European Commission

JRC TECHNICAL REPORTS

Analysis of blast parameters in the near-field for spherical free-air explosions

Vasilis Karlos
George Solomos
Martin Larcher

2016

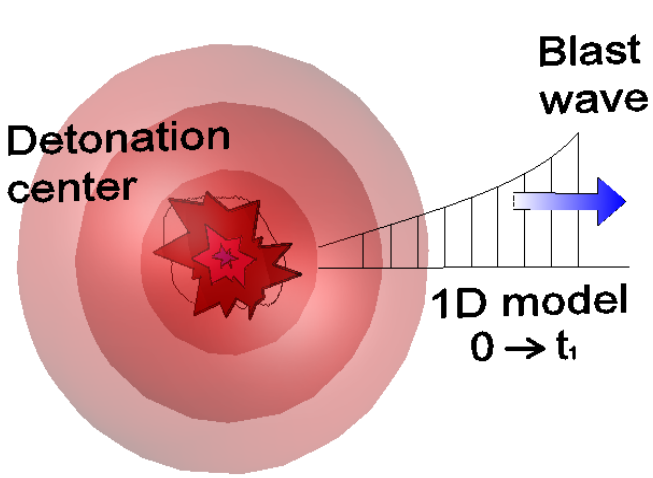

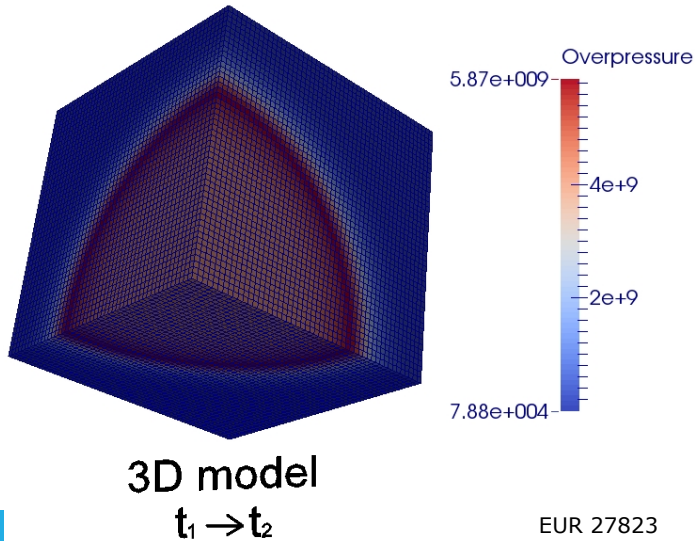

Joint Research Centre

EUR 27823

Analysis of blast parameters in the near-field for spherical free-air explosions

This publication is a Technical report by the Joint Research Centre, the European Commission's in-house science service. It aims to provide evidence-based scientific support to the European policy-making process. The scientific output expressed does not imply a policy position of the European Commission. Neither the European Commission nor any person acting on behalf of the Commission is responsible for the use which might be made of this publication.

Contact information
Name: George Solomos
Address: Joint Research Center, Via Enrico Fermi 2749, TP 480, 21027 Ispra (VA), Italy
E-mail: george.solomos@jrc.ec.europa.eu
Tel.: +39 0332 78 9916

JRC Science Hub
https://ec.europa.eu/jrc

JRC101039

EUR 27823

ISBN 978-92-79-57603-4

ISSN 1831-9424

doi:10.2788/778898

© European Union, 2016

Reproduction is authorised provided the source is acknowledged.

Printed in ITA

All images © European Union 2016, except:

How to cite: Authors; title; EUR; doi

Table of contents

Abstract

The report focuses on the calculation of blast parameters that are used for designing structural elements to resist blast induced loads. It addresses shortcomings encountered with the widely used relationships proposed in the Kingery-Bulmash technical manual. The parameter values in it have proven accurate for medium and large scaled distances, but serious doubts have been raised by researchers on their validity for small scaled distances, i.e. close-in detonations.

As supporting experimental data in this distance range are scarce, numerical simulations have been employed in this investigation. The finite element code EUROPLEXUS is used to study the evolution of spherical blast waves and their parameter values for near and far-field explosions. Modelling of both the explosive (through the JWL equation) and of the air is made. The results from one-dimensional and three-dimensional analyses are favourably compared with those of other specialized programs and with limited actual test data. For the numerical discretisation mesh sensitivity studies are conducted and an equation is proposed that allows the use of a variable cell size in relation to the scaled distance, that ensures both accurate results and reduced computational costs.

From the analysis it is revealed that the Friedlander equation cannot capture the overpressure-time behaviour at small scaled distances as it fails to take into account the effect of the expanding detonation products. At such distances it is also found that there is a big difference between the peak overpressure and positive impulse values proposed by Kingery-Bulmash and those calculated through the numerical simulations, the latter being considerably higher. As a result a new set of equations in terms of scaled distance are proposed that provide improved parameter accuracy for points close to the detonation centre.

1. Introduction

Over the last decades considerable attention has been drawn to the analysis of blast waves and any affected structural components through the use of finite elements. Explosions have always been of interest to the military community, but with the global rise of terrorism they drew the attention of researchers, since their results could have detrimental effects at the structural stability of engineering structures. They can be divided in two categories, with the first containing deliberate explosions as a result of demolition procedures, war acts, excavations, terrorist attacks etc., while the second category consists of accidental explosions.

During an explosion a rapid release of energy takes place due to a very fast chemical reaction. The produced gases expand in the atmosphere with very high velocities forming a pressure wave that travels away from the detonation center. In order to characterize a blast wave, shown in an idealized form in Figure 1, a set of parameters has to be calculated, such as the peak positive P_{so} and negative P_{so-} overpressures, the arrival time t_a, the positive t_o and negative t_{o-} phase duration, the positive i_s and negative i_{s-} impulses, the shock wave speed U and the blast wavelength L_w. Proposals for the calculation of some or all of these parameters can be found in various blast design manuals [1-6].

Simulation of explosions and blast waves with the aid of finite elements can also be an alternative for determining these parameters. It may, however, prove a cumbersome procedure, as, depending on the required accuracy, very fine meshes may be required. Especially if the explosive itself is to be modeled, the number of elements may rise to such a number that the simulation cost becomes prohibitive. There exist procedures for overcoming this obstacle, like that of using a pressure-time function directly applied on the surface of the structure of interest, or that of simulating the explosive material as a compressed air balloon. Every procedure has advantages and disadvantages as has already been described in [7]. In most of the cases, the biggest problem is the need for very small elements in order to achieve good precision, and this leads to small time steps and very large CPU requirements.

For spherical, free-field explosions a way of overcoming this problem is by performing a 1D analysis that can be later mapped into a 2D or a 3D, depending on the existing number of reflecting surfaces in the model. This is the approach followed in the current report which focuses on numerical analyses with the finite element software program EUROPLEXUS. Special attention is given to the calculation, using 1D analysis, of blast parameters at small scaled distances, near the interface between the explosive material and the surrounding air. For this scaled distance range serious doubts have been expressed by researchers on the validity of the relationships proposed in the Kingery-Bulmash technical manual [3]. Several blast examples are computed with the finite element code and are compared with experimental and analytical results from the literature in order to validate, verify and examine the accuracy of the software tool at both near and far field explosions. The proper methodology is proposed, that will produce accurate results without requiring excessive simulation time. Finally, a new set of equations in terms of scaled distance are proposed in the format of the Kingery-Bulmash relationships. They provide improved blast parameter values for points close to the detonation centre in the case of spherical air-bursts for both the incident and the reflected waves.

2. Characterization of the blast wave

The form of the blast wave pressure-time history is usually represented through the Friedlander equation, as shown in Equation 1,that has been adopted to show the decrease of the blast pressure values. This equation is dependent on time t that is measured from the time of the arrival of the blast wave at the point of interest, as shown below:

$$P_s(t) = P_{so}\left(1 - \frac{t}{t_o}\right)e^{-b\frac{t}{t_o}} \tag{1}$$

where, P_{so} is the peak overpressure,

t_o is the positive phase duration,

b is a decay coefficient of the waveform and

t is the time elapsed, measured from the instant of blast arrival.

Figure 1 shows some of the parameters of an ideal blast wave. It can be seen that the pressure increases rapidly to a maximum value, which is referred to as incident or reflected peak overpressure for incident and reflected blast waves respectively. After its peak value, the pressure decays exponentially and reaches the ambient value after a time period known as positive phase duration. This phase is called positive since the resulting blast pressure values are larger than the ambient pressure. The majority of structural and other type of damage during an explosion is usually caused by this positive phase. After the positive phase of the blast, the pressure drops below the ambient value. This negative phase is usually neglected during design of structures to resist an explosion, as the generated peak pressures are generally much less than the respective positive ones and they act in the opposite direction. This means that it is on the conservative side to assume that the negative pressure does not contribute considerably to the created damage. But, if the scaled distance is large or if the affected components are flexible, the negative phase should be taken into account during design. The created impulse for both incident and reflected blast waves is calculated as the area formed between the incident or reflected pressure curve and the time axis respectively.

In all cases, the reflected pressure and impulse is always larger than the incident one and is the value that should be used for design. It should be remembered that the representation of the blast wave pressure-time history through the Friedlander equation is not always valid, especially in the case of small scaled distances, as will be shown in the next sections.

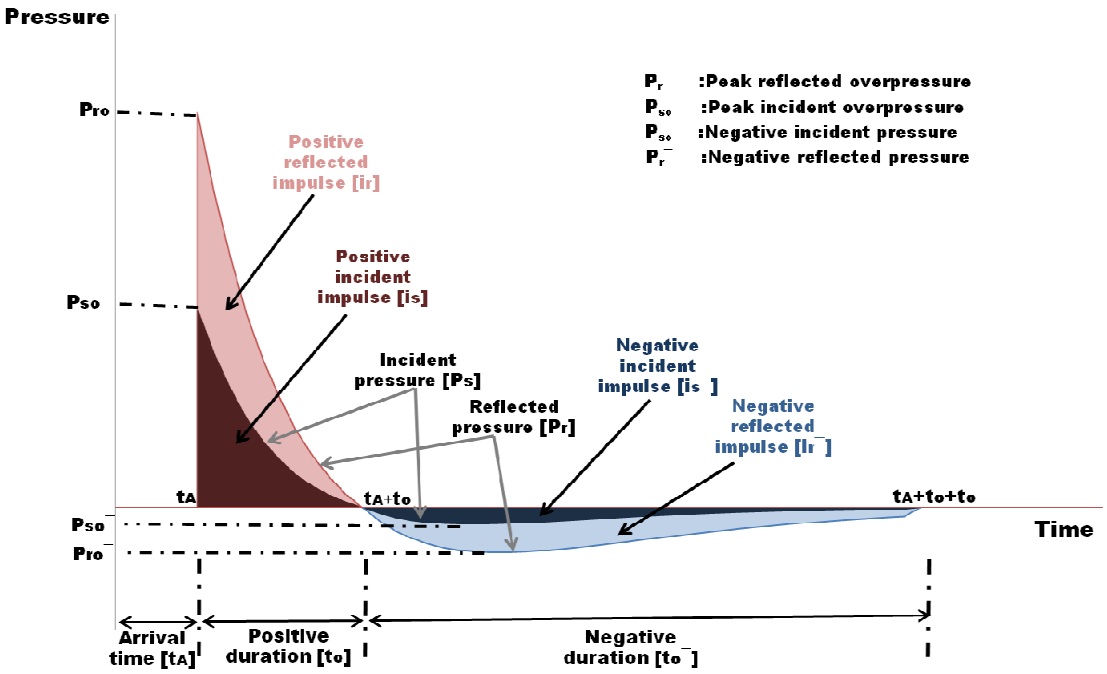

Figure 1: Incident and reflected pressure time histories

The calculation of these parameters can be quite difficult, as an explosion lasts only some milliseconds and releases big amounts of energy. Several textbooks and blast technical manuals exist that give proposals for the calculation of these parameters, as was presented in detail in [8]. Most of the proposed equations are semi-empirical and show good compliance with relevant experiments, especially in the case of far-field loads that can be measured with good accuracy. In the case of near-field loads though, the relevant blast parameters cannot be experimentally measured with precision, as the resulting very big pressure and temperature values make unsuitable the majority of the available measuring equipment. This means that the proposed parameter values at small scaled distances have a big degree of uncertainty, as has been shown by various researchers [9-10], and should be treated with conservatism.

The analysis of a structure to resist a blast load is usually performed by using a proper modeling technique. If the desired accuracy is low, the analysis can be performed by using single degree of freedom models along with the empirical diagrams that are included in many manuals. But, if the importance or complexity of the structure calls for increased precision a computer software finite element code that is able to perform fluid-structure simulations could be used. Of course, in the latter case the amount of time that has to be invested for producing and analyzing the model is far greater, but the results confidence level rises. Modern analysis tools and today's increased computational power have allowed the extensive use of finite element models for simulating many engineering problems. The majority of the available explicit analysis codes uses for the calculation of the blast parameters the equations included in the Kingery-Bulmash manual [3], which are also available in the form of charts in more recent publications [2]. The proposed polynomials [3] are dependent on the scaled distance and allow the calculation of the incident or normally reflected peak pressures and impulses, the positive phase duration and the arrival time of the blast wave for both free-air (spherical blast wave) and surface (hemi-spherical blast wave) detonations.

The Kingery-Bulmash relationships were based on a large number of experimental data, but as described in [10] the available number of experimental readings for small scaled distance values was limited. This means that the proposed blast parameters at scaled distance values $Z<0.4m/kg^{1/3}$ should be treated with caution as they might not be conservative. Moreover, the decay of the peak overpressure at the near-field does not

follow an exponential function as described by the Friedlander equation (Equation 1), because the expanding detonation products and the afterburning effects affect significantly the shape of the pressure-time curve. Nevertheless, these equations are used by various computer finite element codes in order to form the blast pressure-time history that should be applied to a structure or a component. For example, CONWEP and LS-DYNA, which are two of the most commonly used blast software tools, implement these equations for calculating the pressure-time distribution.

3. Blast wave simulation with EUROPLEXUS

3.1 Jones-Wilkins-Lee equation of state

EUROPLEXUS is a finite element program which is developed by CEA and JRC. The program uses an explicit algorithm for the discretization in time, which makes it suitable for fast transient dynamics, such as explosions. For problems with radial symmetry a mapping option is available for expanding the results of a fine mesh 1D analysis into a coarser mesh 2D or 3D analysis. This option allows the transfer of the increased accuracy from fine meshing to coarser models, with relative ease and the advantage of faster computational times. The mapping technology that can be used in EUROPLEXUS has been described with detail in [7]. In summary, the remapping procedure requires calculation of the pressure, density and particle velocity values. A 1D simulation of a spherical blast wave is performed and the results at a certain distance (chosen by the user) from the detonation point are saved into a file and are used as initial conditions in the remapped 2D or 3D configuration.

When simulating a blast wave with the use of finite elements, an equation of state (EOS) is needed for describing the expansion of the detonation products (gases). The EOS describes the relationship among the various variables, such as the pressure, the volume (or density), and the internal energy (or temperature). Many different models exist in the literature [11-12], but when a solid explosive is involved in the calculation procedure, one of the most commonly used EOS is the Jones-Wilkins-Lee (JWL) [13], as described in Equation 2,

$$P = \mathrm{A}\left(1-\frac{\omega}{R_1 V}\right)e^{-R_1 V} + B\left(1-\frac{\omega}{R_2 V}\right)e^{-R_2 V} + \omega\rho e_{\mathrm{int}} \qquad (2)$$

where, P is the pressure [MPa],

A, B, R_1, R_2, ω are material constants that can be obtained from experimental data,

ρ is the current gas density [kg/m^3],

V is the ratio ρ_{sol}/ρ, where ρ_{sol} is the density of the solid explosive,

v_D is the detonation velocity [m/s],

e_{int} is the internal energy per unit mass.

The parameters for the JWL model for the TNT are those proposed by [14] and are included in Table 1.

Table 1. Parameters of the JWL model and material properties.

Parameter	TNT explosive	Air as JWL	Air as ideal gas
A [MPa]	371200	371200	-
B [MPa]	3231	3231	-
R_1	4.15	4.15	-
R_2	0.95	0.95	-
ω	0.30	0.30	0.35
e_{int}[MJ/kg]	4.294	0.22	0.224
ρ [kg/m^3]	1630	1.29	1.275
v_D[m/s]	6930	-	-

By examining Equation 2 we can conclude that for larger volume ratios V the first two terms become very small and the equation becomes similar to that of an ideal gas (third term). Figure 2 shows the contribution of each of the three terms included in Equation 2 to the resulting total pressure. The parameters from Table 1 were used for calculating the relevant pressures, while V= ρ_{sol}/ρ (also equal to the ratio of the current volume of the explosion products to the original explosives volume) varies from 1 to 10. From the graph it can be seen that the 1st and 2nd term of the JWL equation of state practically have a negligible contribution to the resulting pressure values if the volume ratio is larger than 5, i.e. when for the expansion gases their density ρ is such that $\rho_{sol}/\rho>5$.

For the surrounding air the ideal gas equation of state is usually adopted. However, for the analyses that will follow the surrounding air will be also modeled with the JWL equation in order to avoid the use of multi-material finite element models that may cause numerical instability problems during the simulation progress. In addition, as argued above, the JWL equation degenerates into an ideal gas equation for larger V values. For the case of air, with a typical density of approximately 1.29kg/m^3 (depending upon its compression state), it is definitely true that $\rho_{sol}/\rho>>5$.

Included in Figure 2 is also the curve corresponding to this modeling of the air through the JWL equation with parameter values from Table 1. To investigate further this aspect, Figure 3 presents a "zooming" of the above curve in the more realistic range of values of V, around the typical value of V=1263.5 (=1630/1.29). A curve of the ideal gas law, that follows Eq. 3,

$$P = (\gamma - 1)\rho e_{\text{int}} = \omega \rho e_{\text{int}} \tag{3}$$

with typical parameters is also drawn next to it, where γ is the adiabatic expansion constant. The two curves compare well and, as expected, for standard atmospheric conditions (i.e. ρ≈1.29kg/m^3 and V≈1263.5) they both yield a pressure of approximately P≈ 0.1MPa≈ 101kPa, which is the ambient (atmospheric) pressure.

It is finally noted that the EUROPLEXUS code provides a standard version of the JWL and the JWLS, which is the material model used for the TNT in this study. JWLS is an implementation of the Jones-Wilkins-Lee constitutive law, in which the user specifies also the point inside the solid explosive where the detonation starts and the constant speed v_D of propagation of the detonation through the explosive. This possibility has allowed a quite realistic representation of the detonation process.

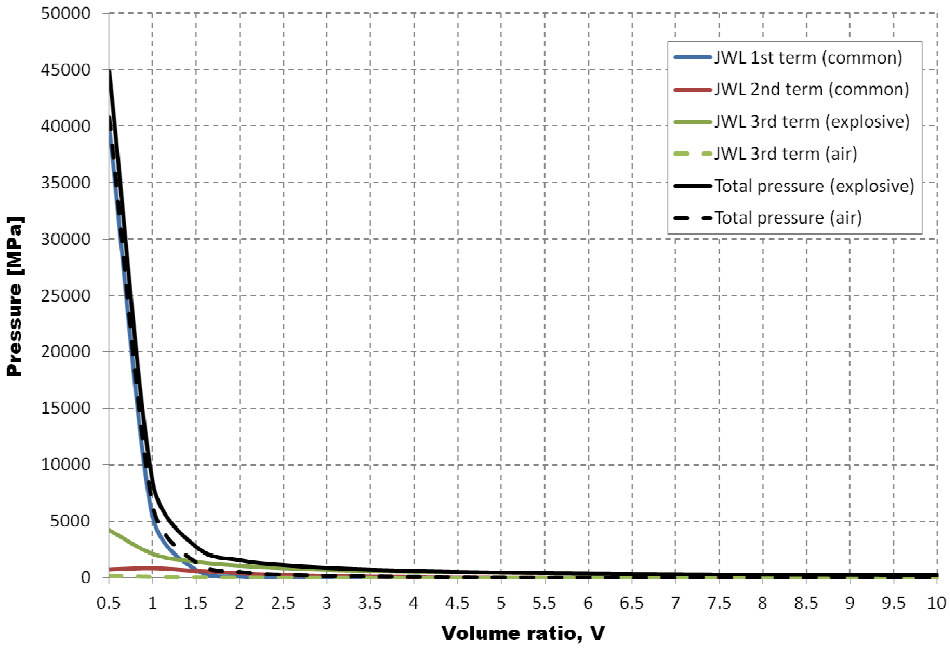

Figure 2: Influence of explosive volume ratio to the JWL equation terms.

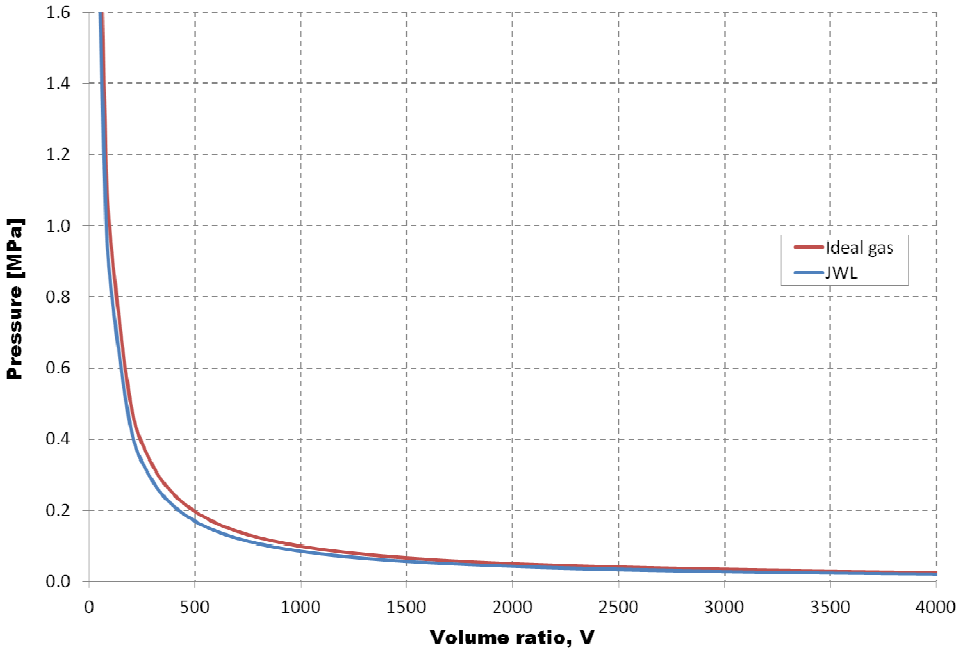

Figure 3: Comparison between ideal gas and JWL EOS for air for larger volume ratios.

3.2 Comparison studies

In his book, Needham [15] has used a computer code in order to describe the evolution of a blast wave in the air, formed by an explosion of a TNT charge in mid-air. An one-dimensional analysis with a Lagrangian code was performed for simulating the resulting

spherical wave. The solid TNT detonation products were represented by the Landau-Stanyukovich-Zeldovits-Kompaneets (LSZK) [16] equation of state. The first term of the LSZK is identical to the first term of the JWL equation of state and they both represent the gaseous part of the blast wave. For simulating the surrounding air the Doan Nickel [17] equation of state was used. The charge consists of 18000kg of TNT with a radius of 1.37m, which is identical to the charge mass used during a series of experiments that took place at the Suffield Experimental Station in Alberta, Canada.

The plots provided by Needham have been digitized and compared below with the results of a similar analysis performed with the software program EUROPLEXUS. As was described earlier, the code uses the JWL equation of state for both the solid TNT detonation products and the surrounding air in order to avoid simulation instabilities, as shown in [7]. 1D calculations based on finite volumes were performed utilizing tube cells whose radius increases linearly with distance from the detonation point. Selection of the minimum and maximum dimensions of the inner and outer cell of the cone follows the suggestions of [7], where it had been noted that when the maximum dimension of the outer element was too big, the simulation ended producing an error since some elements had negative energy. Figure 4 shows a typical mesh of a 1D model in EUROPLEXUS. The detonation is initiated at the center of the spherical explosive. For the current parametric study the angle of the cone is kept constant but the minimum and maximum cross sections are changed as shown in the next sections. The inner cell has necessarily a very small size (e.g. 0.000025m), since a zero value is not accepted by the code. According to the finite volume formulation, the inner and outer elements have at their external borders reflecting boundary conditions.

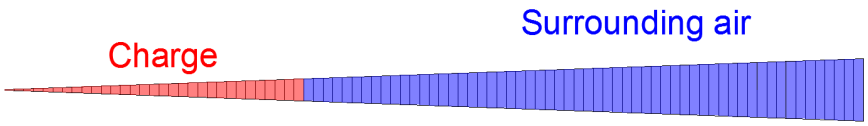

Figure 4: EUROPLEXUS meshed 1D model before detonation.

The figures that follow present the distribution of the blast pressure and density with increasing distance from the explosion center. The derived diagrams show at specific instants the relative overpressure distribution, which is calculated by dividing the overpressure values with the ambient pressure at sea level (equal to P_o=101.3 kPa), and the relative over-density, calculated by dividing the density values with the air density at sea level (equal to D_o= 1.29 kg/m^3). The density of the TNT that was used in the calculations of Needham was slightly lower (1590 kg/m^3) than the density (1630 kg/m^3) used in the current analyses, but this did not affect significantly the produced results.

Figures 5-10 show the relative overpressure at the time when the blast wave front reaches a certain distance from the detonation center. This distance is measured by utilizing an expansion factor which is the ratio of the distance from the explosion center to the charge radius (1.37m). The expansion factors for each of the Figures 5-10 are 1.1, 2.4, 2.6, 4.5, 11.7 and 26 respectively. These diagrams are helpful for monitoring the creation and propagation of the rarefaction wave, as mentioned by Needham. The rarefaction wave is created when the detonation front (still inside the charge) reaches the outer surface of the charge causing the surrounding air to expand and compress. This behavior of the air causes the creation of a wave that travels in the opposite direction to that of the blast wave. Three different cell sizes were used for simulating the propagation of the blast wave. Models with constant element size of 10mm, 5mm and 1mm were used resulting in a total number of 4000, 8000 and 40000 elements respectively for the first 40m from the center of explosion.

Figure 5 shows the relative overpressure distribution when the shock radius (1.51m=1.1*1.37m) has exceeded the charge radius by 10%. The results show that the

pressure at the shock front is very small in comparison to that recorded at the rarefaction wave. The rarefaction wave has not propagated at distances smaller than 0.7m from the detonation center, as is evident by the constant relative overpressure values. All finite element models capture with good accuracy the distribution of pressure values, but the models with a finer mesh give more accurate peak overpressure predictions.

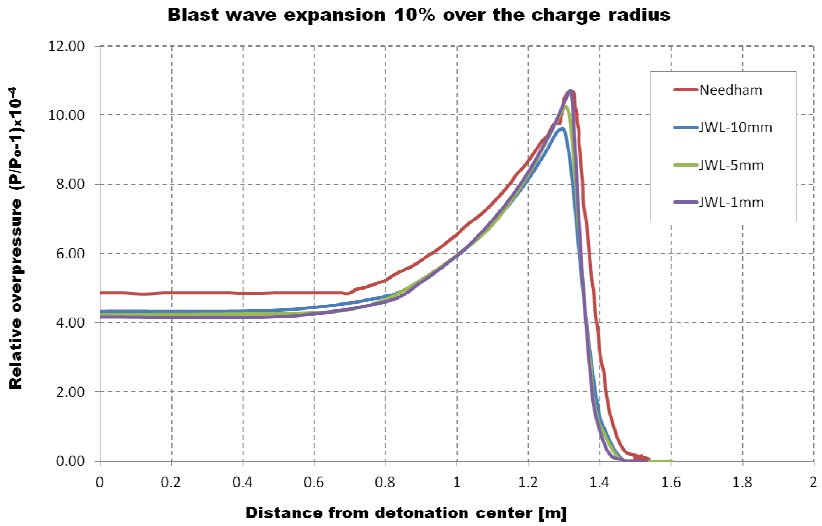

Figure 5: Relative overpressure values at t=0.21ms after detonation.

Figure 6 shows the relative overpressure distribution when the shock radius (3.29m) has exceeded the charge radius by 140%. The constant overpressure near the detonation center shows that the rarefaction wave has still not reached the charge center. The results of the three finite element models are similar to each other and close to the overpressure history provided by Needham. The difference is that in the EUROPLEXUS simulations the rarefaction wave expands faster, as the constant overpressure part near the charge center is smaller in length than that calculated by Needham.

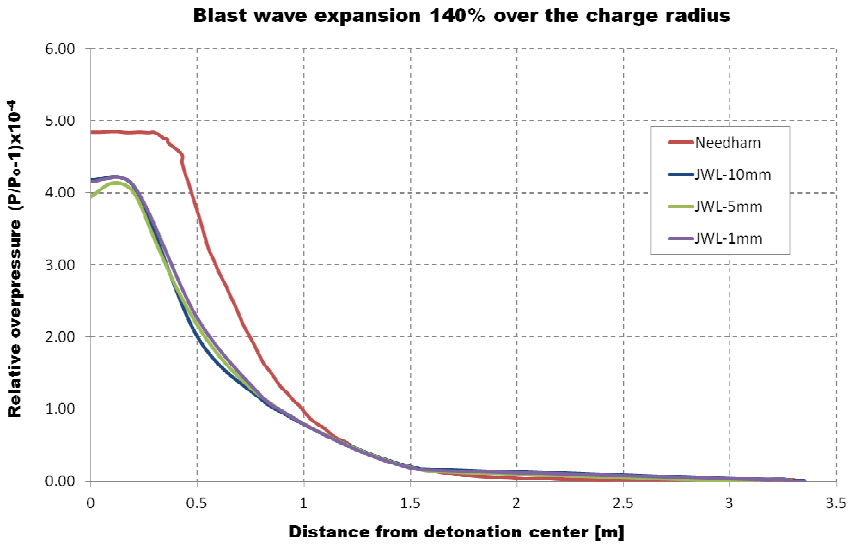

Figure 6: Relative overpressure values at t=0.52ms after detonation.

Figure 7 shows the relative overpressure distribution when the shock radius (3.56m) has exceeded the charge radius by 160%. At this time the rarefaction wave has just reached

the center of the charge, which is shown by the absence of constant pressure values near the center. The overpressure values from all three models are similar to the ones of Needham when the distance from the detonation center is greater than 1m, but for smaller distance values, the finer mesh models provide better accuracy.

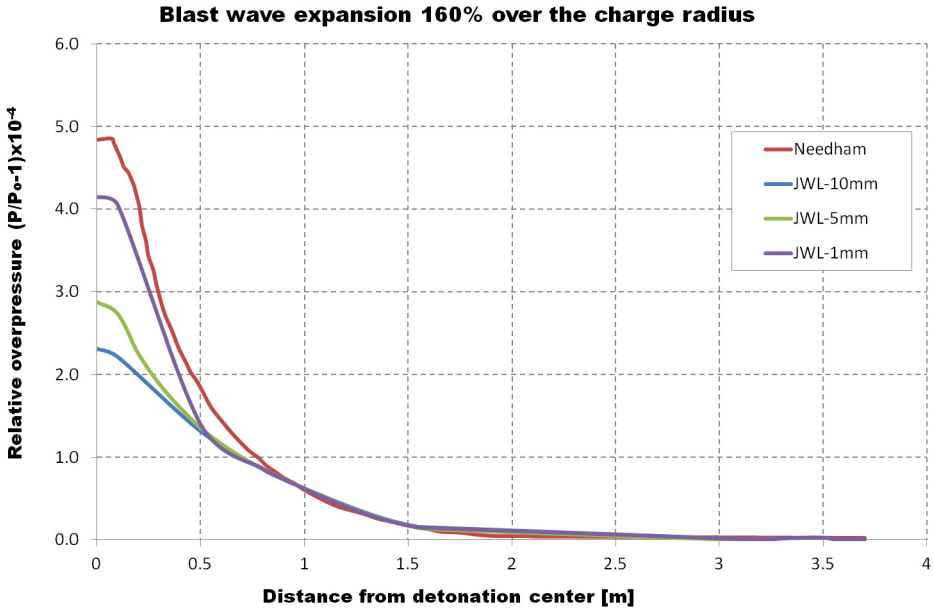

Figure 7: Relative overpressure values at t=0.58ms after detonation.

Figure 8 shows the relative overpressure distribution when the shock radius (6.17m) has exceeded the charge radius by 350%. The overpressure values near the detonation center are overpredicted with the use of EUROPLEXUS, but show greater compatibility with the predictions of Needham at the front of the detonation products which are situated approximately 6m from the charge center.

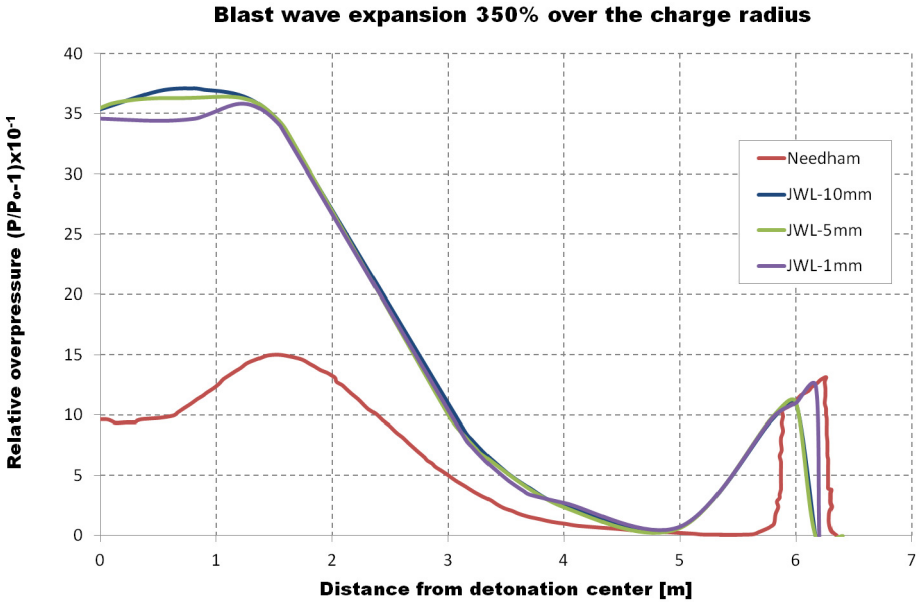

Figure 8: Relative overpressure values at t=1.26ms from after detonation.

Figure 9 shows the relative overpressure distribution when the shock radius (16.03m) has exceeded the charge radius by 1070%. All available models give an overpressure

distribution similar to that of Needham, but the models with finer meshes predict the peak overpressure with greater accuracy.

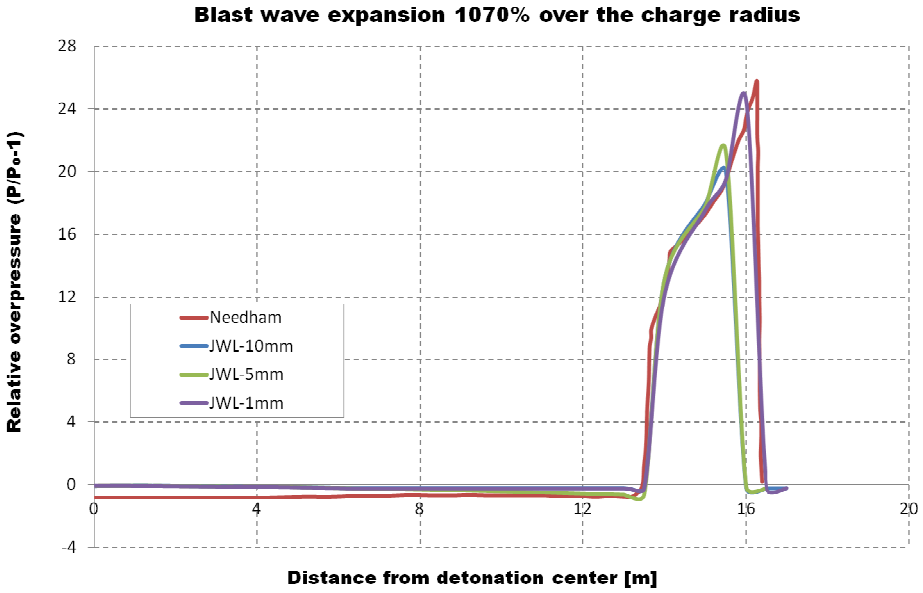

Figure 9: Relative overpressure values at t=5.91ms after detonation.

Figure 10 shows the relative overpressure distribution when the shock radius (35.62m) has exceeded the charge radius by 2500%. The simulations with EUROPLEXUS are in compliance with the predictions of Needham in terms of distribution through the air and peak overpressure values. In this diagram it is interesting to note the difference between the blast front situated at approximately 36m from the charge center and the expanding detonation products whose front is at 22m from the explosion center, as can be noticed by the small kink (instability) at the overpressure distribution. The rarefaction wave that moves in the opposite direction to that of the shock front, causes negative overpressures behind the front of the detonation products. Needham noted that these negative overpressures cause the creation of a second shock wave that moves toward the detonation center and whose front is at approximately 10m at the time instance of Figure 10.

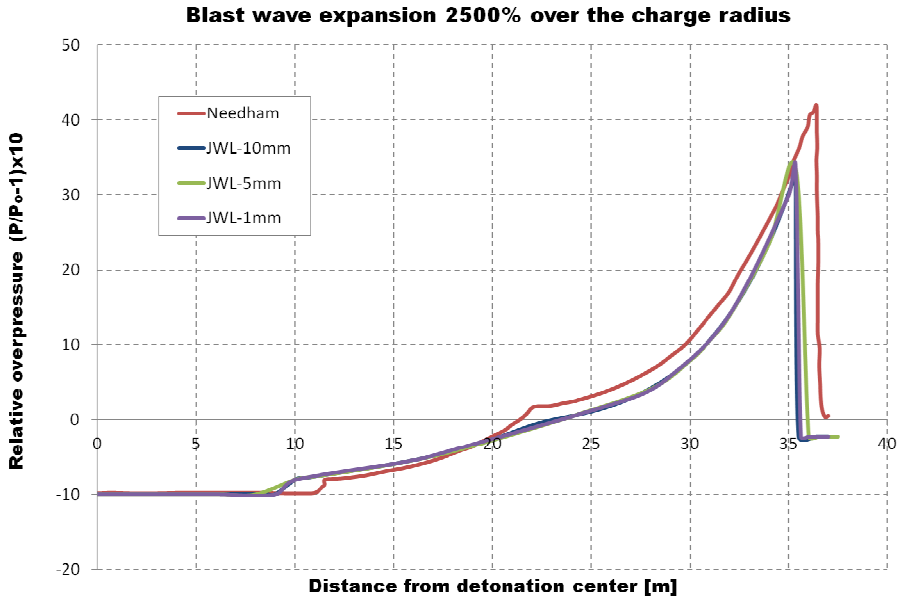

Figure 10: Relative overpressure values at t=27.20ms after detonation.

The conclusions from the relative overpressure distributions are verified by plotting the relative density diagrams at Figures 11-16. The radial expansions selected for these diagrams are identical to the ones already used for the overpressures and span from very small (blast front near the center of the charge) to relatively large. Similarly to the results of the overpressures diagrams, models with finer meshes provide results closer to the ones of Needham, but generally all models capture with good accuracy the evolution of the density distribution. The position of the surface of the expanding detonation gases at 22m when the shock front has exceeded the charge radius by 2500% (commented above in Figure 10) is clearly more evident in the relative density diagram of Figure 16.

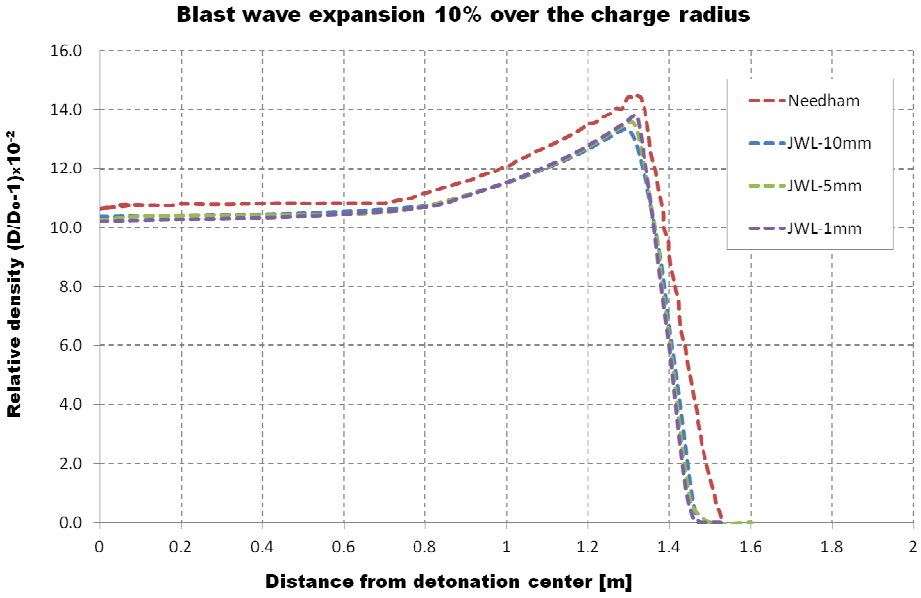

Figure 11: Relative density values at t=0.21ms after detonation.

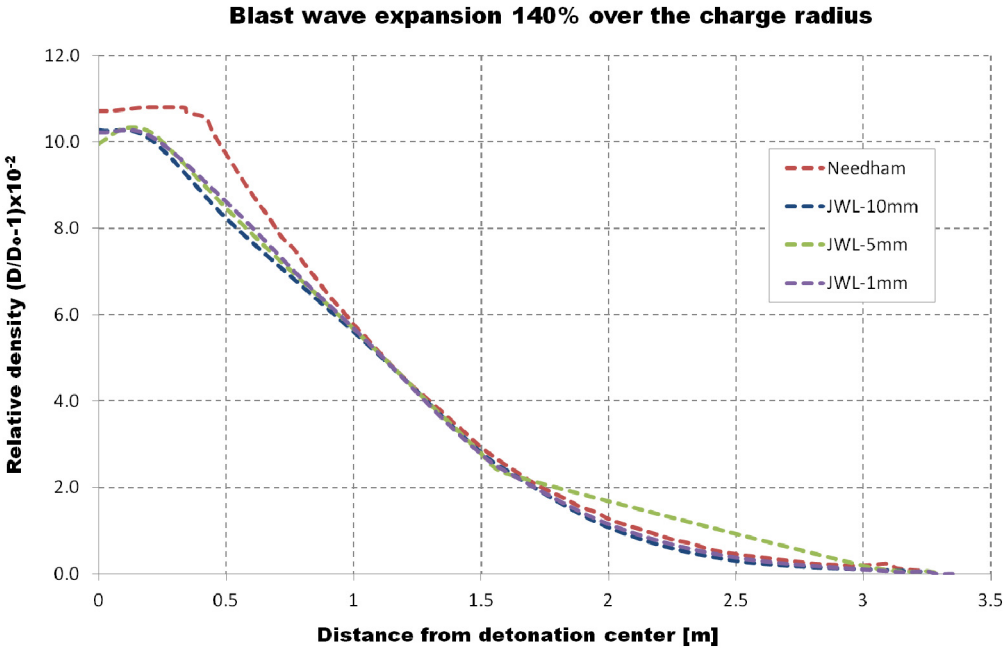

Figure 12: Relative density values at t=0.52ms after detonation.

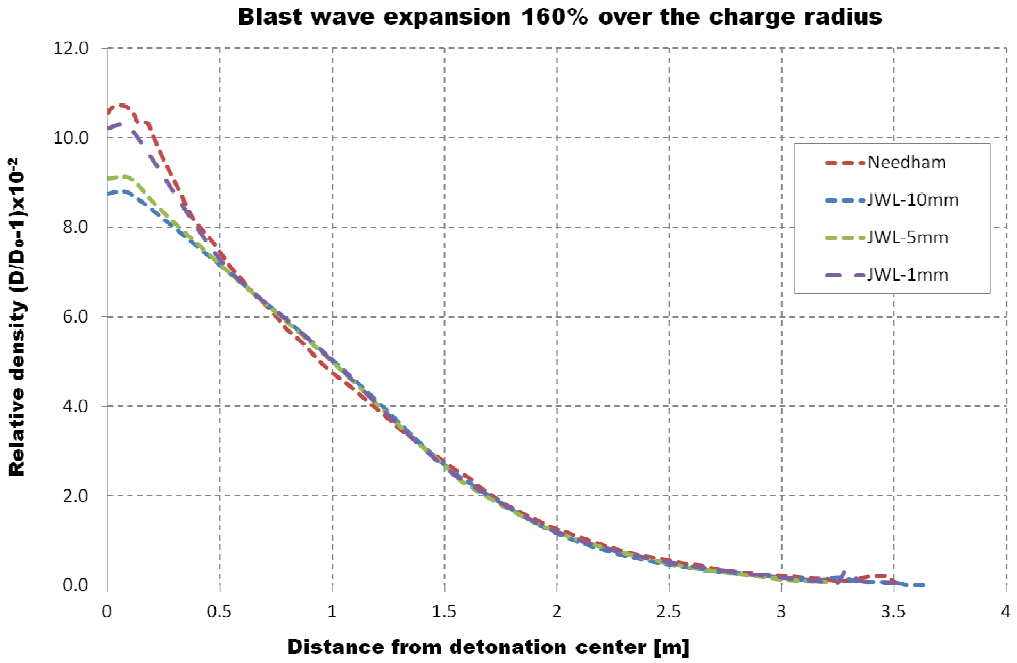

Figure 13: Relative density values at t=0.58ms after detonation.

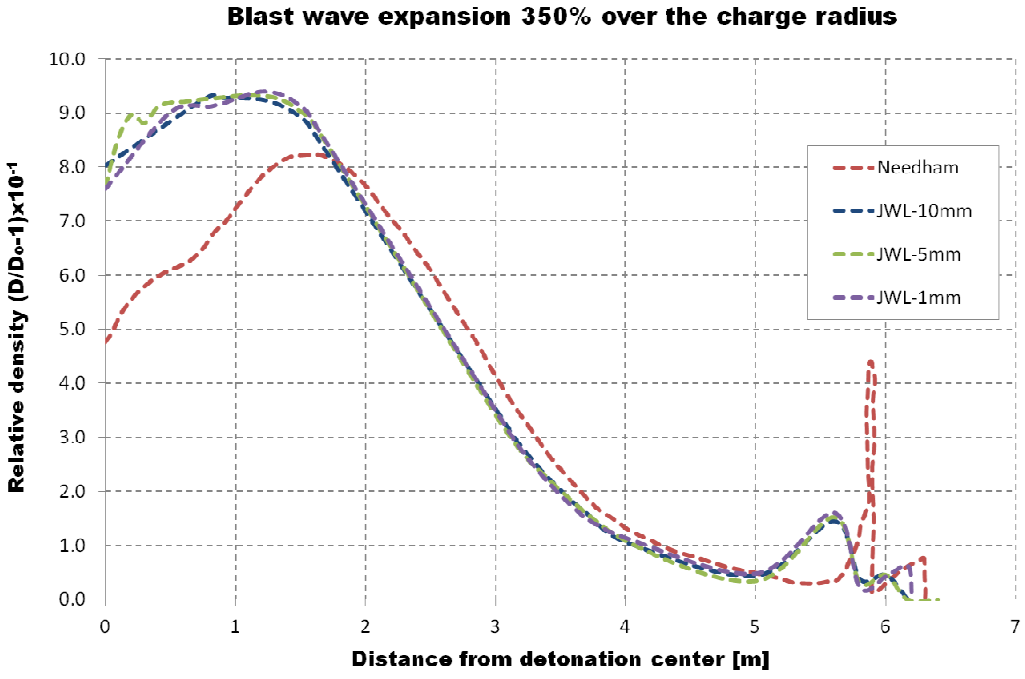

Figure 14: Relative density values at t=1.26ms after detonation.

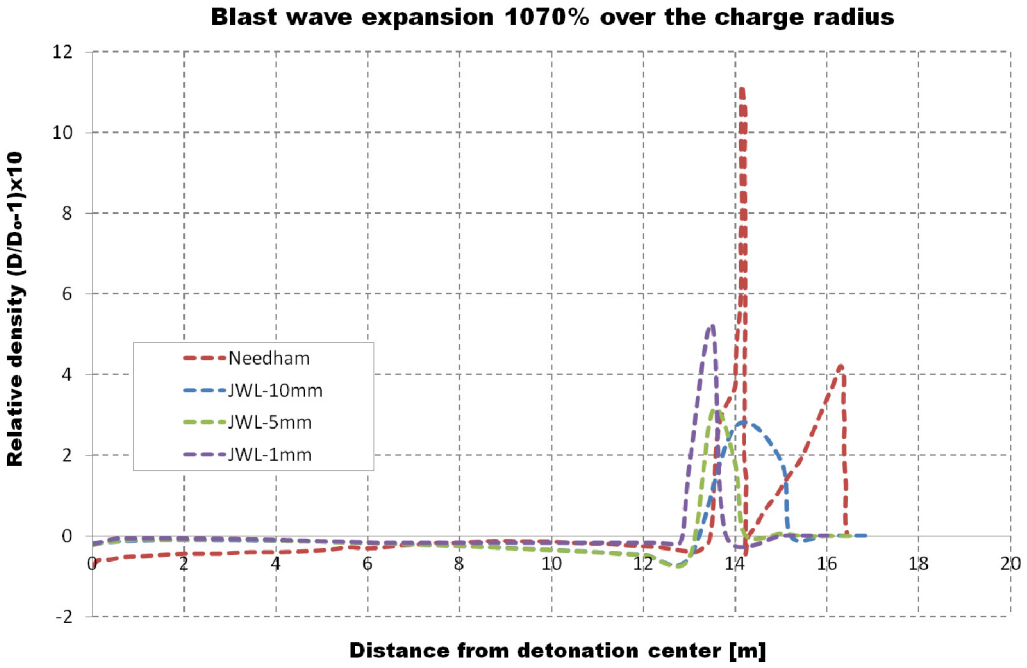

Figure 15: Relative density values at t=5.91ms after detonation.

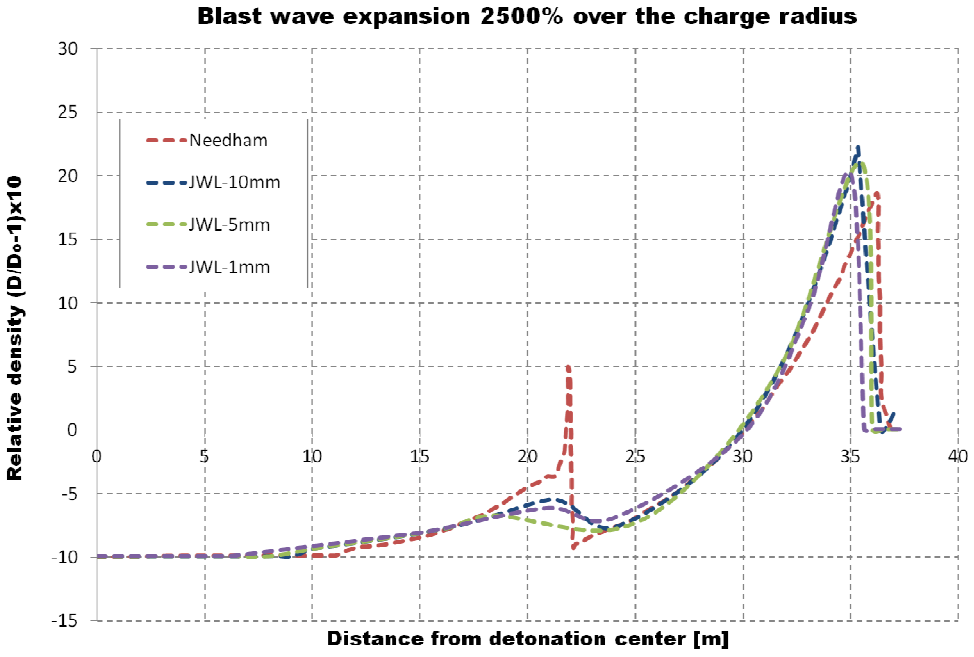

Figure 16: Relative density values at t=27.2ms after detonation.

The propagation of the blast wave through the available space can be also described by the diagrams of the relative overpressure and density with time. The next figures show the overpressure and density time histories at points located at a certain distance from the center of the charge. The distance of these points from the explosion center is identical to the one already used at the previous diagrams for the position of the shock front. The discetization models used for the analysis are characterized by a cell size of 10mm. Figures 17 and 18 show the relative overpressure and relative density time

histories as calculated at 1.51m from the detonation center. The intuitively expected sudden rise of pressure (and density) at this point and its monotonic decay to the ambient pressure are observed.

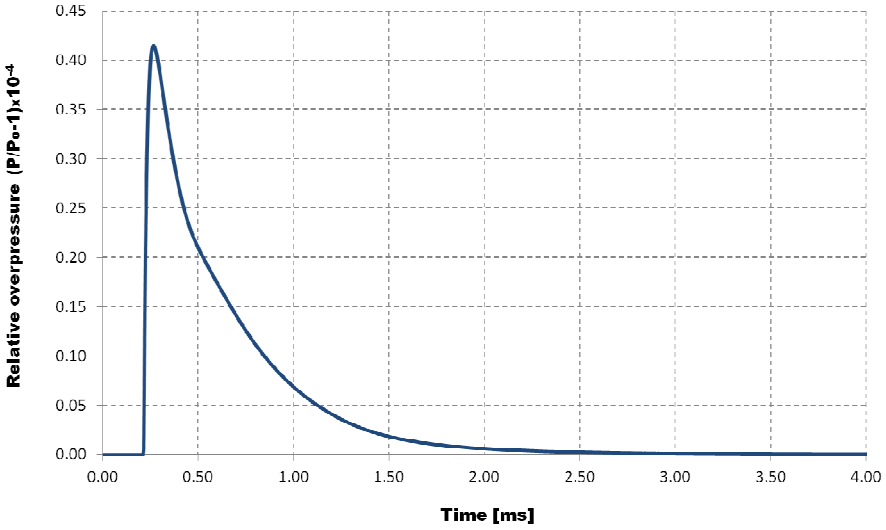

Figure 17: Relative overpressure time history at 1.51m from charge center.

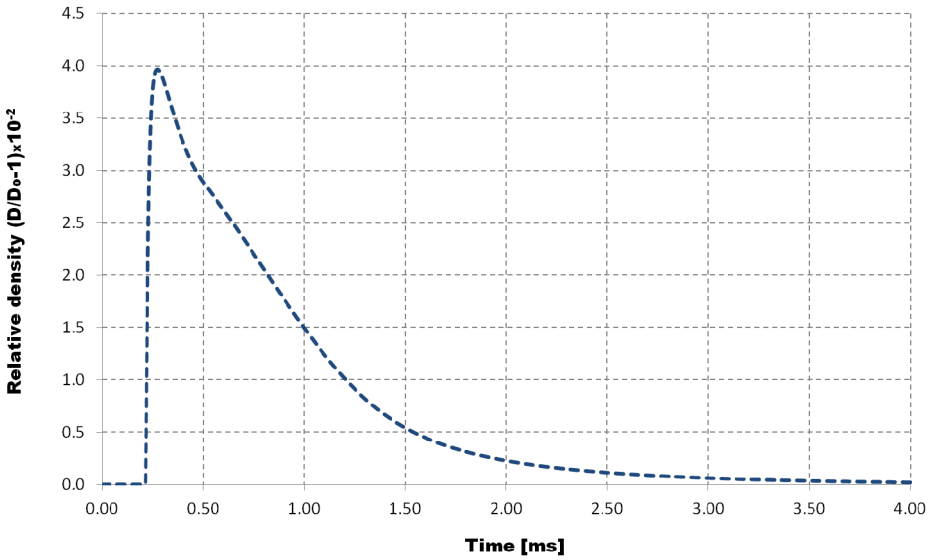

Figure 18: Relative density time history at 1.51m from charge center.

Figures 19 and 20 show the relative overpressure and relative density calculated at 3.29m from the detonation center. The shape of the curves has now drastically changed. The effect of the detonation products is visible, especially at the diagrams of the relative density versus time. One can notice three different peaks, associated with the arrival of the shock front (first and smallest peak), the arrival of the detonation products (second peak) and the outflow of the detonation products (third and largest peak). The arrival of the detonation products is also noticeable at the overpressure diagram, since after the

first higher peak, which is due to the arrival of the shock front, there follows a second related to the detonation products.

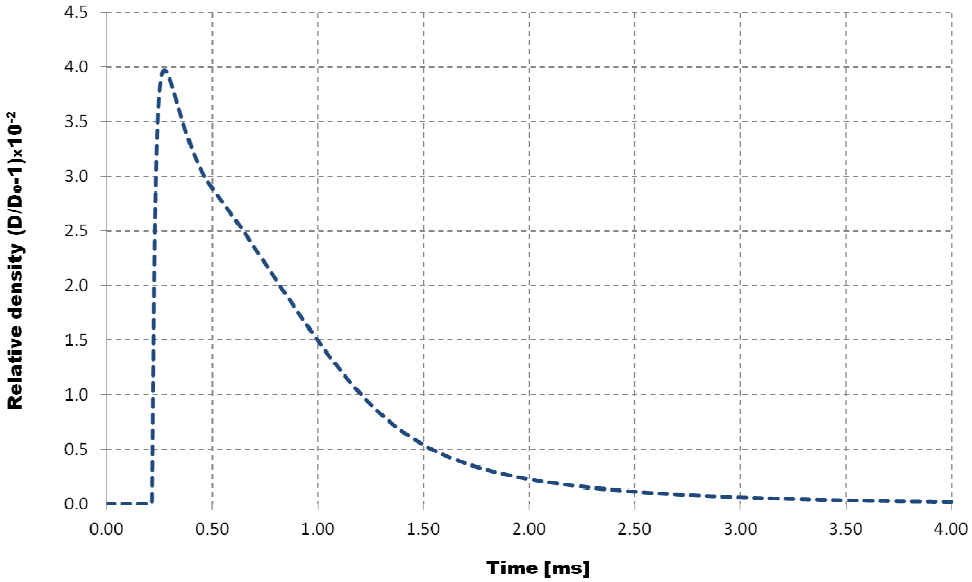

Figure 19: Relative overpressure time history at 3.29m from charge center.

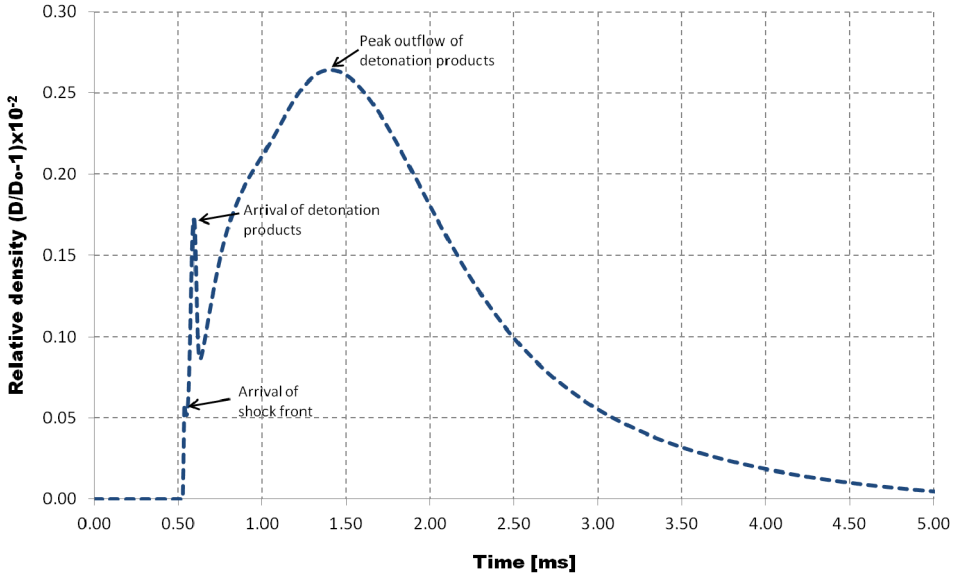

Figure 20: Relative density time history at 3.29m from charge center.

Similar conclusions can be drawn from Figures 21 and 22 that show the relative overpressure and density at 3.56m from the detonation center, where, of course, due to the greater distance from the detonation center, smaller pressure and density values are derived.

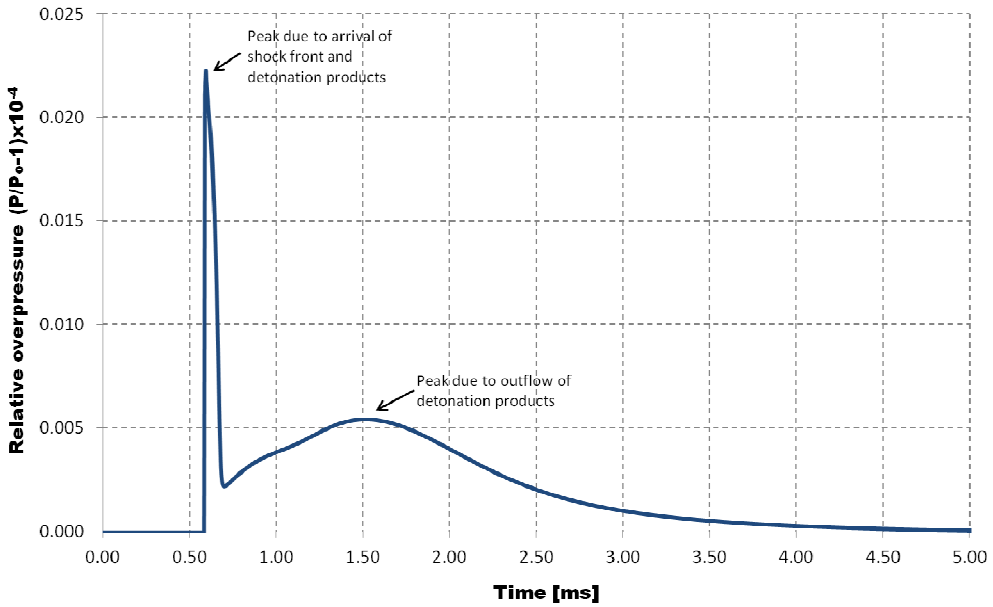

Figure 21: Relative overpressure time history at 3.56m from charge center.

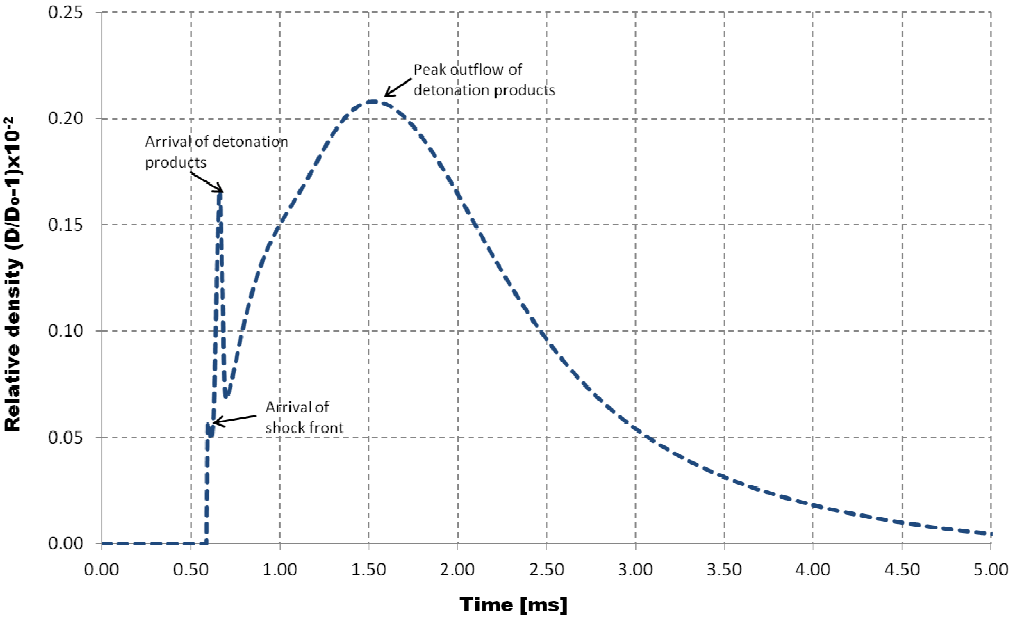

Figure 22: Relative density time history at 3.56m from charge center.

Figures 23 and 24 show the relative overpressure and density at 6.16m from the detonation center, which is equal to a radial expansion factor equal to 4.5. The effect of the detonation products to the calculated overpressures is less pronounced, which implies that at this distance the expanding gases have lost a considerable amount of their speed and energy. However, their arrival is still visible at the relative density plot, where the three distinct peaks define the time instances of the arrivals of the blast front, of the detonation products and of the peak outflow of these products, respectively.

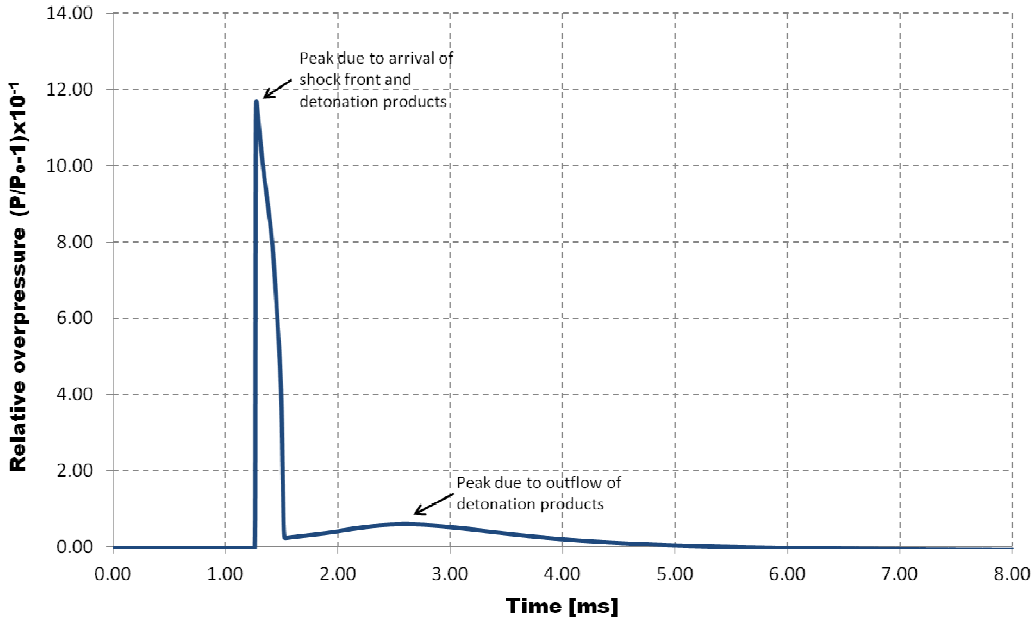

Figure 23: Relative overpressure time history at 6.16m from charge center.

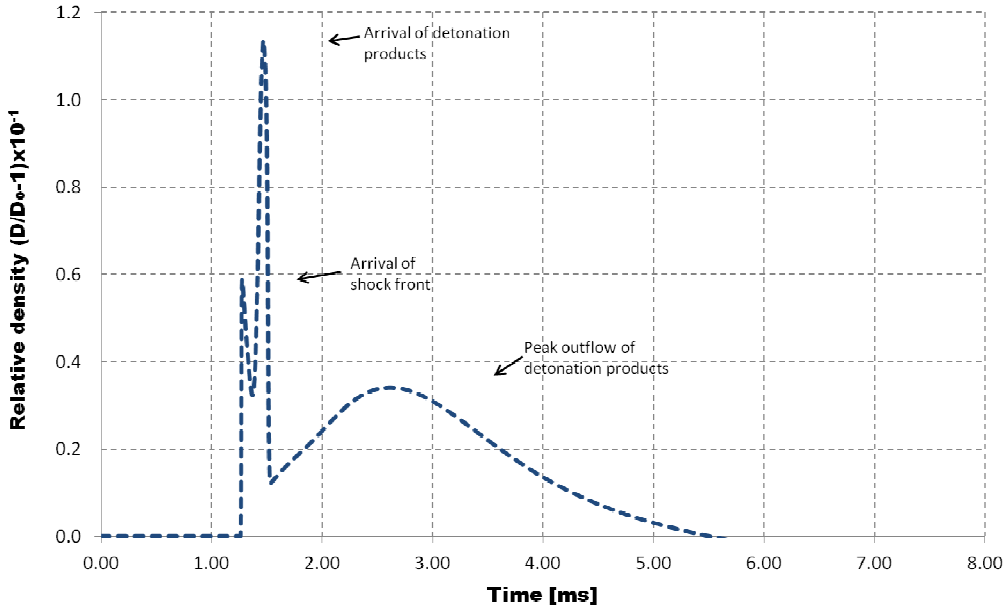

Figure 24: Relative density time history at 6.16m from charge center.

Figures 25 and 26 show the relative overpressure and density at 16.03m from the detonation center. The effect of the existence of the detonation products there can only be noticed at the density diagram, as the relevant overpressures are small compared to the pressure of the blast front.

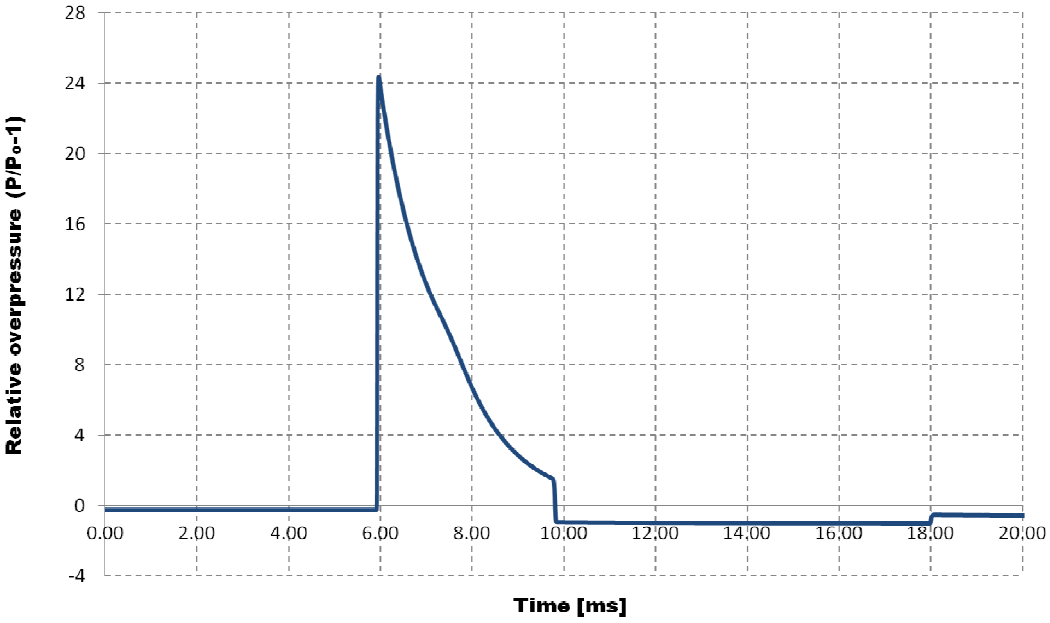

Figure 25: Relative overpressure time history at 16.03m from charge center.

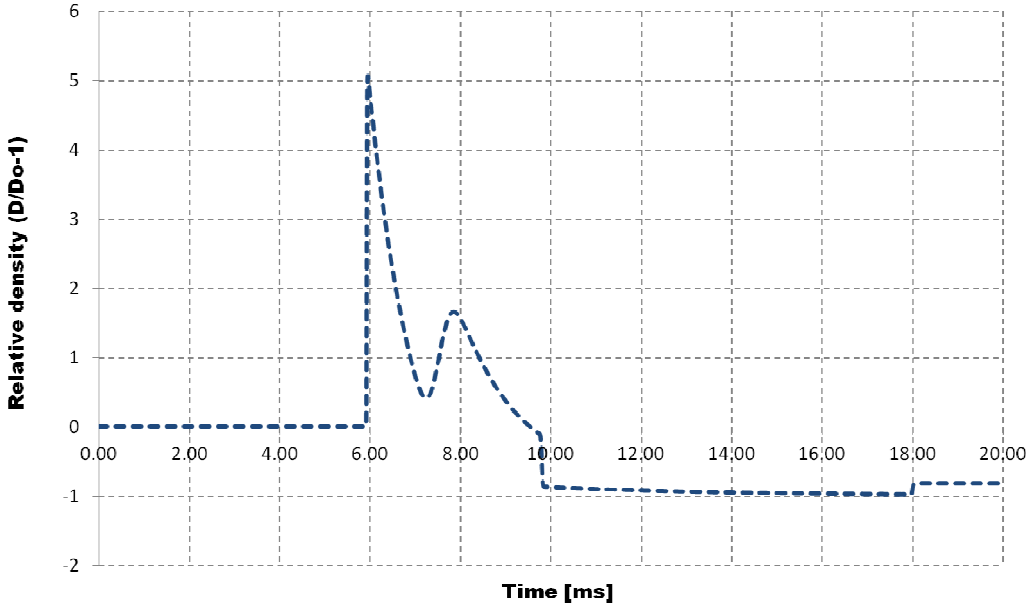

Figure 26: Relative density time history at 16.03m from charge center.

The effect of mesh size on the resulting time histories of overpressure, relative density and impulse is next investigated. The previous results showed that the finer the mesh, the closer the results are to those reported by Needham, especially for small scaled distances. Models with cell sizes of 40mm, 20mm, 10mm, 5mm and 1mm were produced for the analyses. The diagrams that follow in Figures 27-41 show that for small scaled distance values, finer mesh should be used in order to achieve better accuracy, whereas if the scaled distance is larger, the size of the finite elements can also be larger. The relative overpressure and density values are presented (as before) for distances of 1.51m, 3.29m, 3.56m, 6.17m and 16.03m from the charge center. If we consider that the models with the smallest cell size (1mm) provide more accurate results, some criteria can be set and recommended cell sizes for each scaled distance can be proposed.

In this direction the desired degree of accuracy has to be defined, and the results of the model with 1mm element size are chosen as a reference. Then the accuracy of each model size with respect to a certain parameter is assessed by the magnitude of the difference of the calculated results from those of the 1mm cell-size model. If, for example, a 15% difference is considered as a good convergence, then for what concerns the relative overpressure or impulse the appropriate cell sizes would be 5mm, 10mm, 10mm, 20mm and 20mm for expansion factors of 1.1, 2.4, 2.6, 4.5 and 11.7, respectively. If of main interest is the relative density, then larger cell sizes can be used, etc.

From the graphs it can also be noticed that the arrival time of the blast wave is not influenced by the used cell size. The finite element program allows also the use of non-uniform meshing that could, for example, be dependent on the distance from the charge center. The cell sizes of the model can then be chosen larger as the scaled distance increases, which is beneficial in terms of computational time.

As already commented above, from the relative overpressure diagrams it is seen that in many cases the overpressure-time history at a site is quite different from the ideal curve of the Friedlander equation. This difference is attributed to the expansion of the detonation products that affect the shape of the pressure history. This is evident at Figures 29 and 31 that show the relative overpressure-time history for radial expansion factors of 2.4 and 2.6, respectively. At smaller scaled distances (Figure 28) the detonation products are very close to the shock front, so the resulting pressure-time history is not affected to a large extent. Also at larger scaled distances (Figures 33 and 35) the detonation products have lost much of their energy and do not have a significant impact on the shape of the curves.

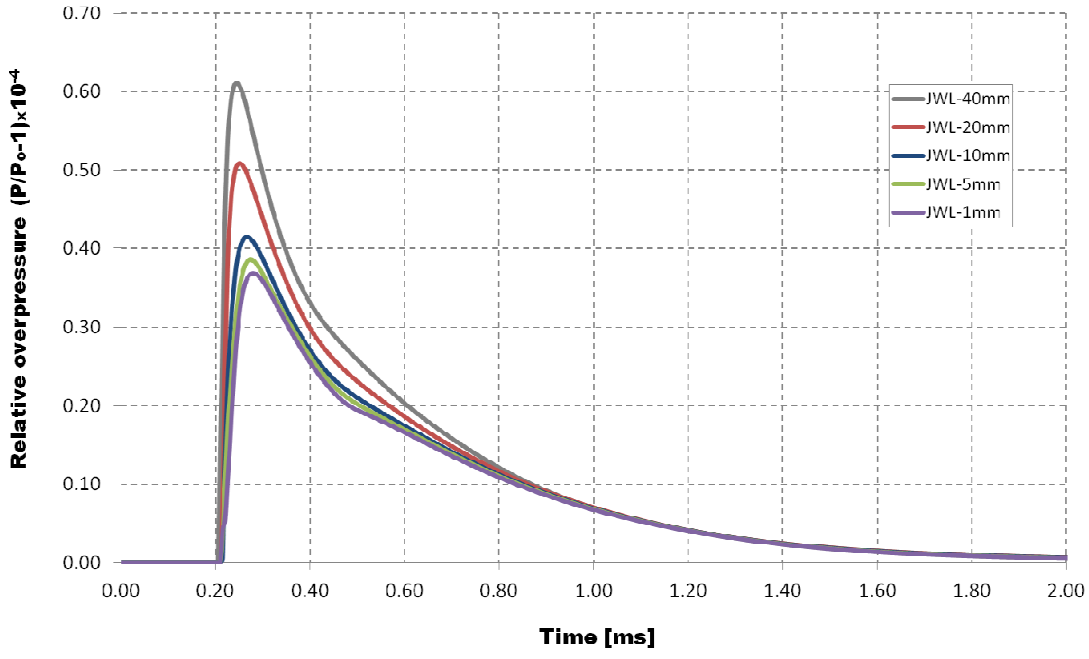

Figure 27: Relative overpressure time history at 1.51m from charge center for different cell sizes.

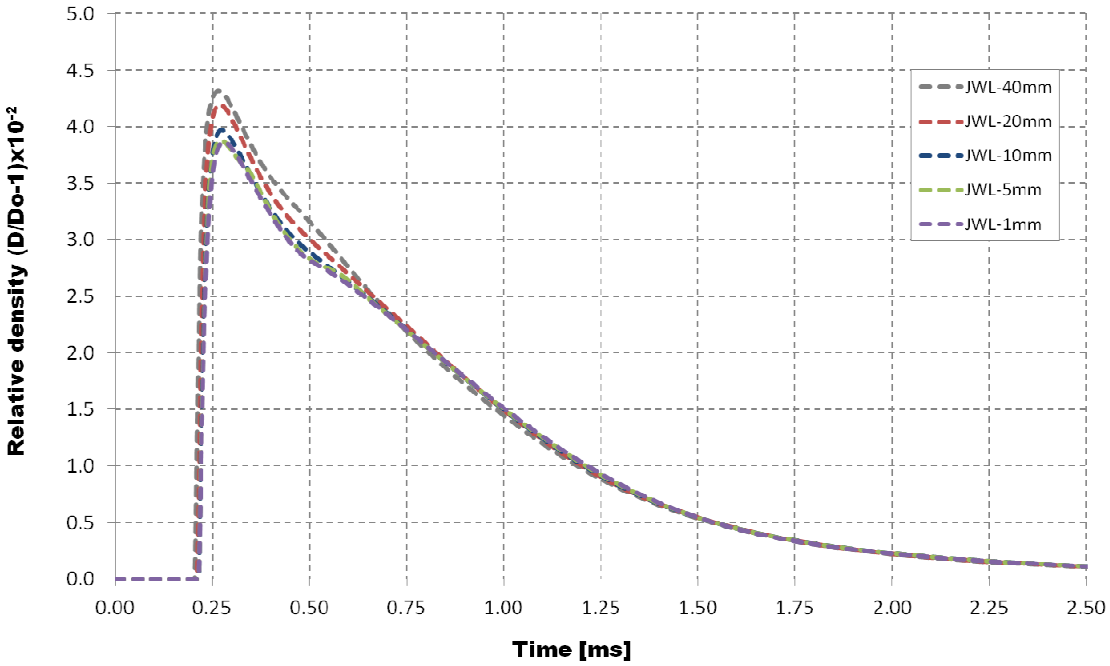

Figure 28: Relative density time history at 1.51m from charge center for different cell sizes.

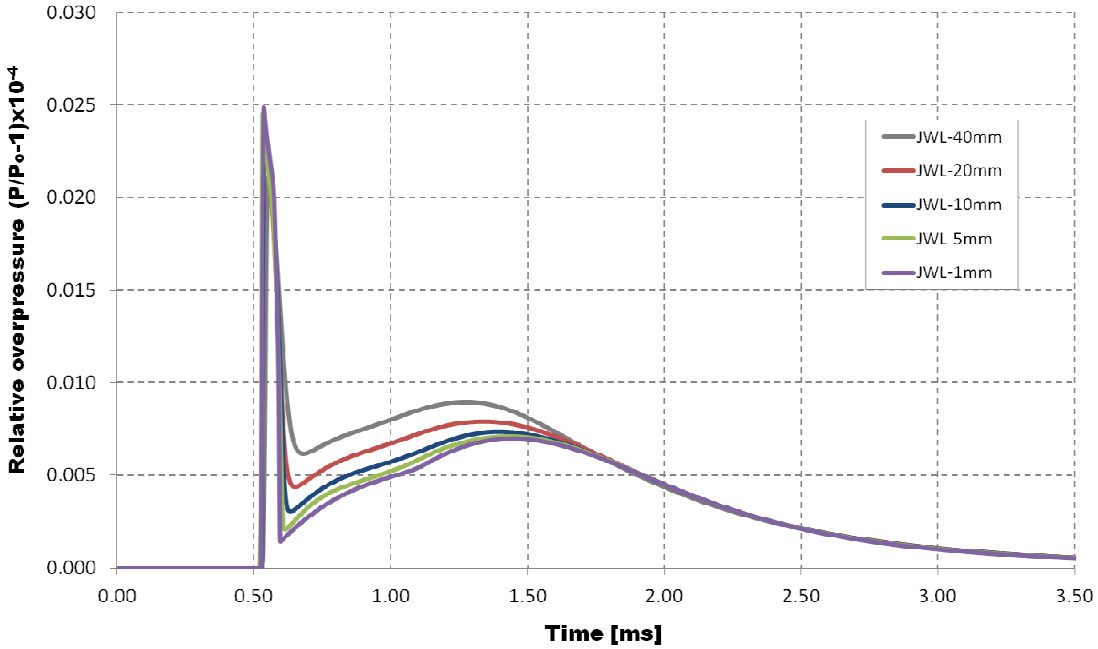

Figure 29: Relative overpressure time history at 3.29m from charge center for different cell sizes.

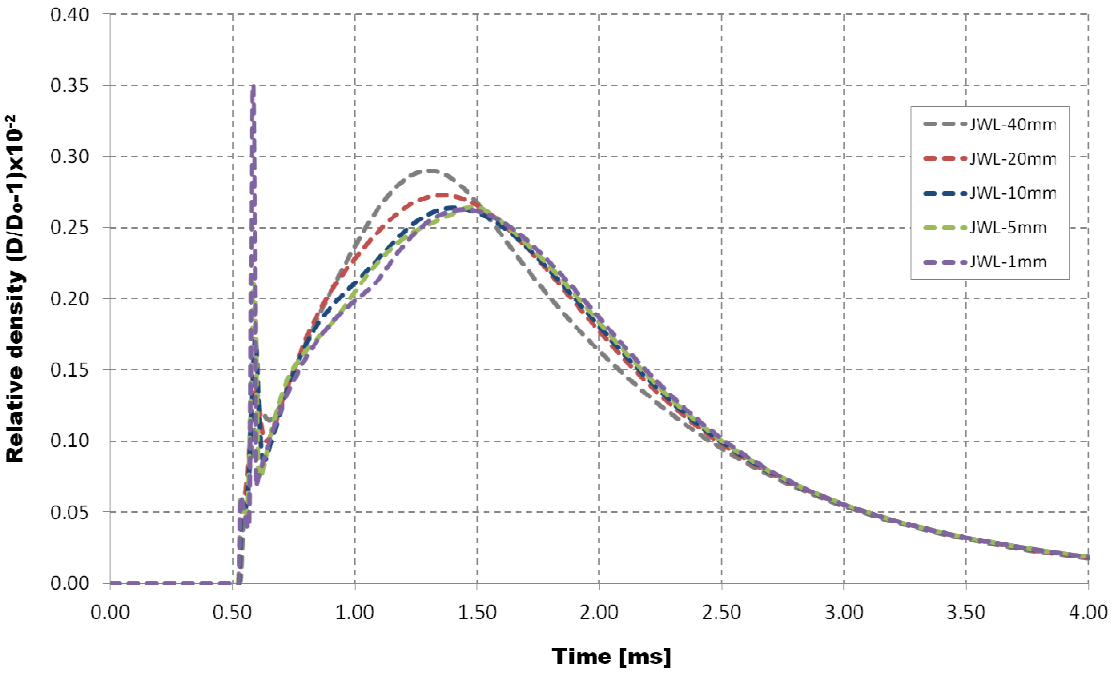

Figure 30: Relative density time history at 3.29m from charge center for different cell sizes.

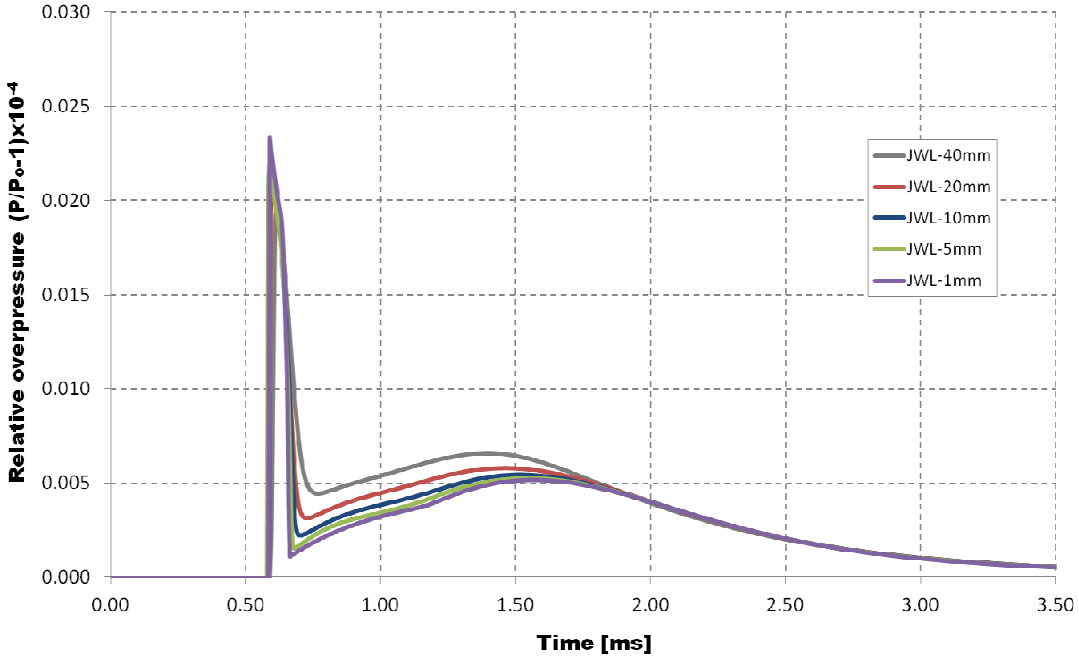

Figure 31: Relative overpressure time history at 3.56m from charge center for different cell sizes.

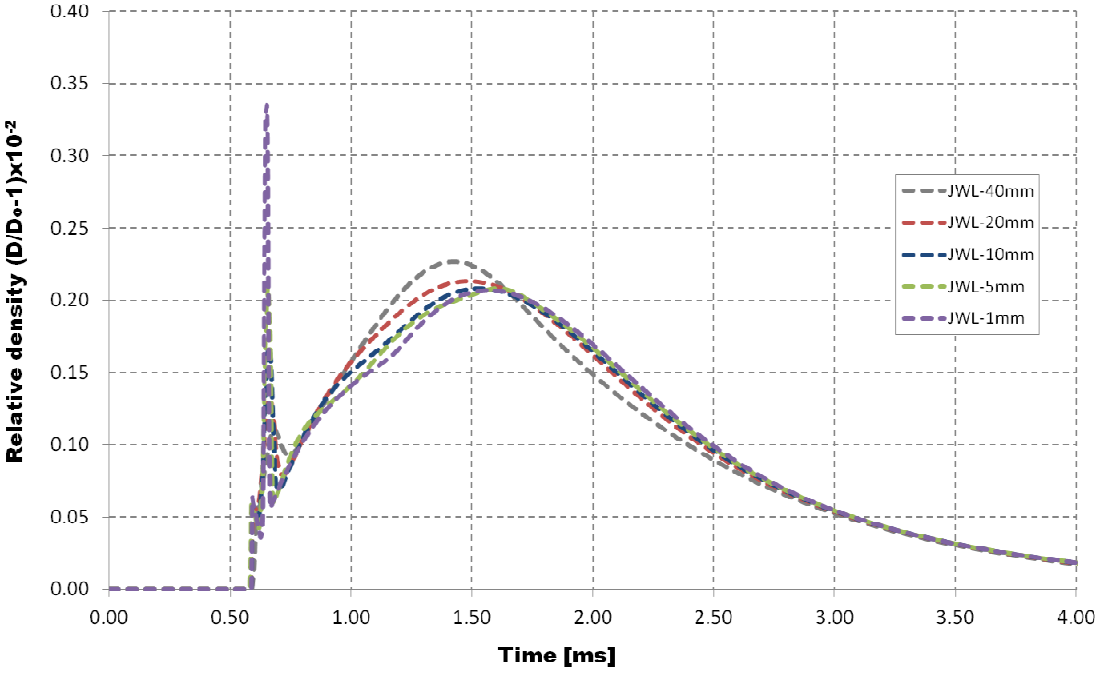

Figure 32: Relative density time history at 3.56m from charge center for different cell sizes.

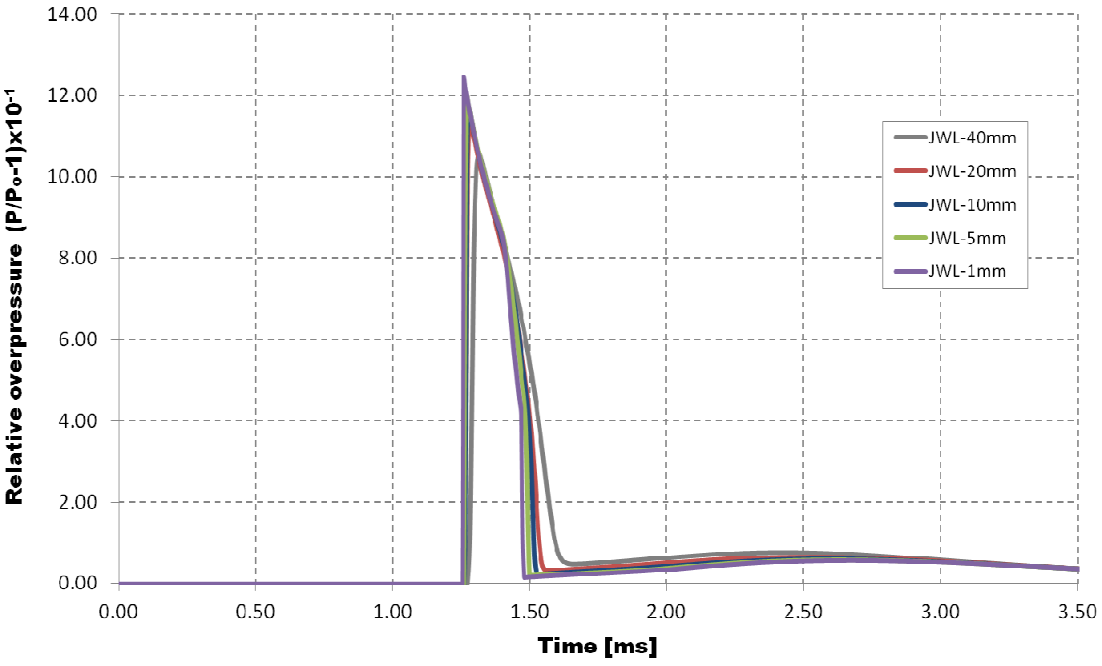

Figure 33: Relative overpressure time history at 6.17m from charge center for different cell sizes.

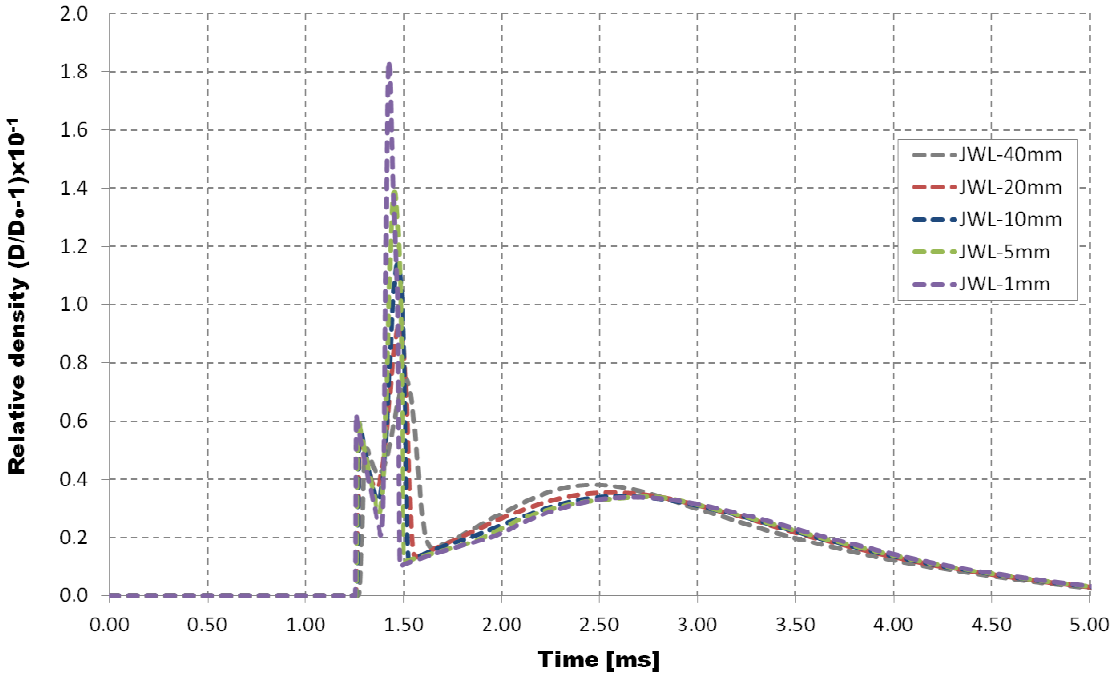

Figure 34: Relative density time history at 6.17m from charge center for different cell sizes.

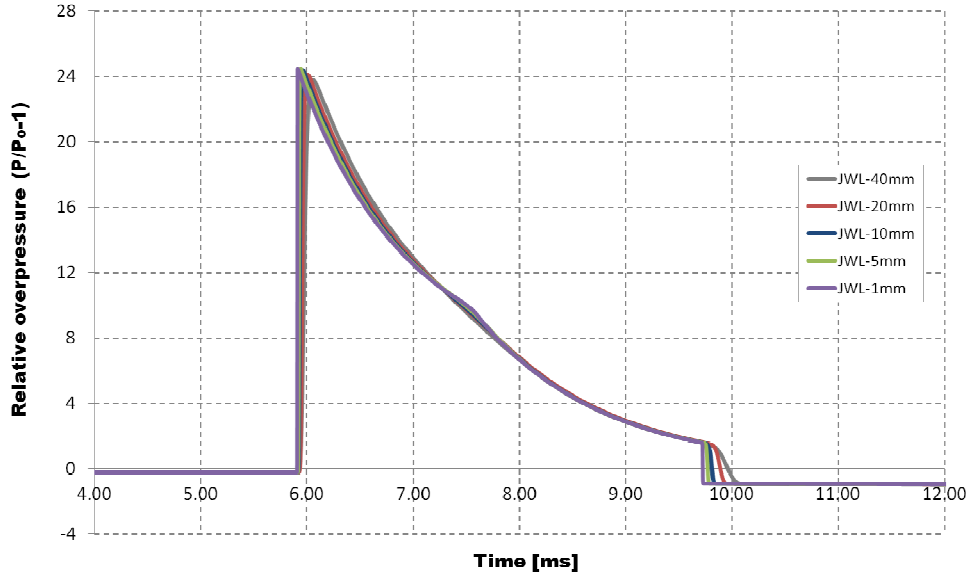

Figure 35: Relative overpressure time history at 16.03m from charge center for different cell sizes.

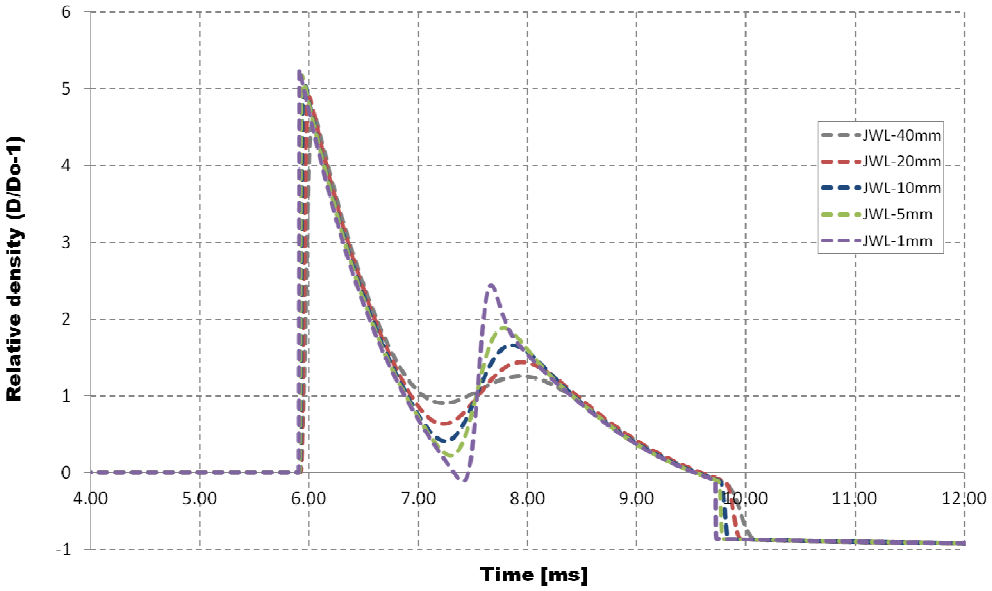

Figure 36: Relative density time history at 16.03m from charge center for different cell sizes.

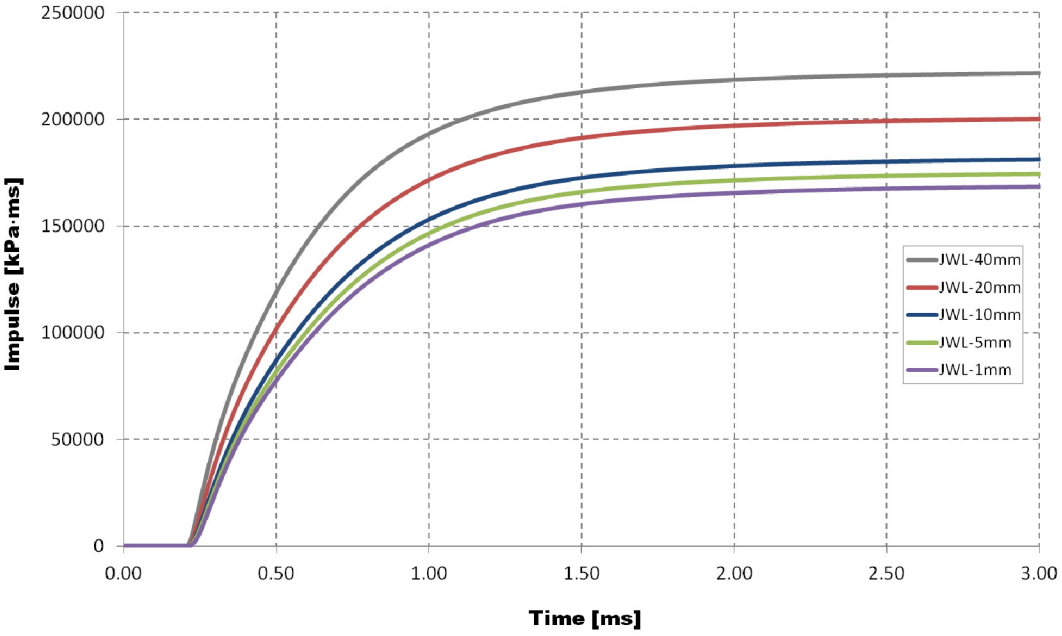

Figure 37: Impulse-time history at 1.51m from charge center for different cell sizes.

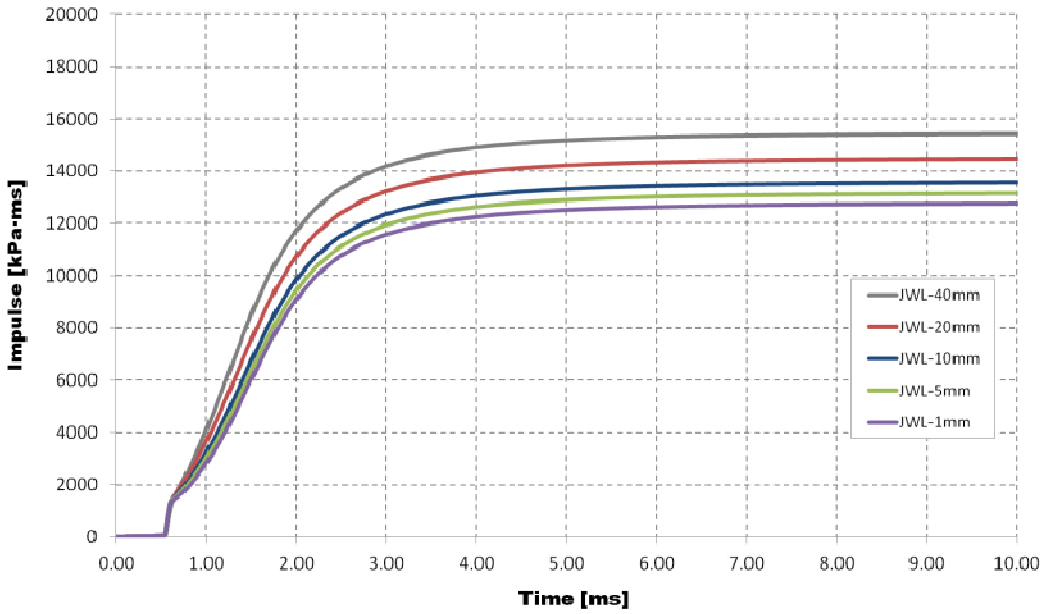

Figure 38: Impulse-time history at 3.29m from charge center for different cell sizes.

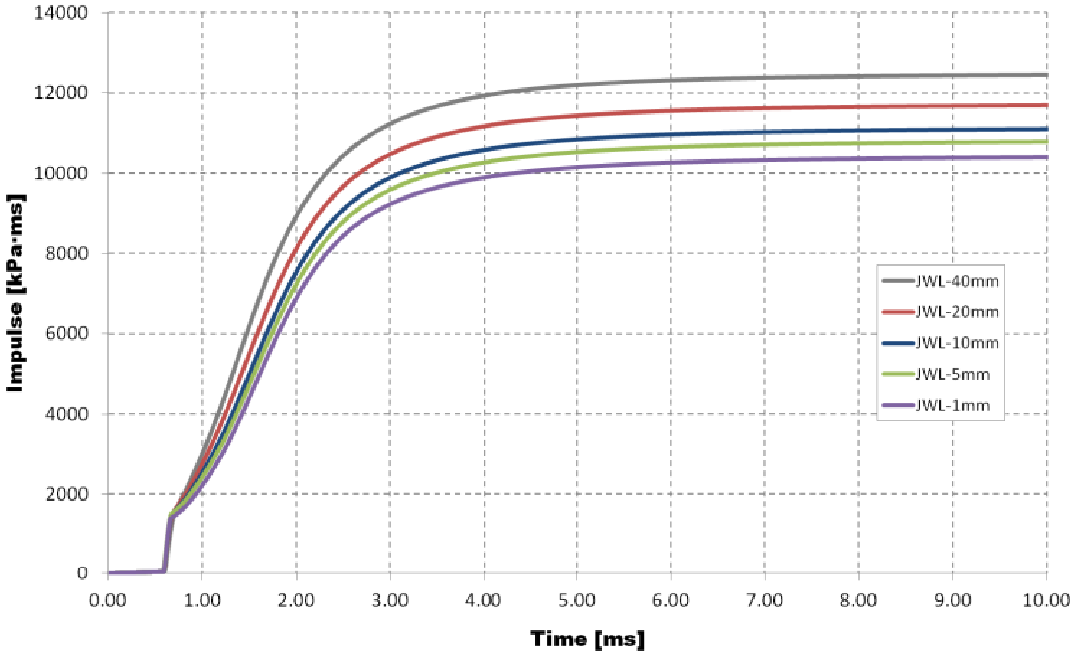

Figure 39: Impulse-time history at 3.56m from charge center for different cell sizes.

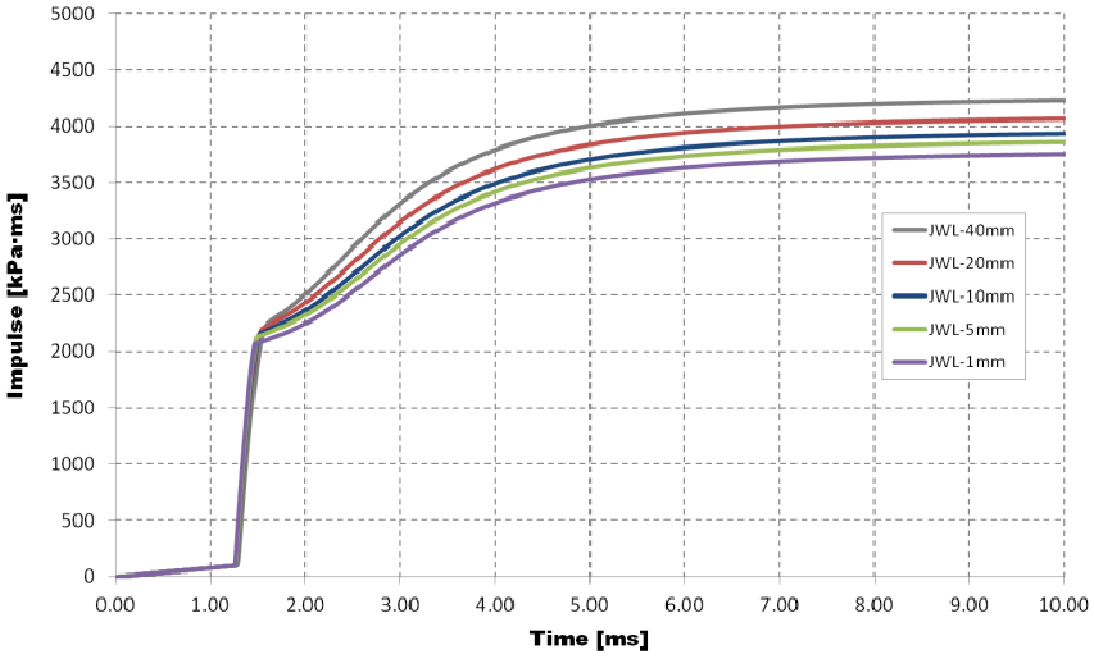

Figure 40: Impulse-time history at 6.16m from charge center for different cell sizes.

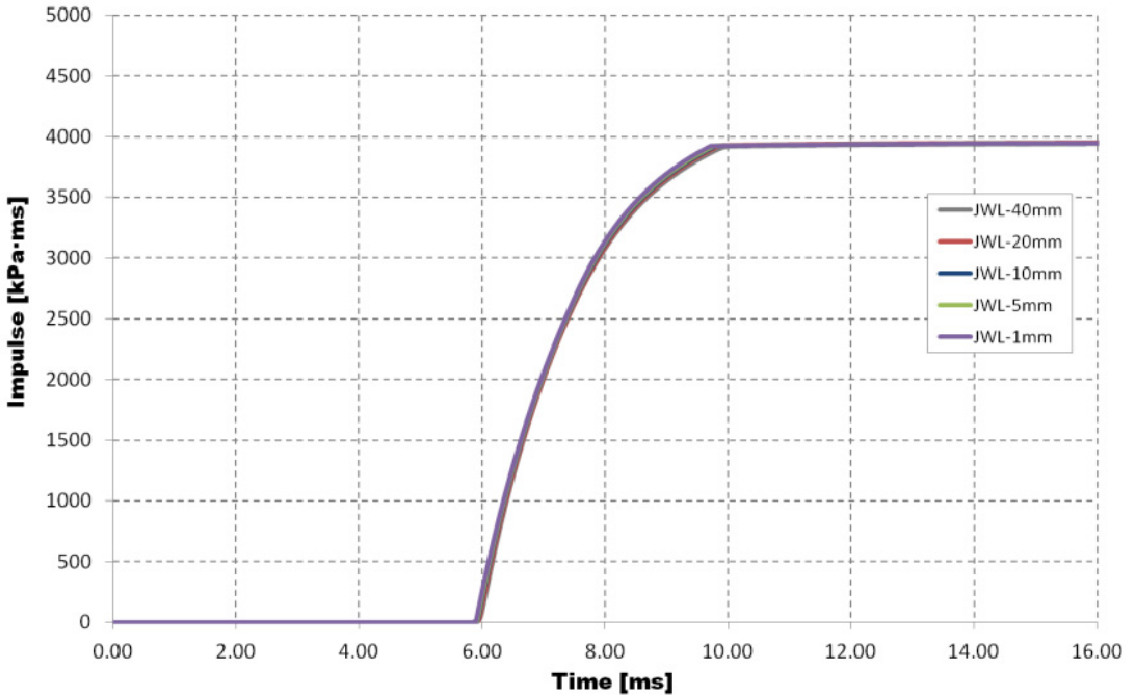

Figure 41: Impulse-time history at 16.03m from charge center for different cell sizes.

From the above diagrams it is shown that a very fine meshing is not necessary if the scaled distance of the point of interest is not small. By using very small cell sizes the computation time rises considerably, while the accuracy of the results is not affected to a

big extent. This means that it would be profitable to define the appropriate cell size, which depends on both the distance from the detonation center and the charge, so as to have accurate results in a relatively short computation time. Some researchers [10] propose the division of the scaled distance range in intervals, each one containing cells of constant size. Even though the procedure is simple it should be used with care, as big changes in the size from one cell to the next should be avoided as they might lead to numerical instabilities.

Based on the above analyses, it appears that a progressive increase in the size of the cell elements, depending on their scaled distance, would be more appropriate. The first cell element at the charge/free-air interface should have a size of 1mm since from the previous section it was found that this yielded good results when used for simulating both the solid charge and the surrounding air. The size of each cell element in the outwards direction could next be calculated through Equation (4),

$$CS = 18.87 \cdot Z, \quad Z \geq 0.053 \tag{4}$$

where, CS is the cell size [mm],

Z is the scaled distance [m/kg$^{1/3}$].

Inside the charge a cell size equal to 1mm should be used as it provides accurate results as will be shown in the nest section. Equation (4) has been applied and tested to several 1D models for various distances and charges. It ensures good convergence of the results (to within 15% maximum difference) to those of a model constructed entirely of cells with 1mm size. Figures 42-47 show a comparison of 1D models that have a fixed cell size of 1mm and others that follow an increasing cell size, as prescribed by Equation (4). The diagrams show the relative overpressure, density and impulse for the case of an 18000kg charge, similar to the one examined in the previous section. Results are presented for distances from the charge center of 1.51m, 3.29m, 3.56m, 6.17m, 16.03 and 20.00m that correspond to expansion factors equal to 1.1, 2.4, 2.6, 4.5, 11.7 and 14.6 respectively (or, equivalently, to scaled distances of 0.058, 0.125, 0.136, 0.235, 0.612 and 0.763m/kg$^{1/3}$). From the following diagrams it appears that the comparison is overall good. It is noticed that appreciable difference between the two approaches is for points near the charge/free-air interface (Z<0.10m/kg$^{1/3}$), whereas for larger distances the corresponding curves are much closer. On the other hand, considerable savings in computation time has been achieved. For instance, for the point at distance 16.03m (expansion factor of 14.4, or, scaled distance of 0.763763m/kg$^{1/3}$) the cell size would be 1mm at the charge/free-air interface and 14.45mm at 16.03m away. The run time of this model in EUROPLEXUS is 24.5 times smaller than that of the model with the constant 1mm cell size.

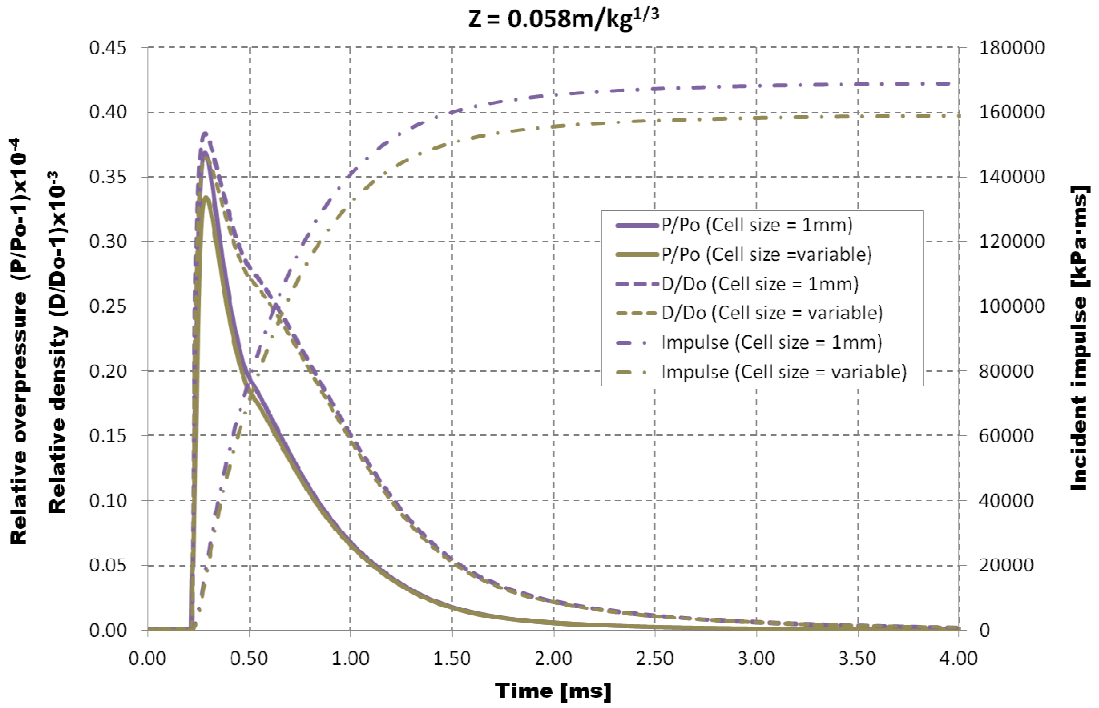

Figure 42: Comparison of blast parameters at 1.51m from charge center for fixed and variable cell size.

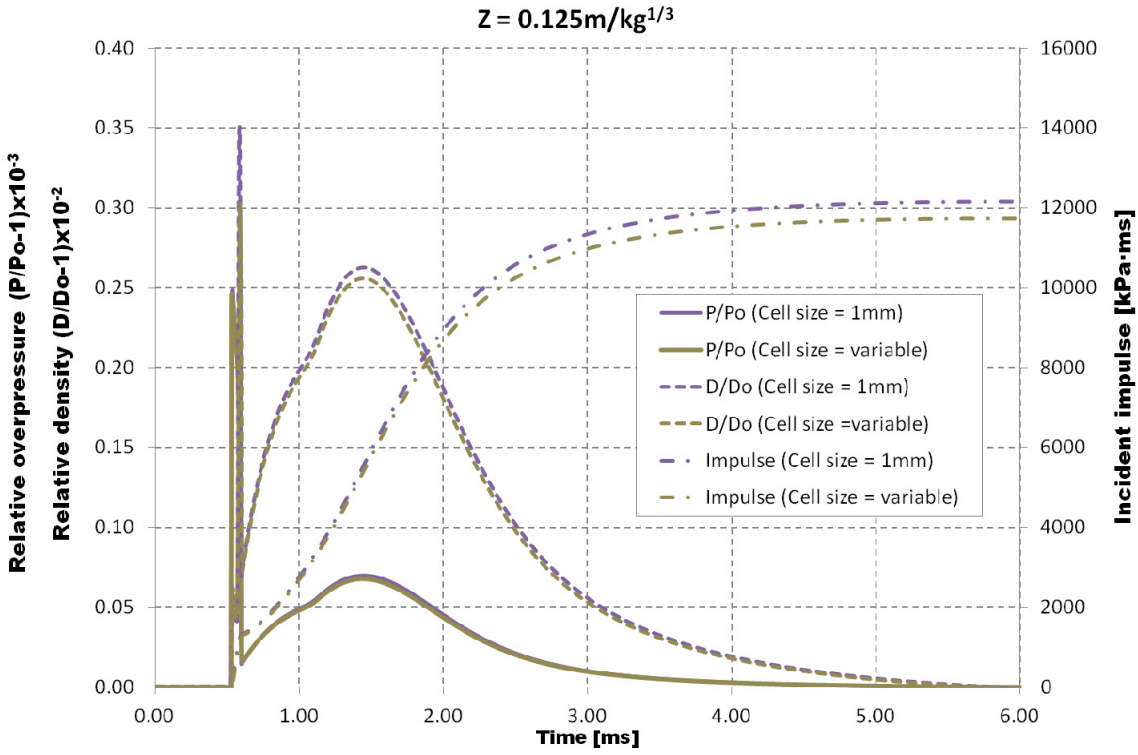

Figure 43: Comparison of blast parameters at 3.29m from charge center for fixed and variable cell size.

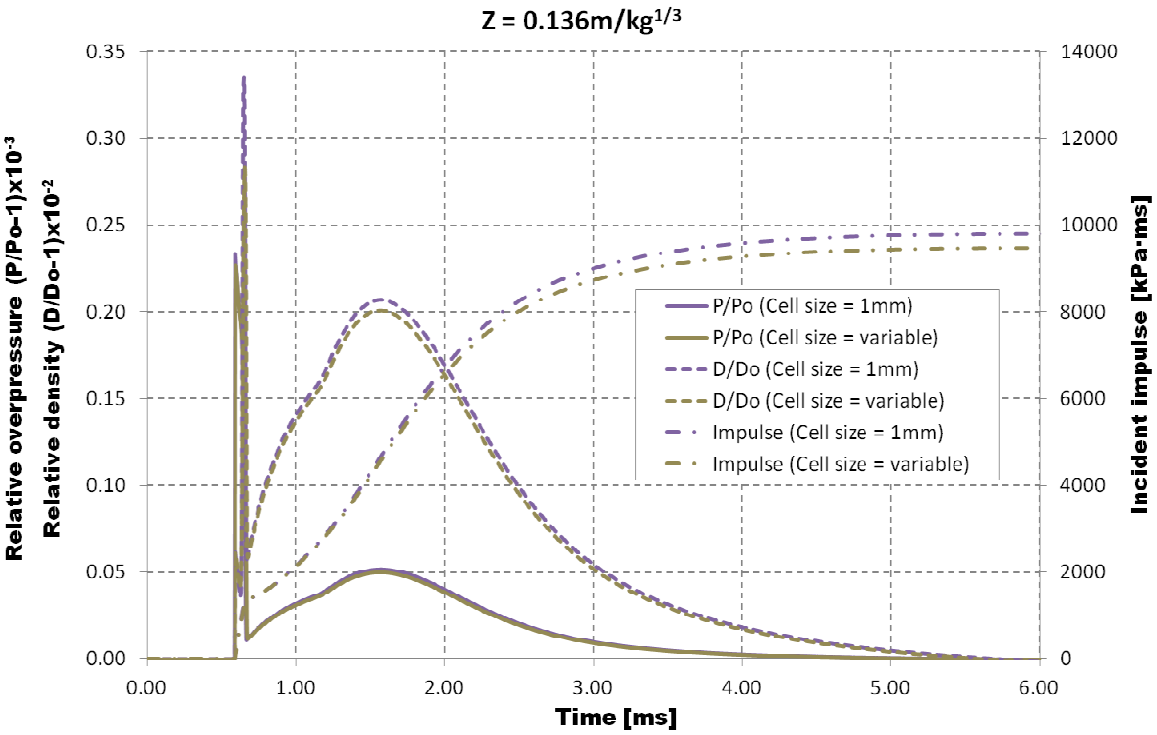

Figure 44: Comparison of blast parameters at 3.56m from charge center for fixed and variable cell size.

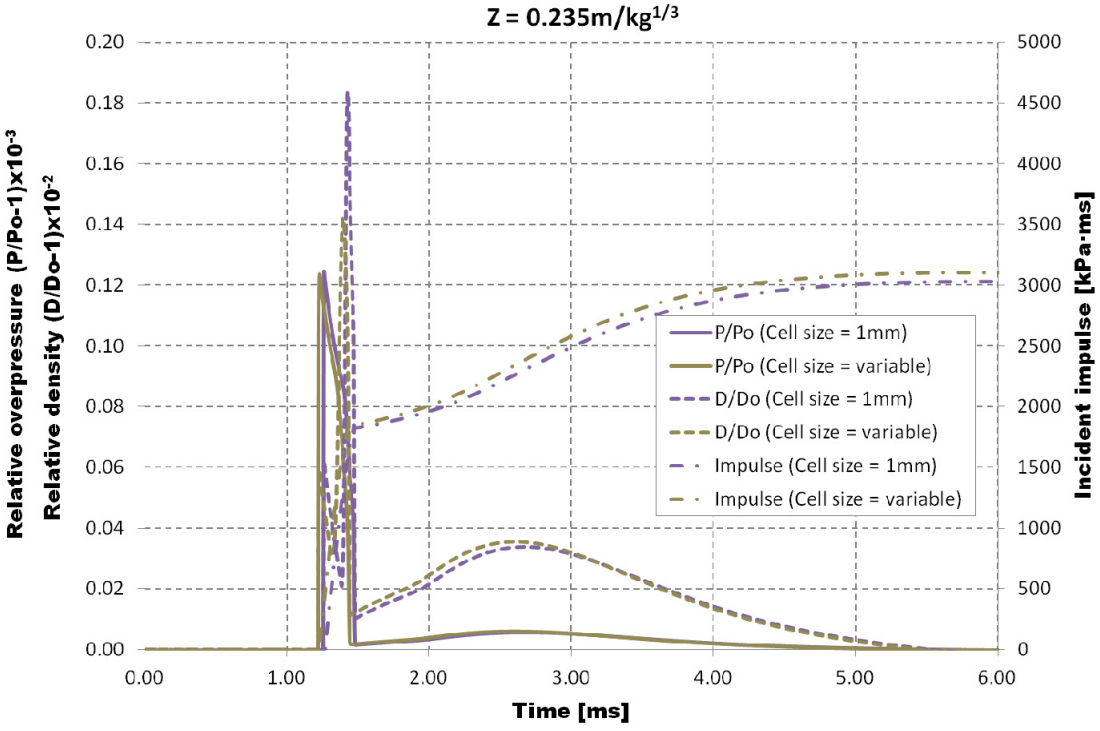

Figure 45: Comparison of blast parameters at 6.17m from charge center for fixed and variable cell size.

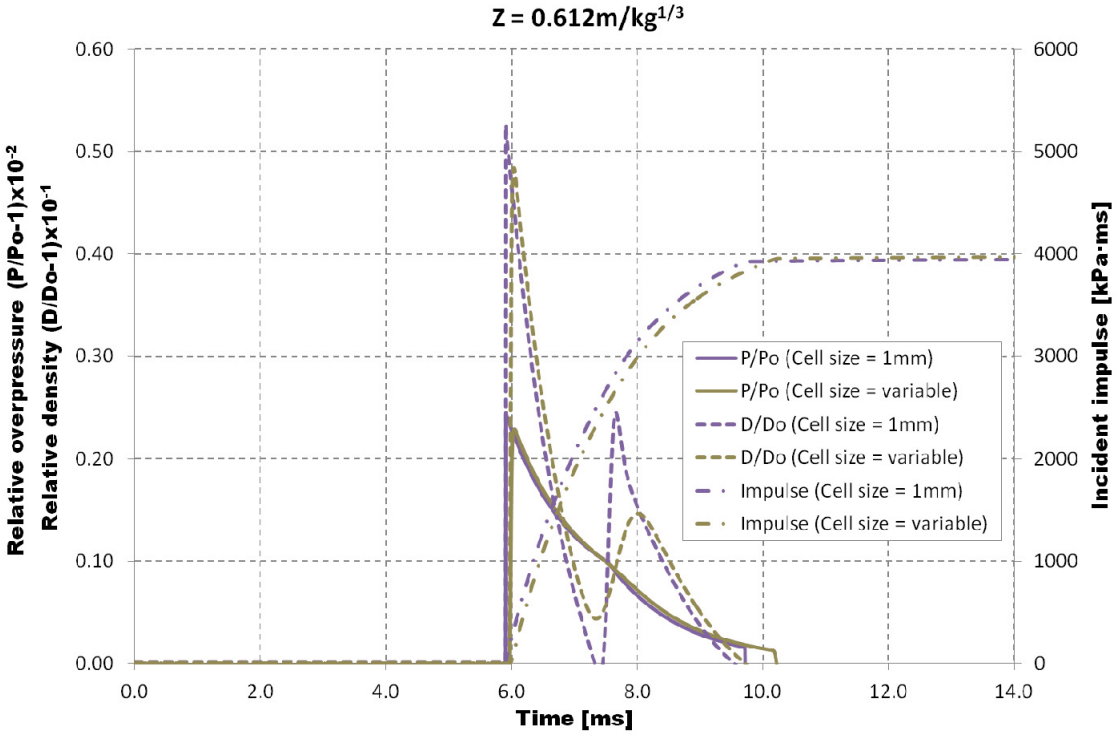

Figure 46: Comparison of blast parameters at 16.03m from charge center for fixed and variable cell size.

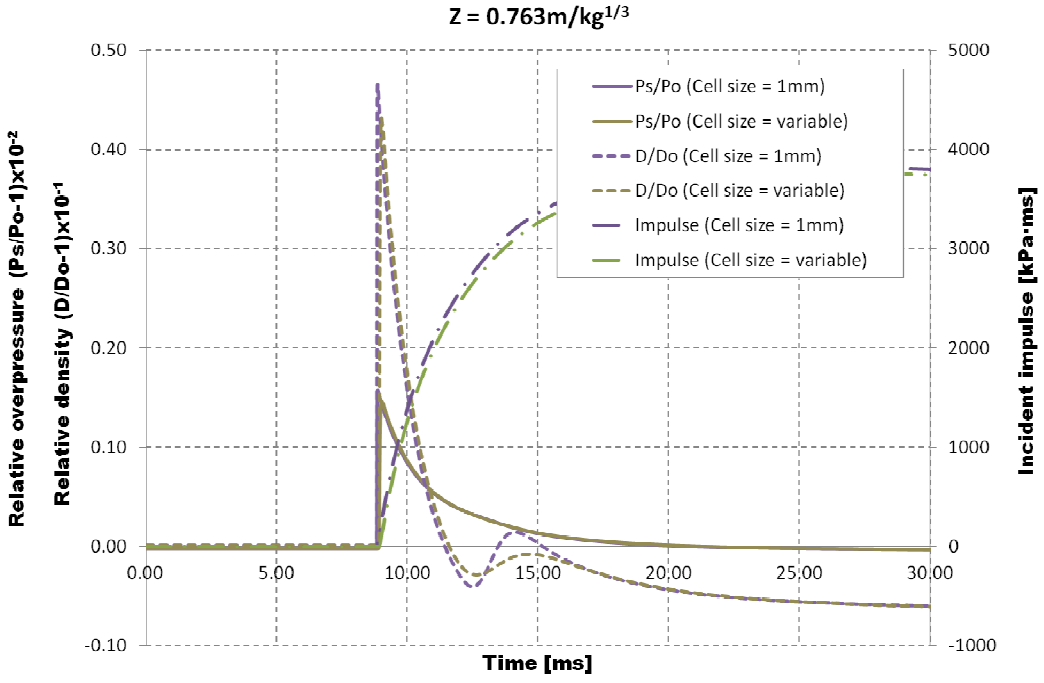

Figure 47: Comparison of blast parameters at 20.00m from charge center for fixed and variable cell size.

The presented diagrams provide confidence with the use of EUROPLEXUS, as the analyses results are close to those presented by Needham. The difference between some of the values can be attributed to many different factors, such as the solvers, the equations of state, the slightly different TNT density value used by Needham, and the numerical models. Cell size has a substantial effect on the calculation of overpressure, density and impulse values, but its influence on the resulting values becomes smaller as the distance from the detonation center increases.

The results from the software code EUROPLEXUS (EPX) can also be compared to the results provided by similar programs. In 2013 Browning [18] used the programs LS-DYNA [19] and CTH [20] to simulate an explosion of 3629kg (8000lb) of TNT, that has a charge radius of 0.81m, with a two-dimensional finite element model. Incident peak overpressure, incident impulse and arrival time results are provided at scaled distances of 1.19, 1.59 and 1.98 m/kg$^{1/3}$ (3, 4 and 5 ft/lb$^{1/3}$) for cell sizes of 25.4, 50.8 and 76.2 mm (1, 2 and 3 in.). Browning [18] used the JWL equation of state for the TNT charge and the relevant parameters are identical to the ones in Table 1. For the surrounding air an ideal gas law was utilized. The simulations were also simulated by Shin [21] in an one-dimensional analysis, while exploring the simulation capabilities of the explicit code AUTODYN.

In Tables 2 and 3 a comparison of the incident peak overpressure and impulse values from these software programs is performed. The results show that all computer codes calculate similar peak incident overpressure values for all of the examined scaled distances. All of them, including EUROPLEXUS, give slightly higher peak overpressure values if a finer mesh is used (except near the charge/free-air interface). The same conclusions are drawn for the incident impulse values, which are usually more important for the design practice since they are used for the dimensioning of structural elements. EUROPLEXUS predicts similar impulse values irrespective of the cell size used during the calculation, so a coarser mesh may be used for analyzing the effect of a blast on structures whose design is mainly governed by the created impulse. From the four different programs, AUTODYN shows the biggest difference among models with different cell sizes. The variations in the results from these programs can be attributed to the different techniques and solvers used in each software when calculating the propagation of the blast wave. Figures 48-50 show the incident overpressure-time history for the different cell sizes as calculated by EUROPLEXUS and Figures 51-53 show the relative incident impulse values.

Table 2. Incident overpressure values [kPa] as calculated from the different software tools.

Z[m/kg$^{1/3}$]	Autodyn	LS-Dyna	CTH	EPX
	Incident overpressures [kPa]			
	Cell size=25.4mm			
1.199	648.8	594.33	550.89	591.19
1.599	321.3	295.1	268.9	264.78
1.989	191.67	177.88	159.96	153.20
	Cell size=50.8mm			
1.199	608.81	570.2	546.75	574.39
1.599	305.44	287.51	262	251.26
1.989	184.09	174.44	155.82	145.04
	Cell size=76.2mm			
1.199	577.78	551.58	525.38	571.97
1.599	293.03	280.62	258.55	243.64
1.989	177.88	171.68	154.44	141.15

Table 3. Incident impulse values as calculated from the different software tools.

Z[m/kg$^{1/3}$]	Autodyn	LS-Dyna	CTH	EPX
	Incident impulse [kPa·ms]			
	Cell size=25.4mm			
1.199	1820.22	1627.16	1482.37	1625.33
1.599	1420.32	1316.9	1206.58	1299.18
1.989	1213.48	1130.74	1041.11	1122.71
	Cell size=50.8mm			
1.199	1785.74	1627.16	1475.48	1631.76
1.599	1399.64	1316.90	1206.58	1305.97
1.989	1199.69	1130.74	1041.11	1127.56
	Cell size=76.2mm			
1.199	1758.16	1634.06	1475.48	1665.77
1.599	1385.85	1316.90	1199.69	1325.11
1.989	1185.90	1130.74	1041.11	1146.96

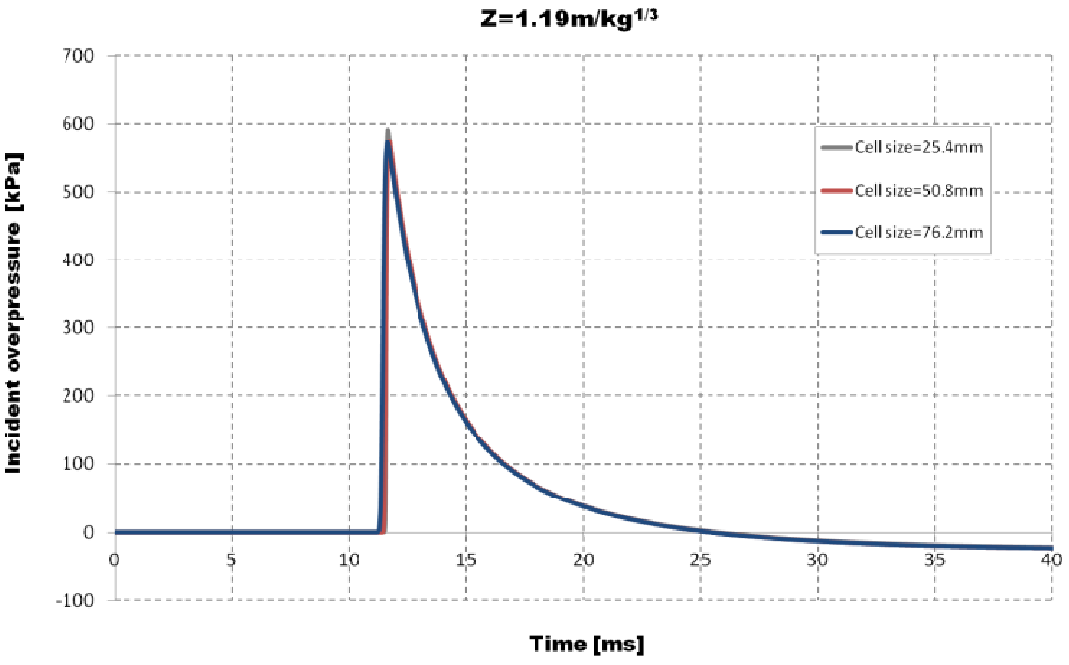

Figure 48: Incident overpressure time history at 18.30m from charge center.

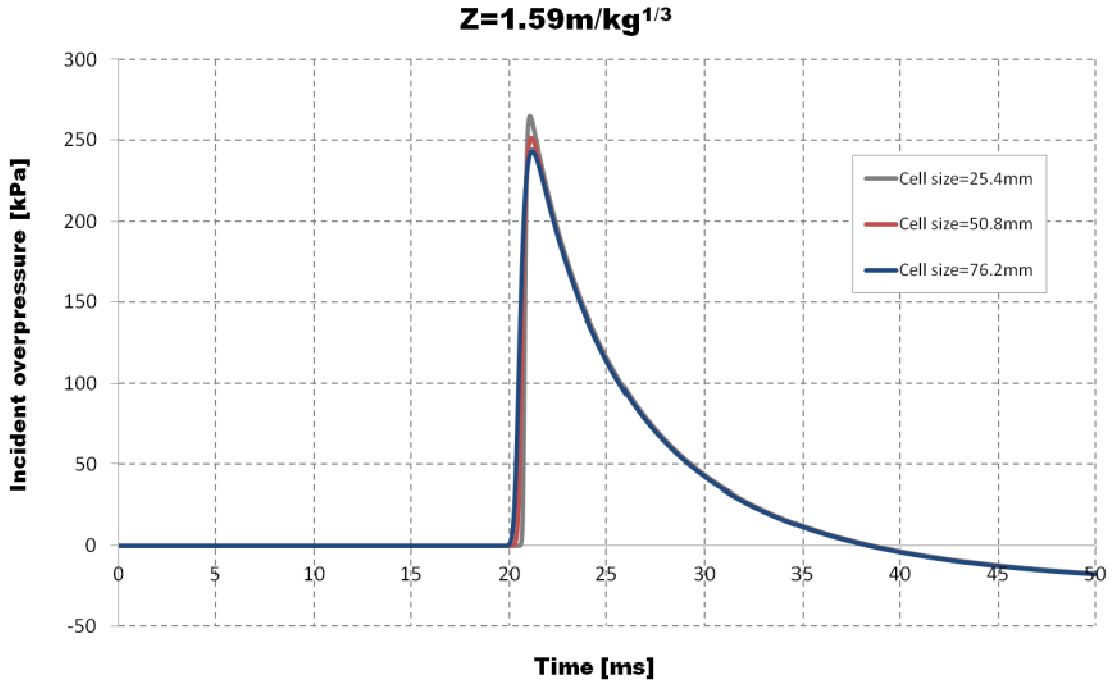

Figure 49: Incident overpressure time history at 24.40m from charge center.

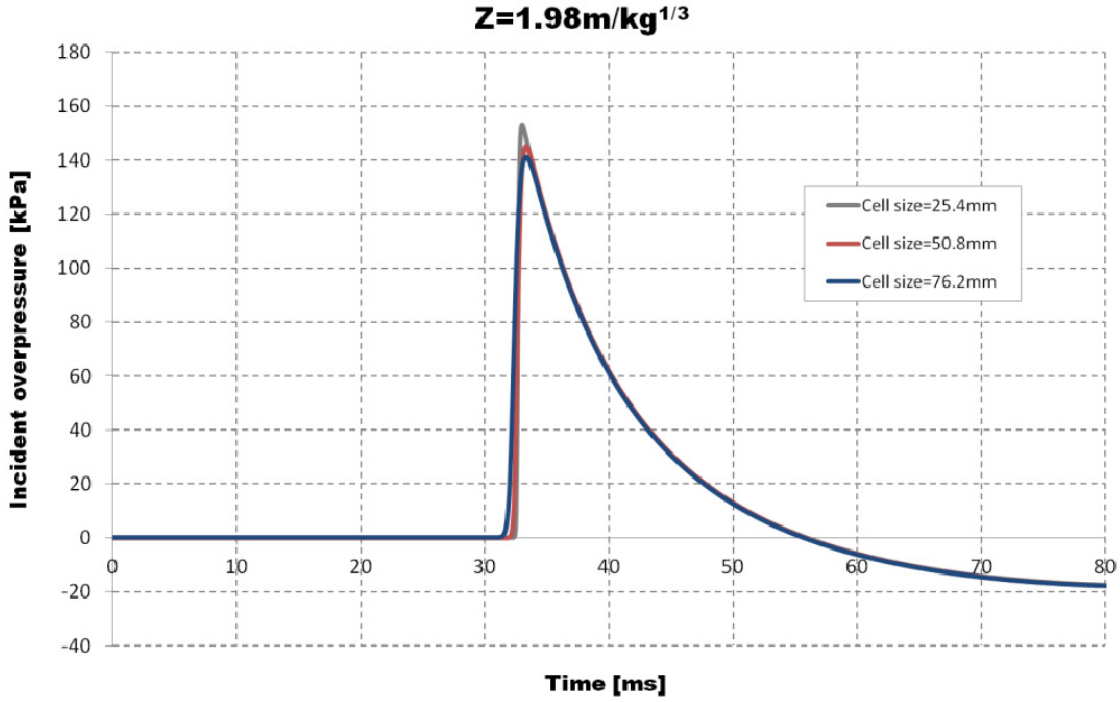

Figure 50: Incident overpressure time history at 30.50m from charge center.

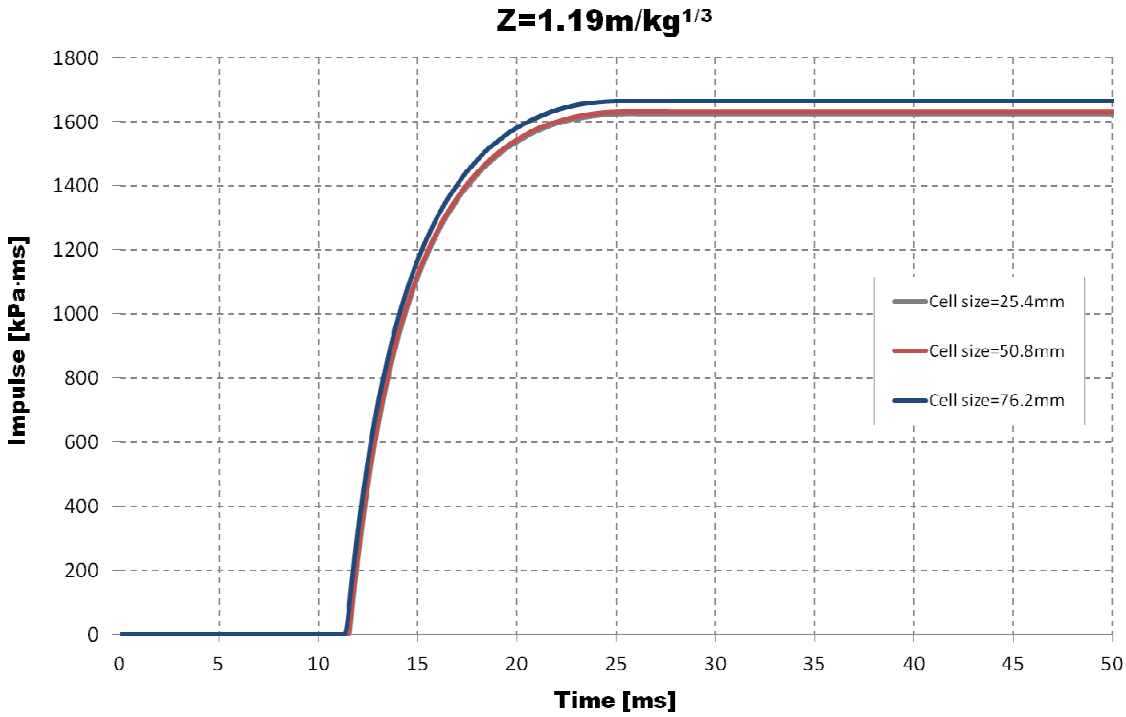

Figure 51: Incident impulse time history at 18.30m from charge center.

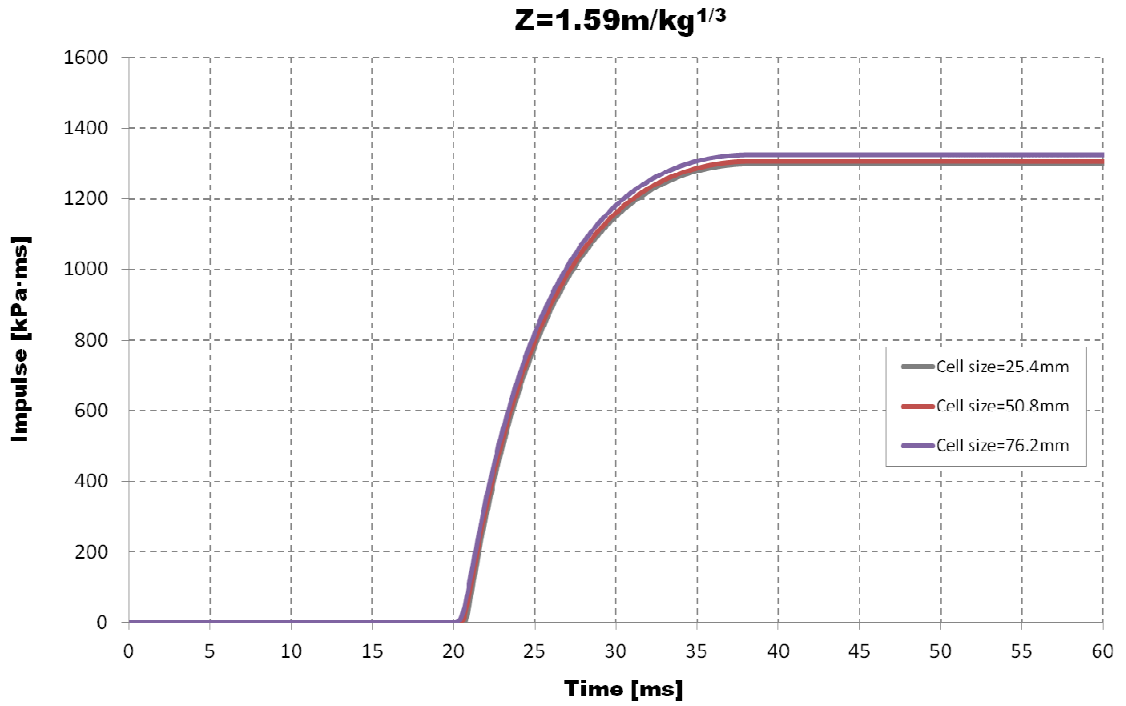

Figure 52: Incident impulse time history at 24.40m from charge center.

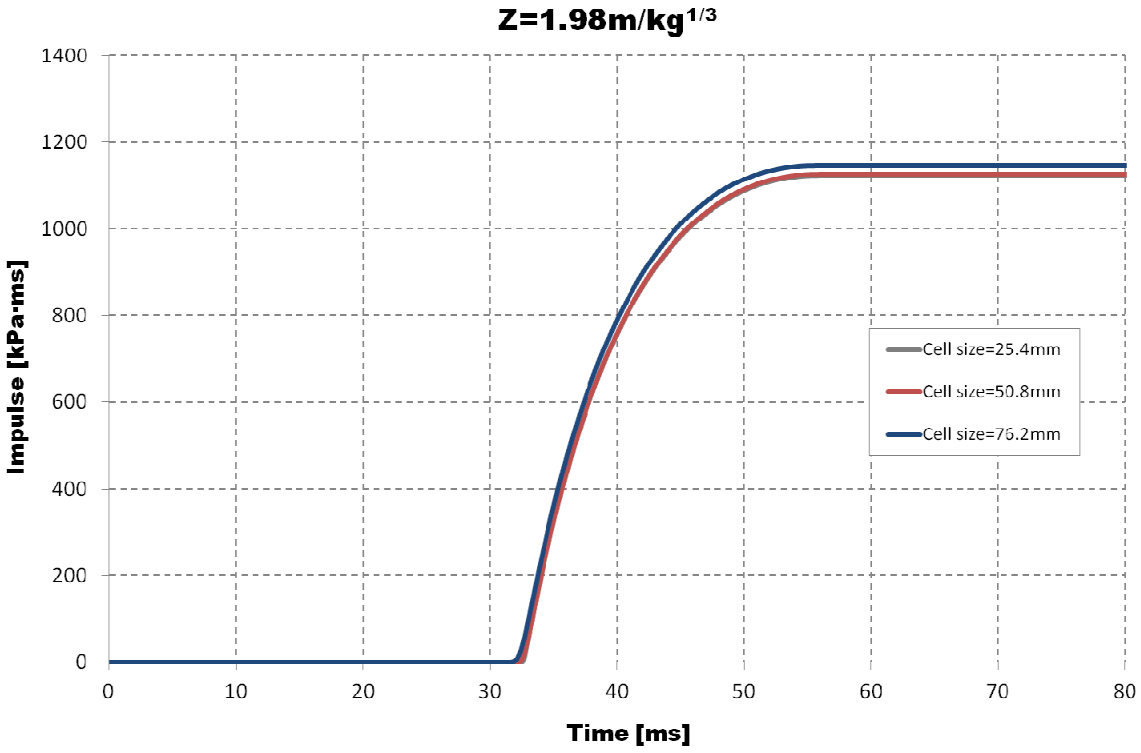

Figure 53: Incident impulse time history at 30.50m from charge center.

3.3 Mesh sensitivity at close range

The response of a structural element under an extreme dynamic load, such as an explosion, depends greatly on the pressure-time history. There are several technical manuals available that contain empirical or semi-empirical relationships and diagrams that allow the calculation of the main blast parameters. The most used ones appear to be special publications from the USA such as the Army Technical Manual 5-1300 [1] and the technical report of Kingery and Bulmash [3]. It has been found from various researchers that the proposed blast parameter values from these manuals are quite accurate for explosions at medium and large scaled distances. But, if the point of interest lies very close to the charge center, the derived values from these manuals may vary considerably from the actual, experimental ones.

Shin [10] in his paper noticed that there is a big difference between the peak overpressure values at the face of an explosive calculated through the Chapman-Jouguet equations and the Kingery-Bulmash diagrams. When the Kingery-Bulmash diagrams were first created, the available test results at small scaled distances were limited and of ambiguous quality, which was also noted by the authors. This means that these diagrams should be used with caution for scaled distances $Z<0.4m/kg^{1/3}$, as they may underestimate the resulting overpressure and impulse values.

To bridge this gap of reliable data, simulation techniques have been proposed and attempted by several researchers. The changes in overpressure values near the face of the charge are simulated in the current work by using the computer software code EUROPLEXUS. In this section a mesh sensitivity analysis is performed at very small scaled distances. Three different TNT spherical charges are examined, equal to 23kg, 960kg and 18000kg. These masses were chosen in order to be in accordance with the ones used by Shin [10]. If the TNT density is equal to $1630kg/m^3$, the charge radius of

each explosive would be equal to 0.149m, 0.52m and 1.37m, respectively. The Jones-Wilkins-Lee equation of state is used for both the explosive products and the surrounding air with the parameters described in Table 1.

The diagrams that follow show the incident overpressure distribution near the face of the charge. It has already been noted by other researchers that the blast characteristics change considerably at the charge/free-air interface. In order to examine the influence of the cell size on the calculated incident peak overpressure, one-dimensional models with element sizes equal to 0.05mm, 0.1mm, 1mm, 5mm, 10mm, 20mm and 40mm are tested for the above charges.

According to Baker [6], the Chapman-Jouguet detonation pressure of TNT is equal to 21GPa for a packing density of 1630kg/m^3. Figures 54-56 show that, generally, the finer the mesh of the numerical model, the closer the detonation pressure is to that reported by Baker. As expected, the smaller the mass of the explosive, the smaller is the cell size that should be utilized for achieving a required level of accuracy. Figures 57-59 are magnified diagrams of the overpressure values just outside the charge radius of each explosive, which is translated to a scaled distance range equal to 0.053m/kg$^{1/3}$<Z<0.07m/kg$^{1/3}$. The diagrams show that the overpressure values for scaled distances over 0.07m/kg$^{1/3}$ practically coincide for all of the examined charge weights, irrespective of the cell size used during the simulation.

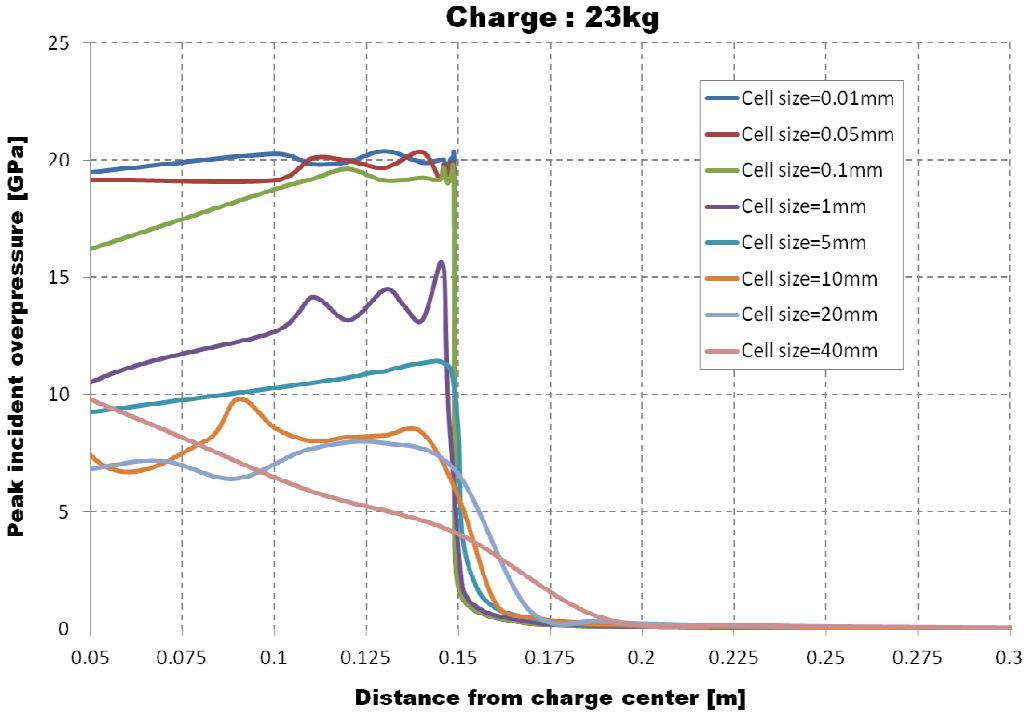

Figure 54: Incident overpressure distribution when the shock front reaches the face of the 23kg charge.

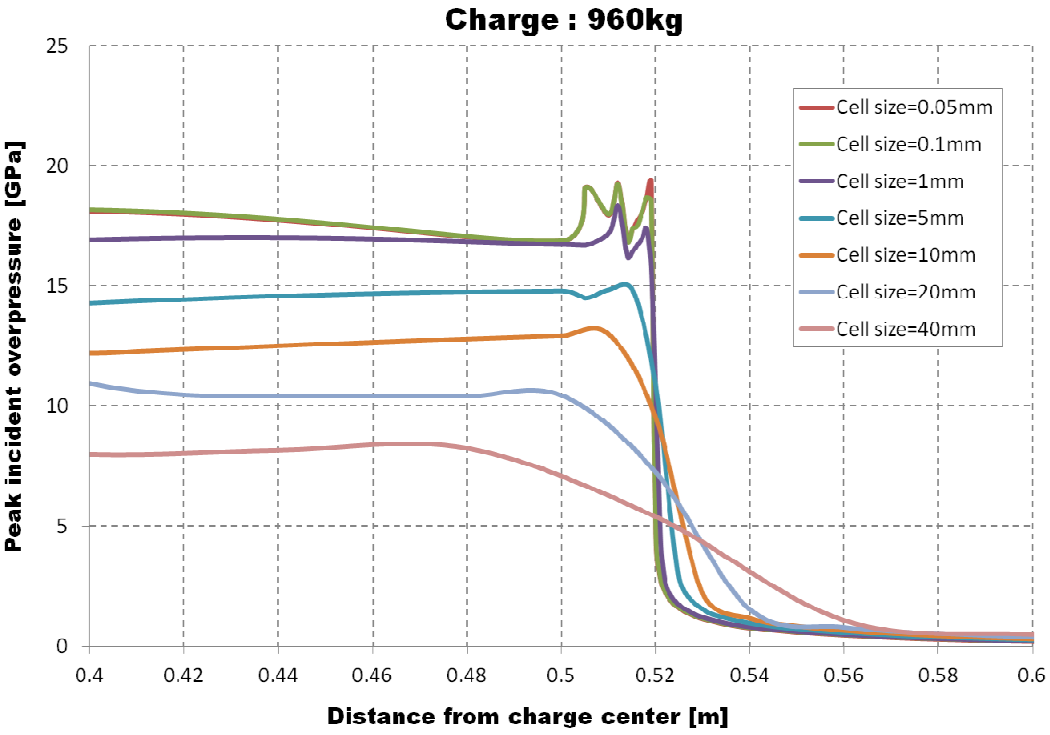

Figure 55: Incident overpressure distribution when the shock front reaches the face of the 960kg charge.

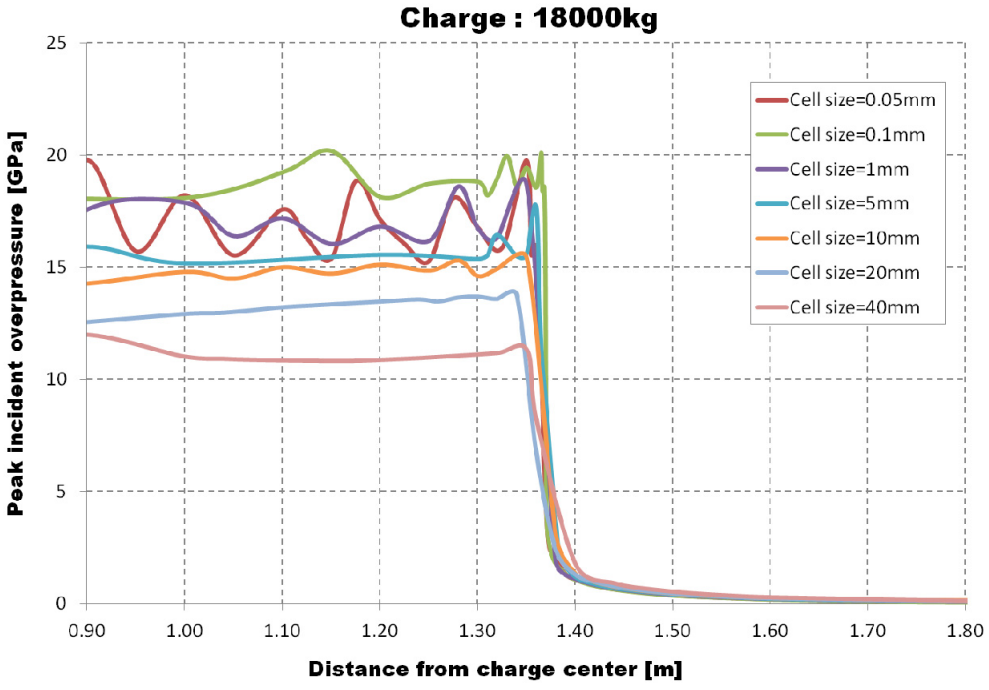

Figure 56: Incident overpressure distribution when the shock front reaches the face of the 18000kg charge.

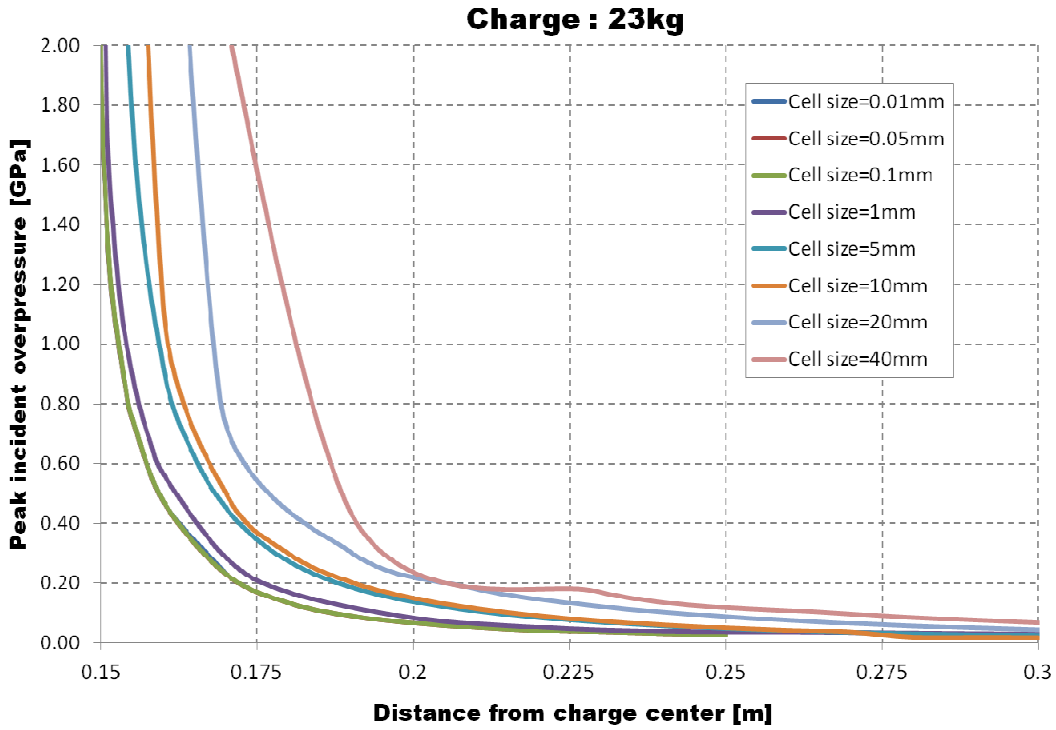

Figure 57: Zoomed-in incident overpressure curves for a 23kg charge for $0.053m/kg^{1/3}<Z<0.10m/kg^{1/3}$.

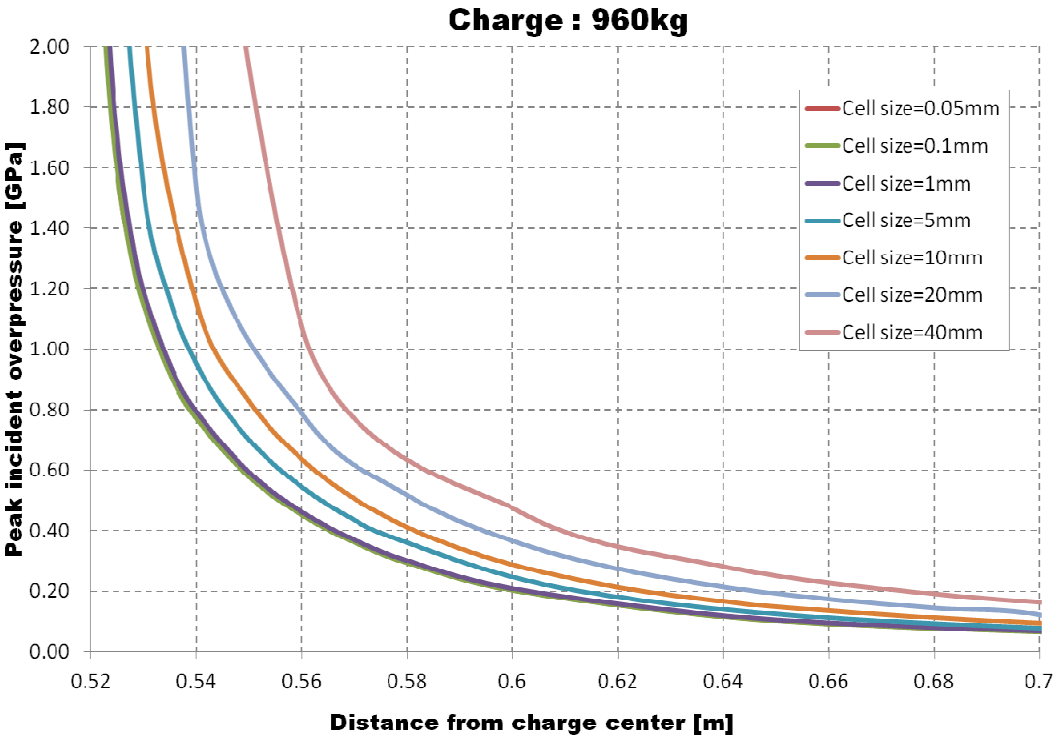

Figure 58: Zoomed-in incident overpressure curves for a 960kg charge for $0.053m/kg^{1/3}<Z<0.10m/kg^{1/3}$.

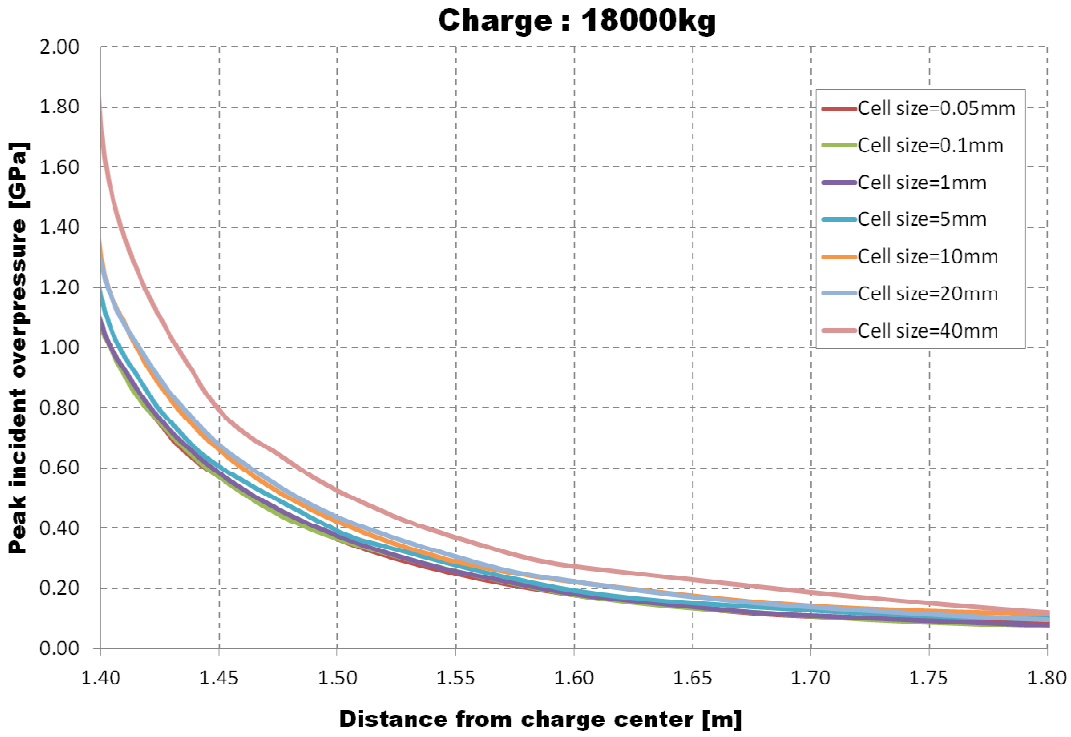

Figure *59*: Zoomed-in incident overpressure curves for a 18000kg charge for $0.053m/kg^{1/3}<Z<0.10m/kg^{1/3}$.

3.4 Incident blast wave parameter

3.4.1 Comparison to Kingery-Bulmash diagrams

One of the most widely used manuals for the calculation of blast parameters is the Kingery-Bulmash technical report [3], which has been included in the UFC 3-340-02 [2] manual. Figure 60 shows the proposed blast parameters for the case of a spherical blast wave. The available diagrams allow the calculation of the positive overpressure, the positive impulse, the shock front velocity, the arrival time, the wavelength and the positive phase duration. These diagrams were based on a large database of experiments, such as [22] and [23], the majority of which were performed at large scaled distances. The limited available experimental data at small scaled distances has been also underlined by Kingery-Bulmash in their report.

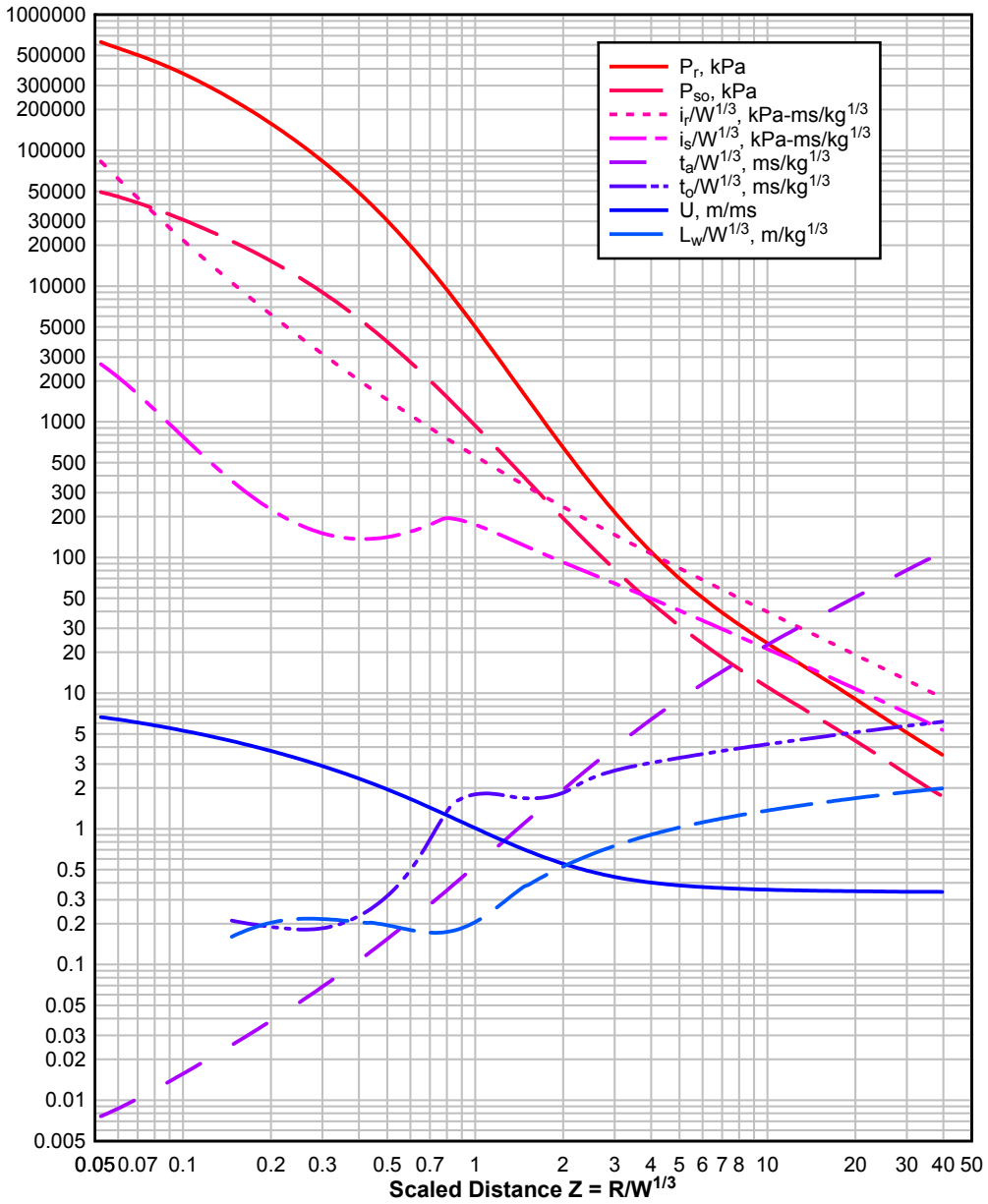

Figure 60: Parameters of positive phase of shock spherical wave of TNT charges from free-air bursts [8].

As has already been shown in [10], there is a large difference between the proposed peak overpressure and impulse values at small scaled distances between Figure 60 and the diagrams calculated through simulations with a 1D analysis. At the current section the results from several EUROPLEXUS simulations are compared to the Kingery-Bulmash proposals. It is reminded that for the analyses with EUROPLEXUS in an 1D formulation a Jones-Wilkins-Lee (JWL) Equation of State is used for both the charge and the surrounding air in order to avoid the use of complicated multi-material models, and the parameters of the EOS used are those of Table 1.

Figure 61 shows in a double-logarithmic diagram the positive phase peak overpressure values as proposed from the UFC 3-340-02 [2] technical manual and as calculated through the analysis with the current numerical models. The results from three different models are included, each corresponding to a different charge. In detail, three TNT charges of 23kg, 960kg and 18000kg were used, each with a packing density of

1630kg/m^3. One common cell size (1mm) over the whole scaled distance range was used for the analyses, but a variable size could have been used (increasing with the distance from the detonation center) without affecting the accuracy of the results and having the advantage of reduced computation cost. The calculated overpressure values from all three models practically coincide for the whole scaled distance range. For scaled distances greater than 0.1m/kg$^{1/3}$ they are very close to the Kingery-Bulmash proposed values, but they are much larger for smaller ranges of scaled distance.

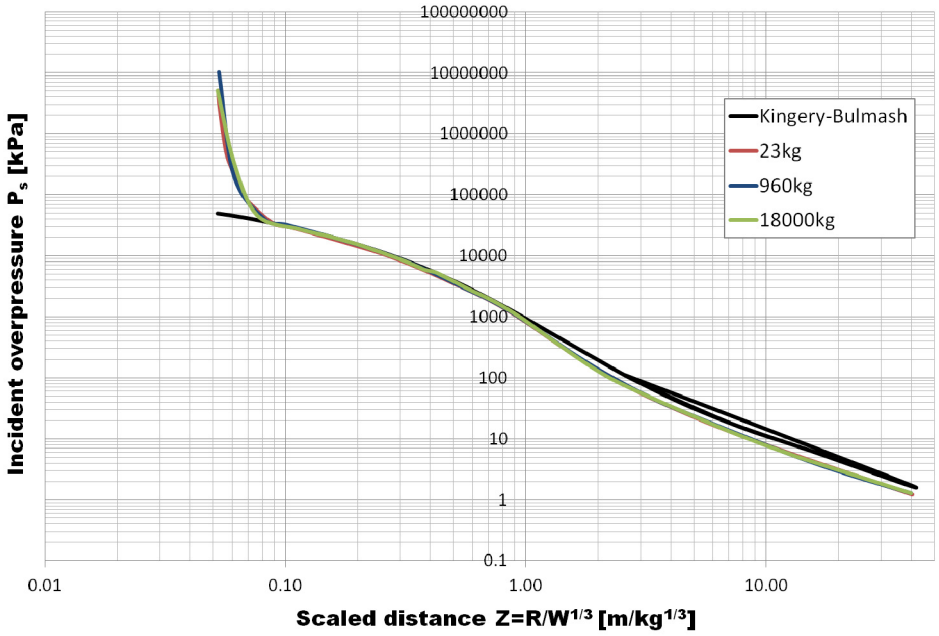

Figure 61: Comparison of peak positive phase overpressure versus scaled distance for different TNT charges for free-air bursts (spherical waves).

Figure 62 is a logarithmic diagram of the positive impulse of a spherical blast wave from a free-air burst as proposed by the Kingery-Bulmash technical manual and as calculated through the numerical analyses described. As seen from the figure, the positive impulse values from the EUROPLEXUS calculations are smaller than the Kingery-Bulmash curve for large and medium scaled distance values. But, similar to Figure 61, near the charge/free-air interface (scaled distance Z<0.1 m/kg$^{1/3}$), the analyses values are much larger than the Kingery-Bulmash predictions.

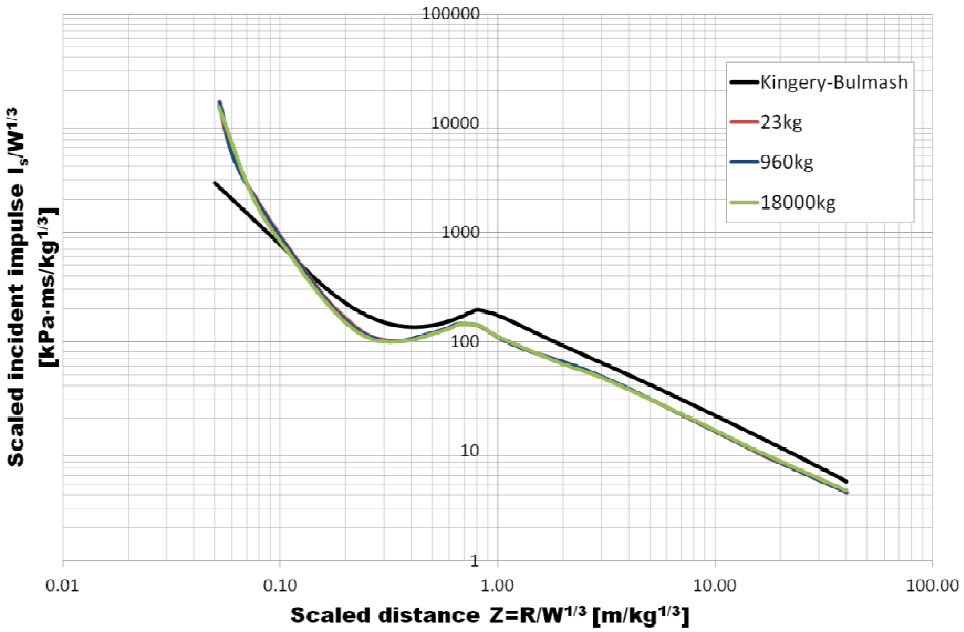

Figure 62: Comparison of positive phase impulse curves versus scaled distance for different TNT charges for free-air bursts (spherical waves).

Figure 63 shows the logarithmic diagram of the arrival time of the shock front for the case of a free-air burst. As can be observed, the arrival times as calculated from the explicit code do not differ much from the Kingery-Bulmash curve over the whole scaled distance range.

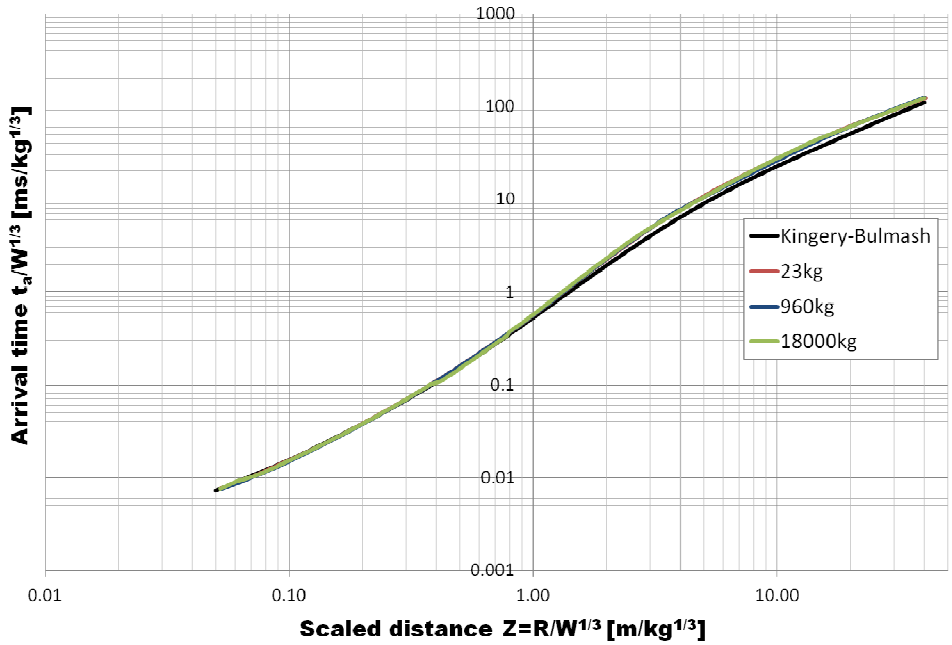

Figure 63: Comparison of arrival time versus scaled distance for different TNT charges for free-air bursts (spherical waves).

Figures 64 and 65, respectively, show the relative difference of the peak overpressure and impulse of a spherical wave, in relation to the values recommended by Kingery-Bulmash as a function of scaled distance. Equation (5) describes the relative difference for the positive overpressure values, where $P_{s.epx}$ is the peak overpressure as calculated by EUROPLEXUS and $P_{s.KB}$ is the proposed value from the Kingery-Bulmash manual, which is considered to be the reference one. For the curves in Figure 65, the overpressure terms of Equation (5) are substituted with the incident impulse values. From both figures we can observe that the biggest relative differences are localized at very small scaled distance values ($Z<0.1$ m/kg$^{1/3}$), i.e. for close-in detonations. The relative difference for the rest of the scaled distance range is smaller, which shows the big uncertainties that are included at the calculation of blast parameters near the charge/free-air interface.

$$RD_{P_s} = \frac{|P_{s.epx} - P_{s.KB}|}{P_{s.King}} \quad (5)$$

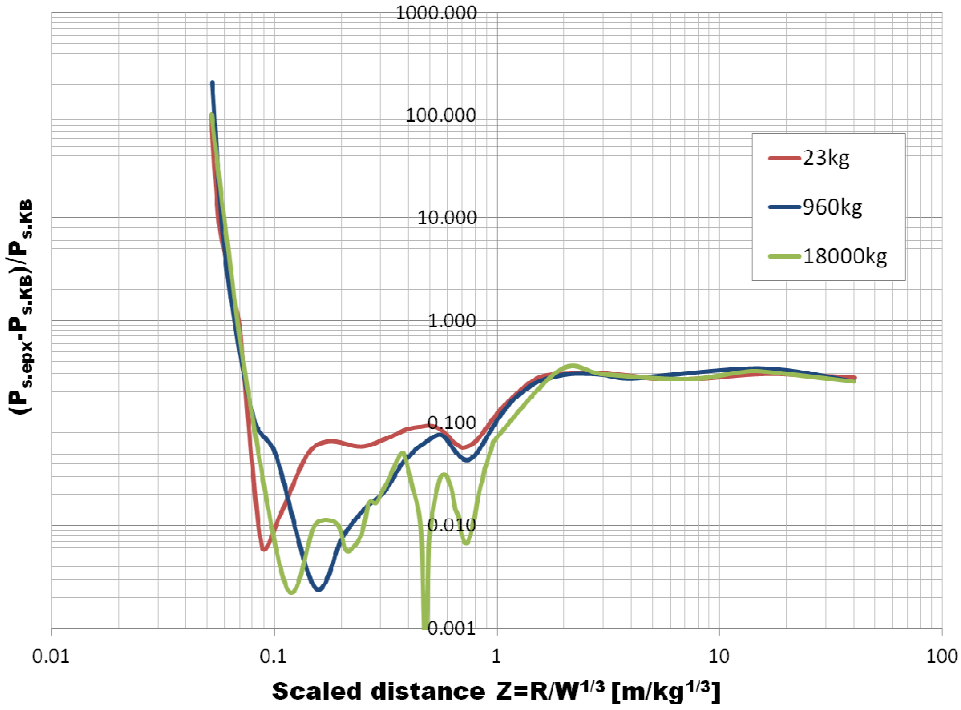

Figure 64: Relative difference of peak positive overpressure in relation to the one of Kingery-Bulmash for free air bursts (spherical waves).

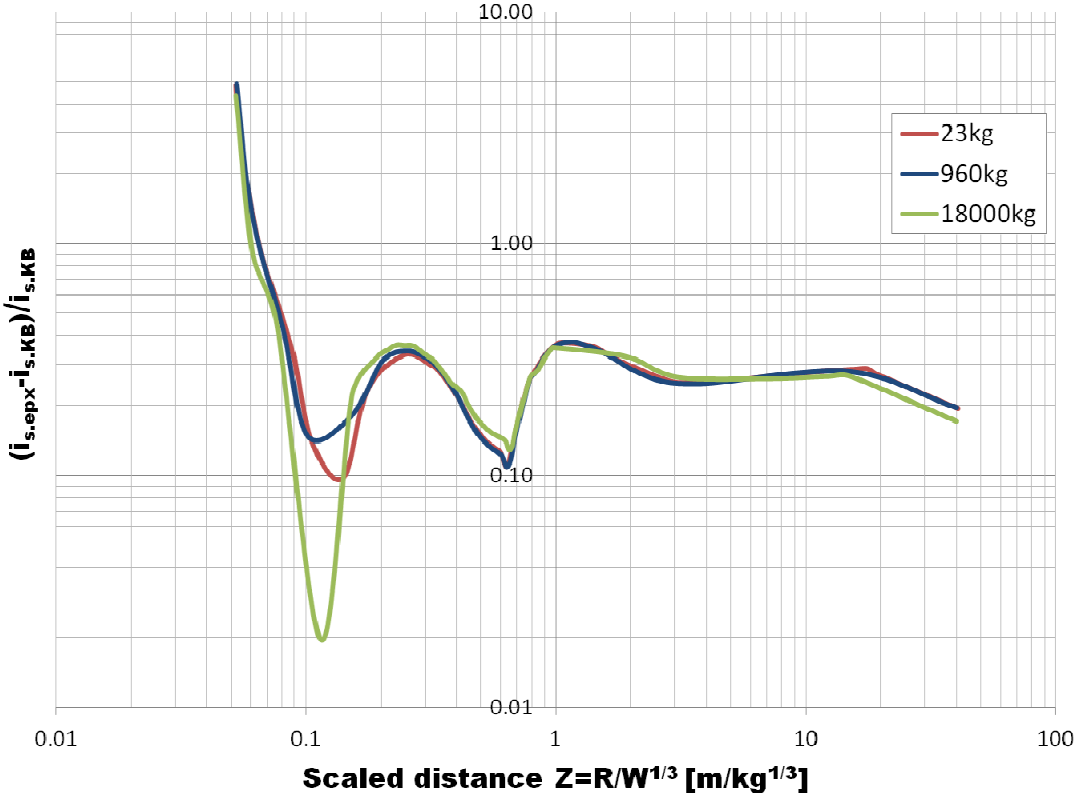

Figure 65: Relative difference of positive impulse in relation to the one of Kingery-Bulmash for free air bursts (spherical waves).

3.4.2 Updated incident parameters polynomial equations

As has already been pointed out in Figure 61 and Figure 62, the peak positive overpressure and positive impulse values for a free-air burst proposed from Kingery-Bulmash technical manual do not agree well with the ones calculated from the EUROPLEXUS explicit program, especially for small scaled distances. For scaled distance values smaller than 0.10m/kg$^{1/3}$ the calculated values are much larger than the ones proposed in the manual. The authors of [3] highlighted the fact that at the time of its publication there were only a few available experimental data at small scaled distances, so the proposed values at this range should only be treated as a suggestion to the order of magnitude of the parameter to be expected.

As an addition to the polynomial equations for the positive peak overpressure proposed by Kingery-Bulmash [3], which cover a scaled distance range of 0.053-40m/kg$^{1/3}$, different relationships are proposed below for the scaled distance ranges $0.053 \leq Z \leq 0.4$m/kg$^{1/3}$ and $0.40 < Z \leq 40.0$m/kg$^{1/3}$ in order to take into account the findings of Figure 61. In this figure the values of the peak incident overpressures are larger even by a factor of 10 in relation to those of Kingery-Bulmash, especially near the face of the charge. For the scaled distance range $0.4 < Z \leq 40$m/kg$^{1/3}$, since the differences between the Kingery-Bulmash proposals and the EUROPLEXUS calculations are smaller, the polynomial equation as included in the Kingery-Bulmash technical manual [3] could be used instead. The scaled distance range $0.053 \leq Z \leq 40.0$m/kg$^{1/3}$ is thus divided in two regions, each characterized by a different equation, so that the designer can decide to apply the modified equation only partially for small scaled distances where the differences in blast parameters are greater.

For the incident positive impulse the largest differences between the Kingery-Bulmash predictions and the EUROPLEXUS calculations are noted at scaled distances smaller than 0.10m/kg$^{1/3}$. At this range the calculated impulse values from the explicit finite element code are much larger than the Kingery-Bulmash proposals. For the rest of the scaled distance range the difference of the impulse values are between 10% and 40%, with EUROPLEXUS predicting smaller values. The positive impulse values as predicted by the finite element program are presented in the form of polynomials again for scaled distance ranges of 0.053≤Z≤0.4m/kg$^{1/3}$ and 0.4<Z≤40m/kg$^{1/3}$.

The polynomial functions that are used for the calculation of the incident positive peak overpressure and impulse are similar to the ones proposed by Kingery-Bulmash in [3]. The form of these functions is shown in Equations (6) and (7)

$$Y = C_0 + C_1 U + C_2 U^2 + \cdots + C_N U^N \quad (6)$$

$$U = K_0 + K_1 T \quad (7)$$

where Y is the common (base 10) logarithm of the blast parameter (in this case positive peak overpressure, P_s or positive impulse, i_s) and T=log(Z) is the common logarithm of the scaled distance and N is the polynomial's order. The rest of the constants (K_0, K_1, C_0, C_1...C_N) are determined through a least squares fitting of the results obtained by the 1D EUROPLEXUS calculations for the charge of 23kg and cell size of 1mm. The order of Equation (5) is chosen so that the difference of the polynomial predictions and the EUROPLEXUS values is smaller than 3%.

Table 4 shows the calculated constants for Equations (6) and (7) for the case of the incident peak positive overpressure and positive impulse. The equations are divided in two groups, with the first being valid for scaled distances 0.053<Z<0.40m/kg$^{1/3}$ and the second for 0.40<Z<40m/kg$^{1/3}$. For the largest scaled distance range (0.40<Z<40m/kg$^{1/3}$) the polynomials of Kingery-Bulmash may also be used as the difference between Kingery-Bulmash and the one-dimensional calculations are small.

Table 4. Constants of the equations of the incident blast parameters of a free-air burst.

	Spherical positive incident blast parameters			
Constant	**Peak overpressure**	**Impulse**	**Peak overpressure**	**Impulse**
	0.053≤Z≤0.40m/kg$^{1/3}$		**0.40<Z≤40m/kg$^{1/3}$**	
K_0	-0.91433	-1.25215	0.55452	0.76008
K_1	-1.45959	-1.65602	-1.13778	-0.73017
C_0	4.06103	2.31971	1.73036	1.13866
C_1	0.97094	1.47803	1.68465	1.3391
C_2	-0.0011	1.27866	0.7919	0.37718
C_3	-1.15856	-3.15442	0.80248	0.13645
C_4	-2.45996	-3.4603	-0.51063	-2.53112
C_5	5.01594	5.19595	-1.998	-5.744957
C_6	-0.3113	9.45267	0.13446	6.41571
C_7	7.4901	5.54576	1.41277	19.26609
C_8	-6.5702	-5.40032	-0.83675	-9.99
C_9	-3.40241	-8.87923	-0.0515	-19.08479
C_{10}	-0.24764	-19.997	1.1813	3.68941
C_{11}	-4.80809	-13.89187	-0.19042	8.13372
C_{12}	8.9989	38.20586	-0.44056	-1.07378

Figure 66 shows in detail the nonlinear fit with the above analytical expressions of the calculated points for the peak positive overpressure of a spherical incident blast wave. The scale of the diagrams is logarithmic and the goodness of fit appears to be very good. It is noted in particular that the value of P_s at the domain division point Z=0.40m/kg$^{1/3}$, calculated by Equation (6) is P_s(0.40-)=5.30MPa and P_s(0.40+)=5.24MPa, i.e. there is a difference of less than 1% between the two values.

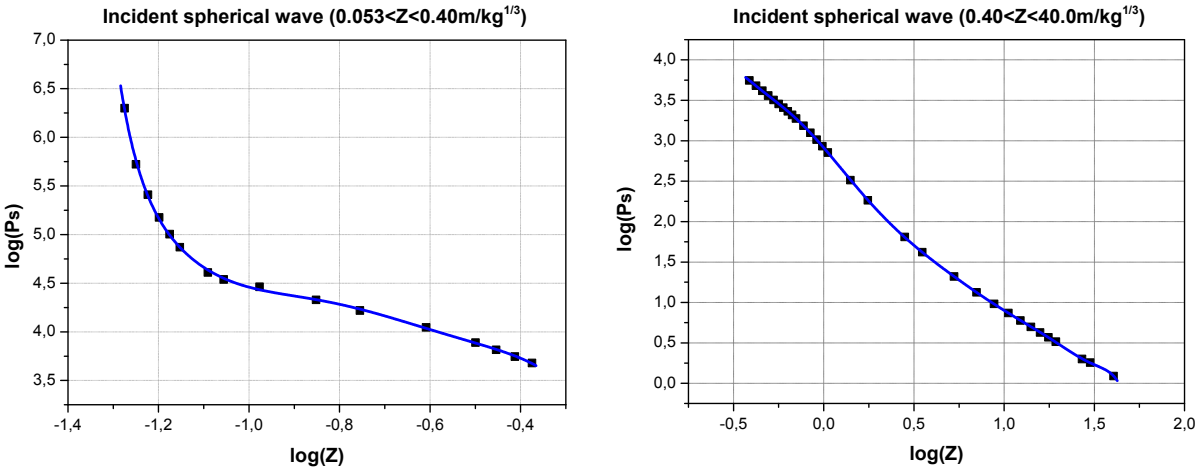

Figure 66: Incident spherical positive peak overpressure in relation to the scaled distance for 0.053≤Z≤0.40m/kg$^{1/3}$ (left) and 0.40<Z≤40.0m/kg$^{1/3}$ (right).

Figure 67 shows the nonlinear fit with the analytical expressions mentioned before for the positive impulse of a spherical incident blast wave. As in the previous figure, the scale of the graphs is logarithmic and the goodness of fit is very good. The value of it at the domain division point Z=0.40m/kg$^{1/3}$, calculated by Equation (6) is i_s(0.40)=103.9kPa·ms and i_s(0.40+)=105.31kPa·ms, i.e. practically the same.

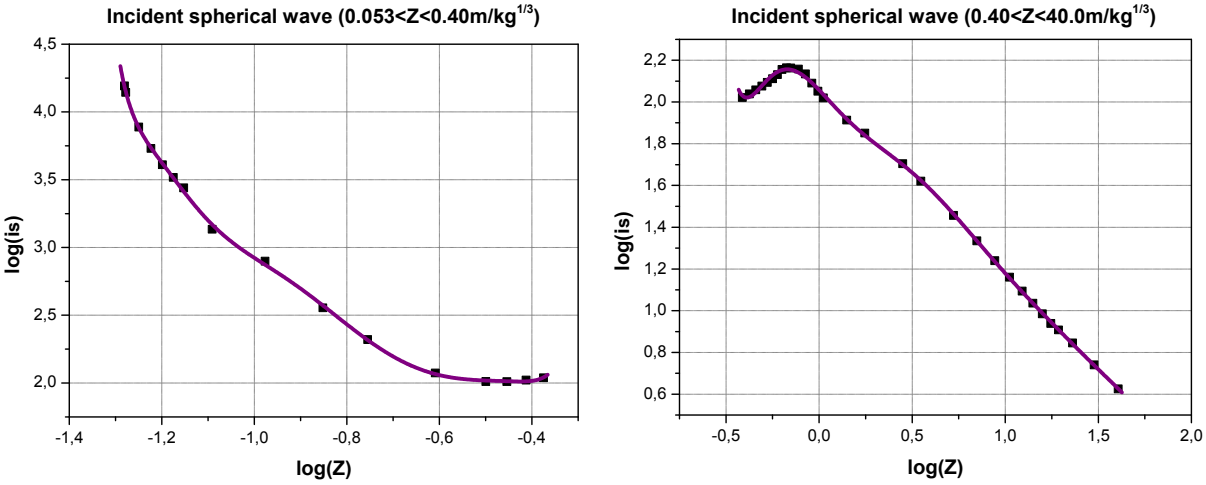

Figure 67: Incident spherical positive impulse in relation to the scaled distance for 0.053≤Z≤0.40m/kg$^{1/3}$ (left) and 0.40<Z≤40.0m/kg$^{1/3}$ (right).

Figure 68 shows the parameters of the positive phase of a spherical wave due to a free-air burst as already shown in Figure 61, but with the addition of the new curves that were calculated through fitting of the EUROPLEXUS simulation results, denoted as "epx".

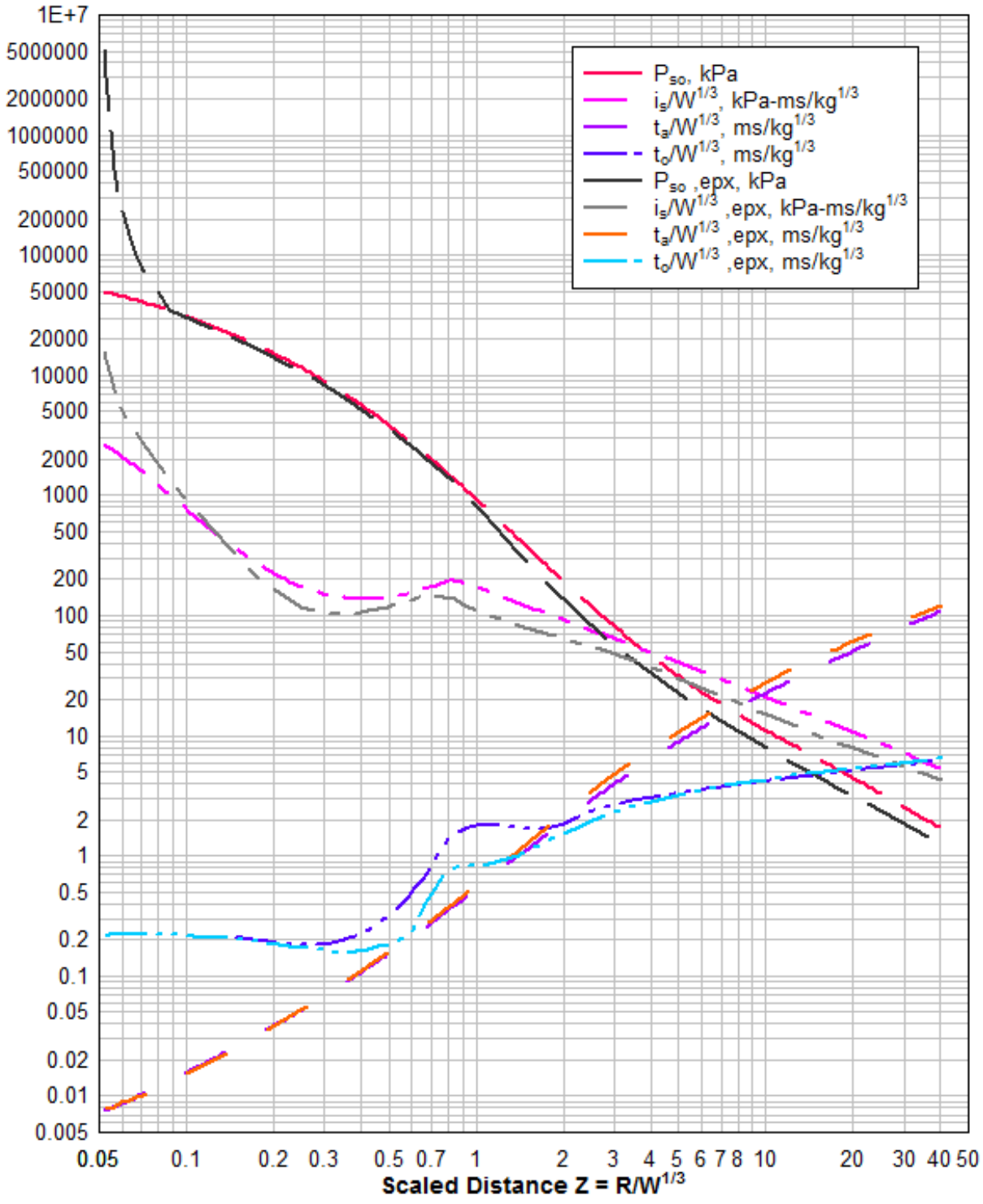

Figure 68: Additional incident parameter curves of positive phase of shock spherical wave of TNT charges from free-air bursts.

3.5 Reflected blast wave parameters

3.4.3 Comparison to Kingery-Bulmash diagrams

When the blast wave comes into contact with an obstacle it is reflected on its surface, thus leading to higher pressure values. The reflected pressure and impulse are more important in terms of design as it is them to be applied to the structural elements that have to sustain an explosion. Figure 60 includes curves for the determination of the positive reflected peak overpressure and impulse in the case of a spherical explosion from a free-air burst. As in the case of the incident blast wave parameters at distances close to the detonation center, there appear to be differences between the proposed reflected wave values of Figure 60 and those of the actual explosions.

The current section deals with the calculation of the normally reflected blast parameters (peak overpressure and impulse) for the same scaled distance range as in UFC-3-340-02 [2], i.e. $0.053 \leq Z \leq 40 m/kg^{1/3}$. The simulations cannot be performed exclusively by means of a one-dimensional (1D) analysis since the insertion of obstacles is not supported, so a three-dimensional (3D) domain is also utilized.

The procedure is divided in two steps. In the first step a 1D analysis is performed with finite volume elements whose diameter increases linearly with the distance from the detonation center, resulting in a cone shape domain. The inner element (at the center of the spherical charge) has a very small size (0.000025m), since it cannot have a zero value, i.e., more precisely, the geometrical model is a truncated cone. These elements at their two external borders have reflecting boundary conditions. This means that at the ends of the created cone it is the reflected pressure that is calculated and not the incident one. This way by constructing one-dimensional models with different lengths (corresponding to the stand-off distances of interest) the reflected overpressure values can be calculated for the whole scaled distance range. But, this procedure cannot be used for calculating the reflected positive impulse, especially at the near-field. When the blast wave reaches the end of the cone, where the reflected overpressure is recorded, it is reflected back towards the detonation center, from where it is reflected once again towards the end of the cone, and this continues until the end of the simulation. Thus for small scaled distances, the decaying reflected overpressure at the end of the cone does not reach the ambient pressure, as another blast wave reflected from the inner element at the charge center will arrive increasing the pressure, as shown in Figure 69. A way to overcome this problem would be to impose an absorbing boundary condition at the inner element of the cone, but this is not supported by EUROPLEXUS in this 1D formulation. However, the approach does not suffer from this problem for long scaled distances, where it is efficiently applied.

To overcome this numerical shortcoming, the solution of remapping the one-dimensional simulations into a three-dimensional model has been utilized. In detail, the 1D blast wave is mapped right before it interacts with the obstacle into a 3D fluid volume and its results are the initial conditions for this new 3D model. This means that the simulation of the 3D model starts at a time increment which has been defined from the 1D analysis and the 1D calculated blast parameters are used as input values for the 3D model. The arrival time of the blast wave in the case of the mapped 3D model is determined by adding the run time of the 1D model. Figure 69 shows the difference between the reflected pressure-time history as calculated from the 1D and the 3D analysis at a point situated 0.19m (near field) from the charge center of a 23kg TNT detonation. As can be seen, the impulse values at the 1D case cannot be correctly calculated as the overpressure does not drop towards the ambient value.

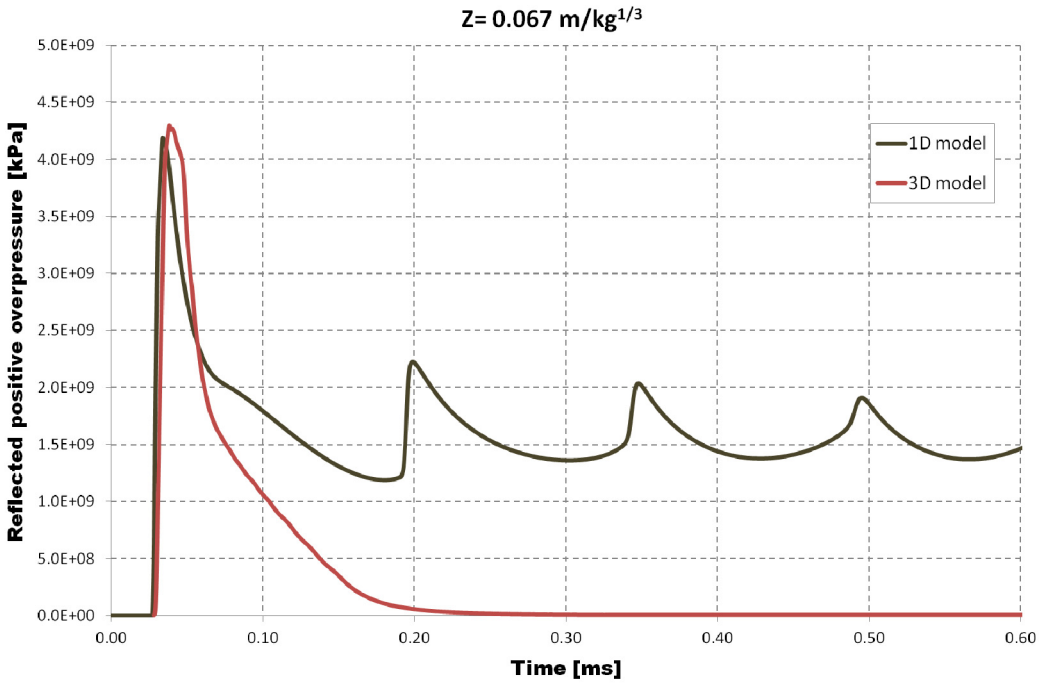

Figure *69*: Reflected pressure-time history at 0.19m distance from the detonation center of a 23kg TNT mass of a free-air burst.

For the calculation of the reflected blast parameters the 1D models were identical to the ones utilized for the incident blast wave. Three different TNT charge masses were used (23kg, 960kg and 18000kg) with a density of 1630kg/m^3. The cell size for all models was 1mm for the total scaled distance range and is identical to the element size of the 3D models. For simplification, the JWL material was used for both the charge and the surrounding air with parameters given in Table 1. The 3D model that was used had a cubic shape and was one eighth of the whole model. Symmetry conditions were applied to three of its faces, a fully absorbing material was applied to the other two and the last was defined as rigid and was used for the calculation of the reflected blast parameters. Figure 70 shows the pressure distribution [kPa] at the mapped 3D model at the beginning of the simulation.

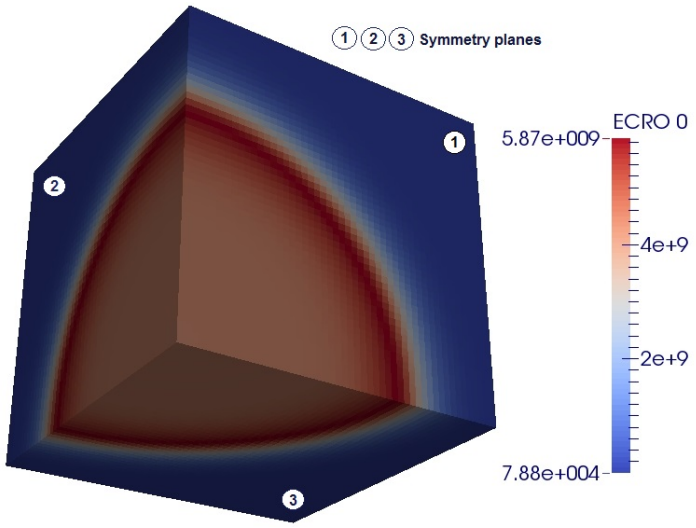

Figure 70: Pressure distribution at the model at the start of the 3D-simulation.

Figure 71 is a logarithmic diagram comparing the peak positive reflected overpressure values as proposed from UFC 3-340-02 [2] technical manual and as calculated from simulations with the above mapping procedure. The results from all three different charges (23kg, 960kg and 18000kg) produced nearly identical curves. From the figure it can be seen that the reflected overpressure values as computed by the EUROPLEXUS simulations are very close to those proposed in UFC-3-340-02 [2] for scaled distance values of Z>0.3 m/kg$^{1/3}$. But for smaller scaled distances, the pressure values predicted through the simulations are much larger. It is reminded that the Kingery-Bulmash predictions were based on a large experimental database, that unfortunately included only a limited number of test results at small scaled distances.

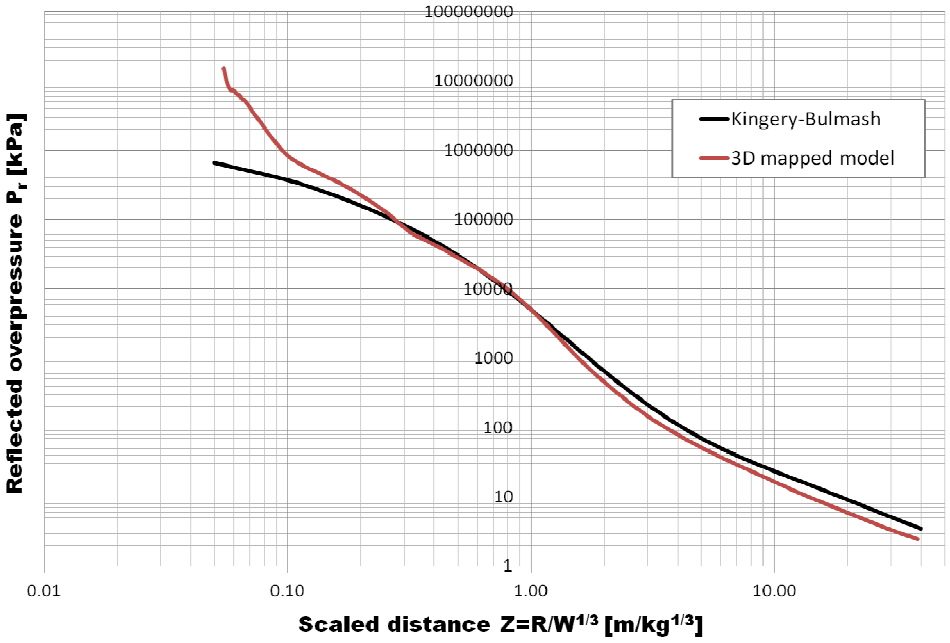

Figure 71: Comparison of peak positive reflected overpressure curves versus scaled distance for free-air bursts (spherical waves).

Figure 72 is a logarithmic diagram of the positive reflected impulse from a free-air burst as included in [2] and as calculated through the mapped 3D model. By comparing the two curves we can deduce that the EUROPLEXUS calculated reflected impulse values coincide very well with the Kingery-Bulmash predictions for both small and large scaled distances.

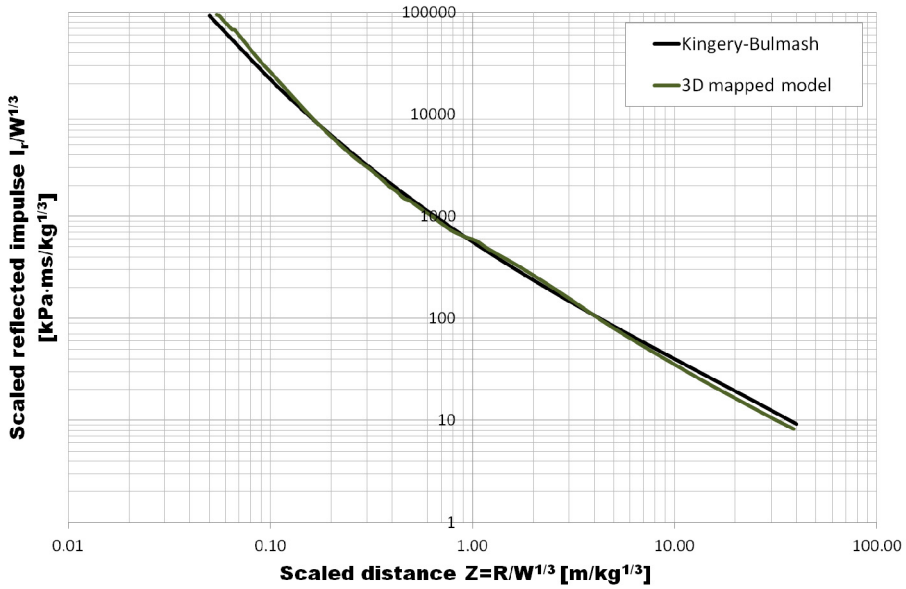

Figure 72: Comparison of positive reflected impulse curves versus scaled distance for free-air bursts (spherical waves).

Figure 73 shows the relative difference of the peak positive reflected overpressure and of the positive reflected impulse of a spherical wave in relation to the values recommended by Kingery-Bulmash as a function of scaled distance. The relative difference was calculated by using Equation (5). From the two diagrams it can be observed that the predicted reflected impulse values from both the Kingery-Bulmash equations [3] and the EUROPLEXUS simulations nearly coincide (less than 10% difference). In the case of the reflected overpressures the results are similar to the ones of the incident case, showing that the biggest differences are observed at small scaled distances.

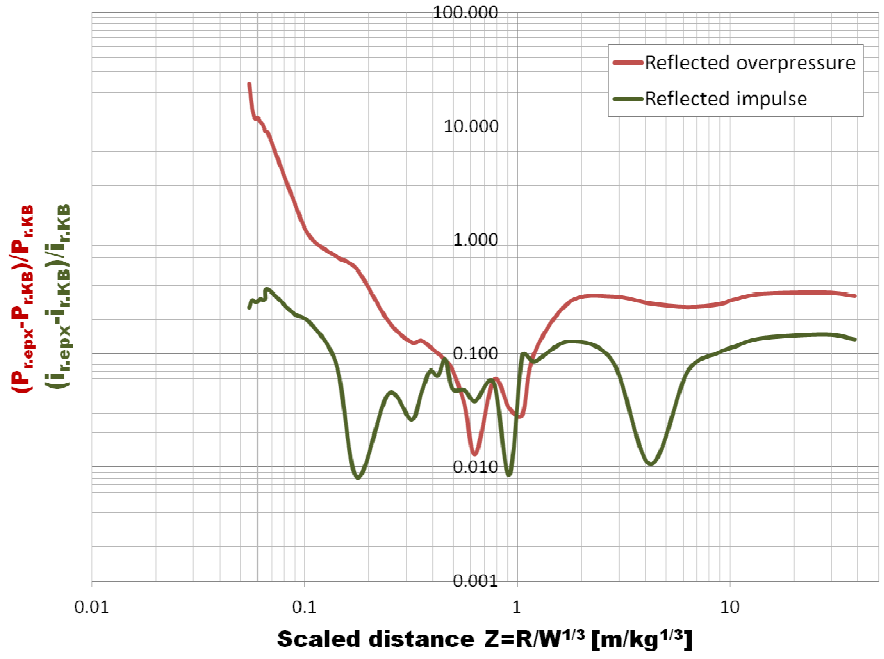

Figure 73: Relative difference of peak positive reflected overpressure and positive reflected impulse in relation to Kingery-Bulmash for free air bursts (spherical waves).

3.4.4 Updated reflected parameters polynomial equations

As can be observed from Figure 65 there is a considerable difference at the proposed peak positive reflected overpressure values at small scaled distances between the technical manual of Kingery-Bulmash [3] and the EUROPLEXUS simulations. Similar to the case of the incident peak overpressure, new polynomial equations are proposed that are based on the finite element analysis results. The scaled distance range is divided in two regions, one for the near-field ($0.053 \leq Z \leq 0.4 m/kg^{1/3}$) and the other for larger scaled distance values ($0.40 < Z \leq 40.0 m/kg^{1/3}$). For the second region the polynomial equations from Kingery-Bulmash can also be used, since the differences are small.

For the case of the reflected positive impulse the differences between the Kingery-Bulmash proposals and the values calculated from the explicit finite element program are relatively small for the whole scaled distance range. This means that even though another set of polynomial equations is provided, which is based on the 3D mapped model graph from Figure 66, the relationships from Kingery-Bulmash technical manual [3] can also be used. The proposed polynomial functions for both the peak reflected positive overpressure and the reflected positive impulse have the form shown in Equations (6) and (7). The constants of these equations are included in Table 5 and are derived by a least squares fitting procedure.

Table 5. Constants of the equations for the reflected blast parameters of a free-air burst.

	Spherical positive reflected blast parameters			
Constant	**Peak overpressure**	**Impulse**	**Peak overpressure**	**Impulse**
	$0.053 \leq Z \leq 0.40 m/kg^{1/3}$		**$0.40 < Z \leq 40 m/kg^{1/3}$**	
K_0	-0.45355	-1.22426	-0.5736	-0.90176
K_1	-1.17991	-1.59396	-1.01474	-0.45548
C_0	4.600	3.91735	4.91457	9.81477
C_1	1.64121	1.32046	1.94421	14.998
C_2	2.11153	0.29047	2.97654	3.16929
C_3	-2.69772	-1.40425	8.999	-14.9883
C_4	-4.68269	0.95869	5.37799	-9.84745
C_5	8.999	6.36189	-0.02422	5.44764
C_6	-3.52406	-6.02756	2.46811	6.14157
C_7	-0.60343	-8.999	4.17288	1.4146
C_8	4.31395	8.38468	1.9687	0.21791
C_9	-3.22106	1.03014	0.30267	0.1034

Figure 74 shows in detail the nonlinear fit for the positive reflected peak overpressure for a free-air burst with the use of the above polynomial expressions. The scale of the diagrams is logarithmic and the goodness of fit is very good. The value of P_r at the domain division point $Z=0.40 m/kg^{1/3}$, calculated by Equations (6) and (7) is $P_r(0.40-)=42.34 MPa$ and $P_r(0.40+)=42.73 MPa$, i.e. there is a difference of less than 1% between the two values.

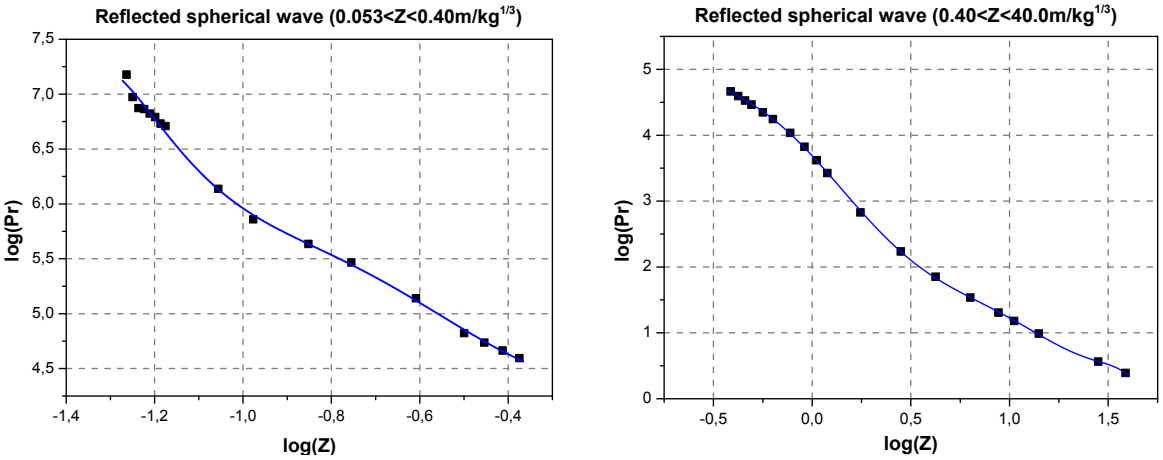

Figure 74: Reflected spherical positive peak overpressure in relation to the scaled distance for $0.053 \leq Z \leq 0.40 m/kg^{1/3}$ (left) and $0.40 < Z \leq 40.0 m/kg^{1/3}$ (right).

Figure 75 shows the nonlinear fit with the analytical expressions of Table 5 for the positive impulse of a spherical reflected blast wave. The scale of the graphs is logarithmic and the values of i_r at the domain division point $Z=0.40 m/kg^{1/3}$, calculated by Equation (6) are $i_r(0.40-)=1875.41 kPa \cdot ms$ and $i_r(0.40+)=1879.48 kPa \cdot ms$, i.e. practically the same.

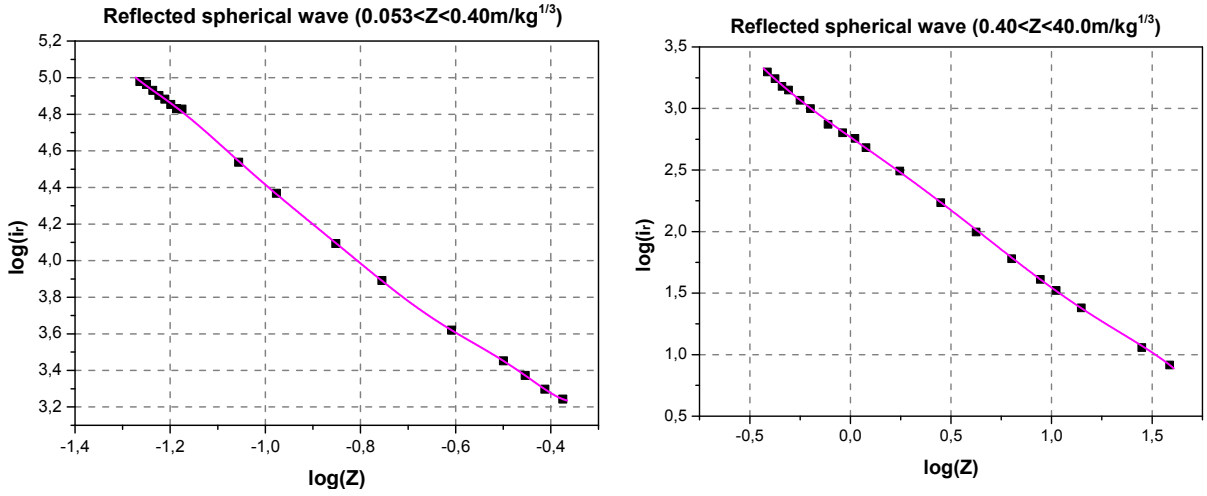

Figure 75: Reflected spherical positive impulse in relation to the scaled distance for $0.053 \leq Z \leq 0.40 m/kg^{1/3}$ (left) and $0.40 < Z \leq 40.0 m/kg^{1/3}$ (right).

Figure 76 shows the reflected parameters of the positive phase of a spherical wave due to a free-air burst as in Figure 60, but with the addition of the new curves that were calculated through fitting of the EUROPLEXUS simulation results ("epx" denotes the simulation derived curves). In Figure 76 the arrival time curve, as calculated through the 3D mapped model, is also included, even though no new set of equations is proposed since the results are nearly identical to the ones of the incident blast wave case.

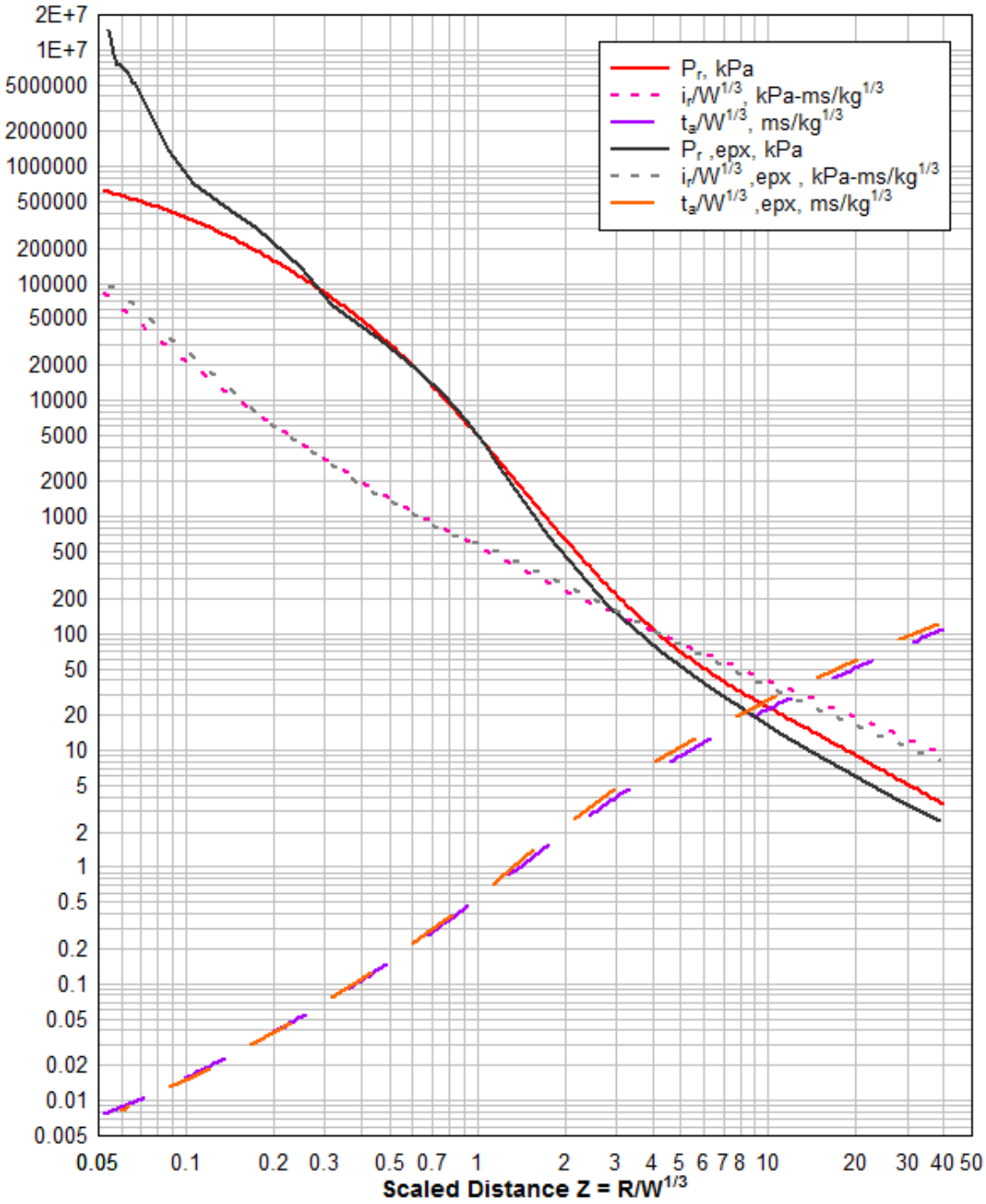

Figure 76: Additional reflected parameter curves of positive phase of shock spherical wave of TNT charges from free-air bursts.

4. Conclusion

When designing structural components to resist blast induced loads, engineers rely on a set of empirical and semi-empirical equations that are available from various technical manuals and other publications. One of the most commonly used set of equations is included in the Kingery-Bulmash technical manual [3]. These equations have been integrated in various explicit finite element programs that are used for the design of structures against several types of explosions. This set of relationships was based on a large number of experimental data and have proven accurate for predicting blast loads at medium and large scaled distances. But, as has been shown by several researchers, the proposed values for small scaled distances should be treated with caution, since the supporting set of test data was extremely limited at the time of publication.

This report has aimed at investigating and confirming the blast parameter values at small scaled distances through the use of the explicit finite element code EUROPLEXUS. Special attention was paid to the region near the charge/free-air interface, where the available experimental data are limited. Near-field explosions were studied by means of computational fluid dynamics analysis and the results were compared with similar findings from other explicit software tools. In detail, EUROPLEXUS was verified for one-dimensional analysis by comparing its results with those of Needham [15] and other specialized programs, such as AUTODYN, LD-DYNA and CTH. The numerical calculations were also compared with the Kingery-Bulmash technical manual and their validity was examined for a large scaled distance range ($0.053 \leq Z \leq 40.0 m/kg^{1/3}$).

It was found that the predictions of Needham [15] are similar to those of EUROPLEXUS for both peak incident overpressure and positive impulse at small and medium scaled distance values. EUROPLEXUS also shows good compliance with similar results from the other widely-used explicit software tools. From the analyses it was shown that the Friedlander equation for describing the overpressure-time curve cannot be used with accuracy near the charge face as it does not take into account the expanding detonation products. If the blast profile at the near-field is of interest, the use of computational fluid dynamics techniques should be considered.

From the mesh dependence studies that were performed it was shown that depending on the vicinity of a point to the explosion center, different cell sizes could be used to achieve good accuracy. The closer the point to the detonation center, the finer the mesh that should be used. For simulating the charge itself, cell sizes of 1mm provide good precision even for small charge masses (23kg), but larger cell sizes may be used if the charge is bigger, without substantially affecting the final results.

Comparisons with the simulation results showed that the Kingery-Bulmash proposed incident blast wave equations give peak positive overpressure and impulse values much smaller than the numerically derived ones for scaled distance values $Z<0.1 m/kg^{1/3}$. For the rest of the scaled distance range both the peak positive overpressure and positive impulse values from the EUROPLEXUS simulations are slightly smaller than the ones proposed from [2]. Similarly, there is a big difference between the peak reflected overpressure values at small scaled distances between the simulation and the Kingery-Bulmash predictions, whereas the differences between the reflected positive impulse values are much smaller for the whole scaled distance range.

A new set of equations as a function of scaled distance was introduced by curve fitting the results from the numerical simulations. These equations may be used independently or as a supplement to the ones of Kingery-Bulmash. Thus, the peak positive overpressure and positive impulse at a point due to a free-air burst can be calculated with improved accuracy and inserted into an explicit code for quantitatively assessing the effects of an explosion onto a structure. It is reminded though, that the blast phenomenon at very small distances from the charge center is very complex and the evolution of the chemical reactions taking place may vary depending on the charge type.

In particular, the afterburning effect may have to be taken into account, an issue which has been totally ignored in this work. This means that the blast parameter values at very small scaled distances should always be treated with caution. In order to be more confident with the use of certain values, further research and especially more experimental data from small scaled distances would be necessary.

References

[1] U.S. Department of the Army, (1990) "Structures to resist the effects of accidental explosions", Technical Manual 5-1300.

[2] Unified Facilities Criteria (2008), "UFC 3-340-02 Structures to Resist the Effects of Accidental Explosions", U.S. Army Corps of Engineers, Naval Facilities Engineering Command, Air Force Civil Engineer Support Agency.

[3] Kingery C. N., Bulmash G., (1984) "Technical report ARBRL-TR-02555: Air blast parameters from TNT spherical air burst and hemispherical burst", AD-B082 713, U.S. Army Ballistic Research Laboratory, Aberdeen Proving Ground, MD.

[4] Brode H. L., (1955) "Numerical solution of spherical blast waves", Journal of Applied Physics, American Institute of Physics, New York.

[5] Kinney G. F., Graham K.J., (1985) "Explosive Shocks in Air", Springer, Berlin.

[6] Baker W.E., Cox P.A., Westine P.S., Kulesz J.J., Strehlow R.A., (1983) "Explosion Hazards and Evaluation", Elsevier, Amsterdam.

[7] Larcher M., Casadei F., Solomos G., (2014) "Simulation of blast waves by using mapping technology in EUROPLEXUS", JRC Technical Report, EUR 26735EN, Luxembourg.

[8] Karlos V., Solomos G., (2013) "Calculation of blast loads for application to structural components", JRC Technical Report, EUR 26456EN, Luxembourg.

[9] Bogosian D., Ferritto J., Shi Y., (2002) "Measuring uncertainty and conservatism in simplified blast models", 30th Explosive Safety Seminar, Atlanta.

[10] Shin J., Whittaker A., Cormie D., (2015) "Incident and normally reflected overpressure and impulse for detonations of spherical high explosives in free air", Journal of Structural Engineering, Vol. 141, Issue 12.

[11] Mader L., (1963) "Detonation Properties of Condensed Explosives Computed Using the Becker-Kistiakosky-Wilson Equation of State", Los Alamos Scientific Laboratory Report LA-2900, New Mexico.

[12] Tanaka K., (1985) "Detonation Properties of High Explosives Calculated by Revised Kihara– Hikita Equation of State", Proc. 8th Symp. (Int.) on Detonation, Albuquerque/New Mexico/Washington, DC.

[13] Lee E., Horning J., Kury J., (1968) "Adiabatic expansion of high explosives detonation products", Lawrence Livermore National Laboratory, University of California, Livermore, TID 4500-UCRL 50422.

[14] Dobratz B., Crawford P., (1985) "LLNL Explosives Handbook", Lawrence Livermore National Laboratory, University of California, Livermore.

[15] Needham C., (2010) "Blast Waves", Springer-Verlag, Berlin, Germany.

[16] Lutsky M., (1965) "The flow behind a spherical detonation in TNT using the Landau-Stanyukovoch Equation of State for detonation products", NOL-TR 64-40, U.S. Naval Ordnance Laboratory, White Oak, MD.

[17] Doan L., Nickel G., (1963) "A subroutine for the equation of state of air", RTD TN63-2, Air Force Weapons Laboratory.

[18] Browning S., Sherburn A., Schwer E., (2013) "Predicting blast loads using LS-DYNA and CTH", Proceedings, ASCE Structures Congress, Pittsburgh.

[19] LSTC, (2013) "Keyword User's Manual Ver.7.0", Livermore Software Technology Corporation, Livermore, CA.

[20] McGlaun M., Thompson L., Elrick G., (1990) "CTH: a three-dimensional shock wave physics code", International Journal of Impact Engineering, 10(1-4), 351-360.

[21] Shin J., Whittaker A., Amjad A., (2014) "Air-blast effects on civil structures", Technical Report MCEER-14-0006, University of Buffalo, NY.

[22] Kingery C. N., (1966) "Air blast parameters versus distance for hemispherical TNT surface bursts", Ballistic Research Laboratories, Aberdeen Proving Ground, Maryland.

[23] Kingery C. N., Coulter G. A., (1983) "Reflected overpressure impulse on a finite structures", Ballistic Research Laboratory, Aberdeen Proving Ground, Maryland.

List of abbreviations and definitions

P_{so}: Peak positive incident overpressure

P_{so-}: Peak negative incident overpressure

t_a: Arrival time

t_o: Positive phase duration

t_{o-} : Negative phase duration

i_s: Positive incident impulse

i_{s-}: Negative incident impulse

U: Shock wave speed

L_w: Blast wavelength

b: Blast wave decay coefficient

P_{ro}: Peak positive reflected overpressure

P_{ro-}: Peak negative reflected overpressure

I_r: Positive reflected impulse

I_{r-}: Negative reflected impulse

Z: Scaled distance

$A,B,R1,R2,\omega$: Material constants for the Jones-Wilkins-Lee (JWL) model

ρ: Gas density

ρ_o: Explosive density

D: Detonation velocity

e_{int}: Internal energy per unit mass

CS: Cell size

$P_{s.KB}$: Peak positive incident overpressure according to Kingery-Bulmash manual

$P_{s.epx}$: Peak positive incident overpressure according to EUROPLEXUS calculations

$i_{s.KB}$: Positive incident impulse according to Kingery-Bulmash manual

$i_{s.epx}$: Positive incident impulse according to EUROPLEXUS calculations

W: Charge mass

List of figures

List of tables

Europe Direct is a service to help you find answers to your questions about the European Union
Free phone number (*): 00 800 6 7 8 9 10 11
(*) Certain mobile telephone operators do not allow access to 00 800 numbers or these calls may be billed.

A great deal of additional information on the European Union is available on the Internet.
It can be accessed through the Europa server http://europa.eu

How to obtain EU publications

Our publications are available from EU Bookshop (http://bookshop.europa.eu),
where you can place an order with the sales agent of your choice.

The Publications Office has a worldwide network of sales agents.
You can obtain their contact details by sending a fax to (352) 29 29-42758.

LB-NA-27823-EN-N

JRC Mission

As the Commission's in-house science service, the Joint Research Centre's mission is to provide EU policies with independent, evidence-based scientific and technical support throughout the whole policy cycle.

Working in close cooperation with policy Directorates-General, the JRC addresses key societal challenges while stimulating innovation through developing new methods, tools and standards, and sharing its know-how with the Member States, the scientific community and international partners.

Serving society
Stimulating innovation
Supporting legislation

Publications Office

doi:10.2788/778898

ISBN 978-92-79-57603-4